Thermal and Electrical Phenomena in Chaotic Conductors

PROEFSCHRIFT

TER VERKRIJGING VAN DE GRAAD VAN DOCTOR AAN DE RIJKSUNIVERSITEIT TE LEIDEN, OP GEZAG VAN DE RECTOR MAGNIFICUS DR. W. A. WAGENAAR, HOOGLERAAR IN DE FACULTEIT DER SOCIALE WETENSCHAPPEN, VOLGENS BESLUIT VAN HET COLLEGE VOOR PROMOTIES TE VERDEDIGEN OP DONDERDAG 3 SEPTEMBER 1998 TE KLOKKE 15.15 UUR

DOOR

Stijn Alexander van Langen

geboren te Nijmegen in 1971

Promotiecommissie:

Promotor: Prof. dr. C. W. J. Beenakker
Referent: Prof. dr. ir. W. van Saarloos
Overige leden: Prof. dr. P. J. van Baal
Prof. dr. M. Büttiker (Université de Genève)
Prof. dr. L. J. de Jongh
Prof. dr. J. M. J. van Leeuwen
Prof. dr. L. W. Molenkamp (Rheinisch-Westfälische Technische Hochschule Aachen)

Het onderzoek beschreven in dit proefschrift is uitgevoerd als onderdeel van het wetenschappelijke programma van de Stichting voor Fundamenteel Onderzoek der Materie (FOM) en de Nederlandse Organisatie voor Wetenschappelijk Onderzoek (NWO).

The research described in this thesis has been carried out as part of the scientific program of the Foundation for Fundamental Research on Matter (FOM) and the Netherlands Organization for Scientific Research (NWO).

Aan mijn ouders

Contents

1 Introduction 7
1.1 Scattering theory . . . 7
1.1.1 Landauer formula . . . 7
1.1.2 Thermopower . . . 9
1.1.3 Shot noise . . . 11
1.1.4 Optical speckle . . . 13
1.2 Disordered waveguides . . . 14
1.2.1 Semiclassical theory of weak localization . . . 14
1.2.2 Herbert-Jones-Thouless formula . . . 17
1.2.3 Dorokhov-Mello-Pereyra-Kumar equation . . . 17
1.3 Chaotic cavities . . . 19
1.3.1 Random-matrix theory of a closed cavity . . . 20
1.3.2 Random-matrix theory of an open cavity . . . 22
1.4 This thesis . . . 23

2 Nonperturbative calculation of the probability distribution of plane-wave transmission through a disordered waveguide 31

3 Fluctuating phase rigidity for a quantum chaotic system with partially broken time-reversal symmetry 41

4 Quantum-statistical current correlations in multi-lead chaotic cavities 49

5 Thermopower of single-channel disordered and chaotic conductors 59
5.1 Introduction . . . 59
5.2 Disordered wire . . . 60
5.2.1 Analytical theory . . . 60
5.2.2 Numerical simulation . . . 61
5.2.3 Finite temperatures . . . 61
5.3 Chaotic quantum dot . . . 64
5.4 Conclusion . . . 65

6 Berry phase and adiabaticity of a spin diffusing in a non-uniform magnetic field 69
6.1 Introduction . . . 69
6.2 Spin-resolved transmission . . . 70
6.2.1 Formulation of the problem . . . 70
6.2.2 Diffusion approximation . . . 72
6.2.3 Comparison with Monte Carlo simulations . . . 76

6.3 Weak localization 76
  6.3.1 Formulation of the problem 76
  6.3.2 Diffusion approximation 78
  6.3.3 Comparison with Loss, Schoeller, and Goldbart 81
6.4 Conclusions 84

Samenvatting **89**

List of publications **93**

Curriculum Vitae **94**

1 Introduction

In this thesis we study electrical and optical transport properties of systems in which the dynamics of the electrons or photons is chaotic. We concentrate on two types of geometries, waveguides and cavities. In waveguides, the chaotic dynamics arises due to the scattering on randomly placed impurities, whereas in cavities it can be due to the irregular shape of the boundaries. The behaviour of such systems in quantum mechanics or wave optics can be quite different from what is known in classical mechanics or geometrical optics, due to the interplay of multiple scattering and wave interference. In electrical conductors this interplay affects the conductance and other transport properties like the shot noise and the thermopower. In optical systems the speckle pattern of transmitted radiation reveals the chaotic dynamics of the photons. In this first chapter we introduce the techniques we will use to describe disordered waveguides and chaotic cavities, as well as the physical quantities that we will study.

1.1 Scattering theory

1.1.1 Landauer formula

The Landauer formula [1] relates the zero-temperature conductance G to the quantum-mechanical transmission matrix t,

$$G = \frac{2e^2}{h} \mathrm{Tr}\, t t^\dagger. \tag{1.1.1}$$

It provides the link between optics and electronics, because the transmission matrix — unlike the conductance — can also be defined for classical waves. It can also be generalized to other transport properties, such as the shot noise [2] and the thermopower [3]. Before discussing these generalizations, we give an elementary derivation of Eq. (1.1.1).

Consider a metal sample connected to two electron reservoirs as in Fig. 1-1. In the leads between the sample and the reservoirs, the eigenstates are of the form

$$\psi_n^\pm(\mathbf{r}) = \frac{1}{\sqrt{k_n}} \mathrm{e}^{\pm i k_n x} \chi_n(y, z), \tag{1.1.2}$$

where the plus (minus) sign is for the right (left) moving state. The transverse wave functions $\chi_n(y, z)$ are solutions of the wave equation in a confining potential $V(y, z)$,

$$\left[-\frac{\hbar^2}{2m} \left(\frac{d^2}{dy^2} + \frac{d^2}{dz^2} \right) + V(y, z) - E_n \right] \chi_n(y, z) = 0. \tag{1.1.3}$$

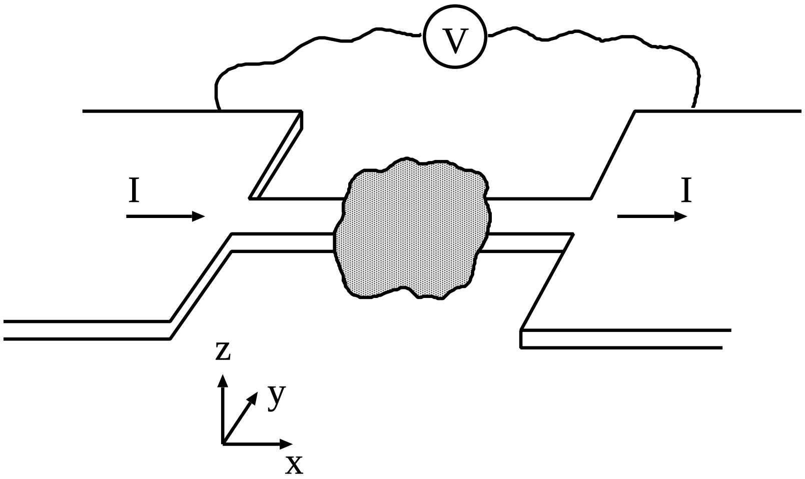

Figure 1-1. Conductor (shaded) coupled to two electron reservoirs by leads. A current I is passed through the leads for a voltage difference V between the reservoirs. The conductance of the system is $G = I/V$.

The longitudinal wave-number k_n at the Fermi energy E_{F} is given by

$$\hbar k_n = \sqrt{2m(E_{\mathrm{F}} - E_n)}. \tag{1.1.4}$$

For long enough leads only the N modes with real k_n can carry current.

A general incoming state is a superposition of all incoming modes from the left and from the right, the $2N$ coefficients forming vectors c_{L}^{+} and c_{R}^{-}. Similarly, the outgoing state is described by a $2N$ vector $(c_{\mathrm{L}}^{-}, c_{\mathrm{R}}^{+})$. The scattering matrix S relates the amplitudes of the incoming and outgoing modes,

$$\begin{pmatrix} c_{\mathrm{L}}^{-} \\ c_{\mathrm{R}}^{+} \end{pmatrix} = S \begin{pmatrix} c_{\mathrm{L}}^{+} \\ c_{\mathrm{R}}^{-} \end{pmatrix}, \quad S = \begin{pmatrix} r & t' \\ t & r' \end{pmatrix}, \tag{1.1.5}$$

where r and t (r' and t') are the $N \times N$ reflection and transmission matrices for scattering from the left (right). Flux conservation requires that S is a unitary matrix, $SS^{\dagger} = 1$. In the absence of a magnetic field the matrix S is also symmetric, $S = S^{\mathrm{T}}$.

Consider now the situation that a voltage difference V is applied between the reservoirs at zero temperature. In the left (right) reservoir all states below $E_{\mathrm{F}} + eV$ (E_{F}) are occupied, while the other states are empty. Only states in the interval $E_{\mathrm{F}} < E < E_{\mathrm{F}} + eV$ contribute therefore to the current. If the leads are connected ideally to the reservoirs, the current carried by the right-moving state n in this energy interval is $\int_{E_{\mathrm{F}}}^{E_{\mathrm{F}}+eV} ev_n \rho_n \, dE$, where v_n and ρ_n are the group velocity and density of states of the one-dimensional subband. It follows from $v_n = dE_n/\hbar dk$ and $\rho_n = 2\,(2\pi dE_n/dk)^{-1}$ that the injected current equals the universal amount $2e/h$ per channel, per unit of energy. The factor of 2 accounts

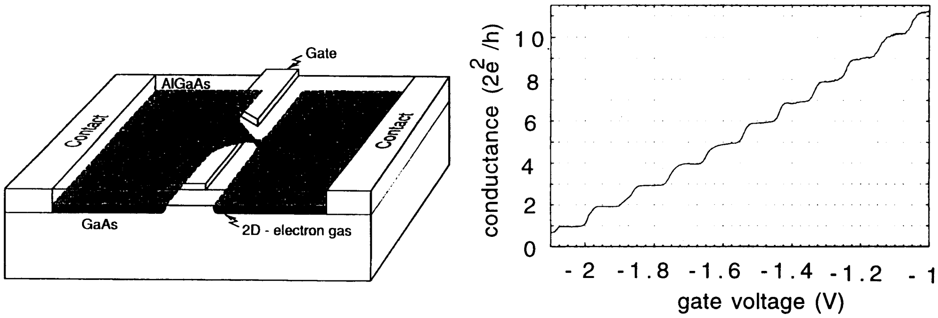

Figure 1-2. Left: schematic view of a quantum point contact. The width is adjustable by the voltage on a gate electrode. Right: conductance as a function of gate voltage, showing conductance quantization. (From Ref. [5].)

for spin degeneracy. A fraction $\sum_m |t_{mn}|^2$ is transmitted to the right lead, therefore the total current is

$$I = \frac{2e}{h} \sum_{m,n=1}^{N} \int_{E_\mathrm{F}}^{E_\mathrm{F}+eV} dE \, |t_{mn}|^2. \tag{1.1.6}$$

The conductance G is the ratio I/V in the limit $V \to 0$, hence we obtain the Landauer formula

$$G = \frac{2e^2}{h} \sum_{m,n=1}^{N} |t_{mn}|^2 = \frac{2e^2}{h} \mathrm{Tr}\, tt^\dagger. \tag{1.1.7}$$

The Landauer formula has been successfully applied to a great variety of mesoscopic systems [4]. We illustrate its application to what is perhaps the most basic system, the quantum point contact (QPC). A QPC is a constriction in a two-dimensional electron gas of variable width W, comparable to the Fermi wavelength λ_F. For ballistic motion through the QPC the eigenvalues of $tt^\dagger$ are equal to zero or one with good accuracy. According to the Landauer formula the conductance is quantized,

$$G = \frac{2e^2}{h} N_\mathrm{QPC}, \tag{1.1.8}$$

where $N_\mathrm{QPC} \simeq 2W/\lambda_\mathrm{F}$ is the number of unit eigenvalues of $tt^\dagger$. The stepwise increase of G with increasing width of the QPC is shown in Fig. 1-2.

1.1.2 Thermopower

Electrical conduction at zero temperature is determined by quantum mechanical scattering at the Fermi energy. Thermo-electrical properties probe the energy dependence of these scattering processes. In this thesis we will consider the thermopower.

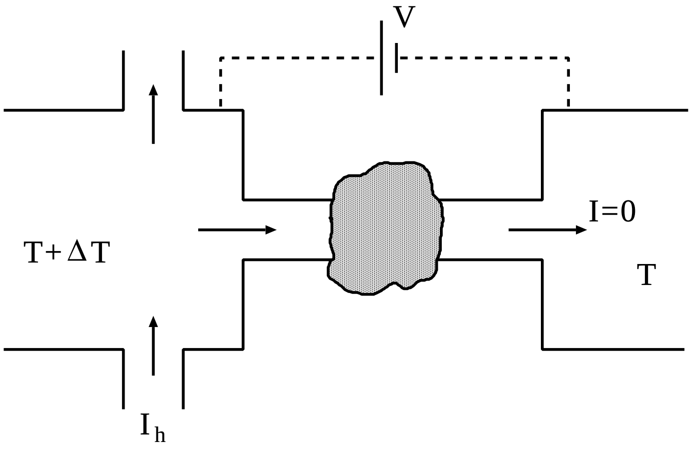

Figure 1-3. Schematic view of an experiment to measure the thermopower. A heating current I_h is passed on the left side of the conductor, to create a temperature difference ΔT. A voltage V is applied to compensate the resulting electrical current I.

When a temperature difference $\Delta T = T_1 - T_2$ is maintained between the two reservoirs an electrical current will flow. This current can be compensated by applying a voltage V yielding a current in the opposite direction. The thermopower S is defined as the (negative) ratio of V and ΔT such that the net current vanishes, in the limit $\Delta T \to 0$,

$$S = - \lim_{\Delta T \to 0} \left. \frac{V}{\Delta T} \right|_{I=0} . \tag{1.1.9}$$

Thermo-electric transport can be described in terms of the transmission matrix [3] by generalizing Eq. (1.1.6) to finite temperatures,

$$I = \frac{2e}{h} \sum_{m,n=1}^{N} \int dE \left[f(E - eV, T + \Delta T) |t_{mn}|^2 - f(E,T) |t'_{mn}|^2 \right], \tag{1.1.10}$$

where $f(E,T)$ is the Fermi-Dirac distribution,

$$f(E,T) = \frac{1}{1 + \exp\left[(E - E_{\rm F})/k_{\rm B}T\right]}. \tag{1.1.11}$$

Expansion in V and ΔT yields

$$I = \frac{2e}{h} \int dE \left(\frac{E - E_{\rm F}}{T} \Delta T - eV \right) \mathrm{Tr}\, (tt^\dagger) \frac{d}{dE} f(E). \tag{1.1.12}$$

Thus the thermopower is given by the Cutler-Mott formula

$$S = -\frac{1}{eT} \frac{\int dE\, (E - E_{\rm F}) \mathrm{Tr}\, (tt^\dagger)\, df/dE}{\int dE\, \mathrm{Tr}\, (tt^\dagger)\, df/dE}. \tag{1.1.13}$$

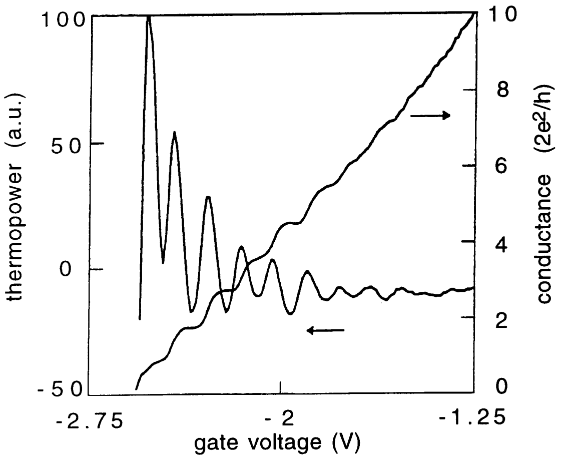

Figure 1-4. Thermopower and conductance of a quantum point contact as a function of gate voltage. The peaks in the thermopower line up with the steps in the conductance. (From Ref. [6].)

If $k_B T$ is smaller than the energy scale at which $\mathrm{Tr}\, tt^\dagger$ varies, the energy integrals can be done using partial integration and the Sommerfeld expansion, yielding

$$S = -\frac{\pi^2}{3} \frac{k_B^2 T}{e} \left. \frac{\frac{d}{dE}\mathrm{Tr}\,(tt^\dagger)}{\mathrm{Tr}\,(tt^\dagger)} \right|_{E=E_F} . \tag{1.1.14}$$

Fig. 1-4 shows the measured thermopower of a quantum point contact, plotted together with the conductance. As expected from Eq. (1.1.14), the thermopower peaks at the transitions between conductance plateaux.

In Chapter 5 we consider the thermopower of a chaotic electron cavity. Fig. 1-5 shows an experimental result on such a system. Plotted is the distribution of the thermopower, sampled over different values of the magnetic field and a gate voltage changing the shape of the cavity. The result compares well with a random matrix simulation, and is clearly non-Gaussian.

1.1.3 Shot noise

The conductance describes the time-averaged current. Two fundamental sources for time-dependent fluctuations in the current are thermal noise and shot noise [2, 8]. Thermal noise arises because at finite temperatures the occupation of states around the Fermi level fluctuates. Shot noise is still present at zero temperature, and arises due to discreteness of the charge.

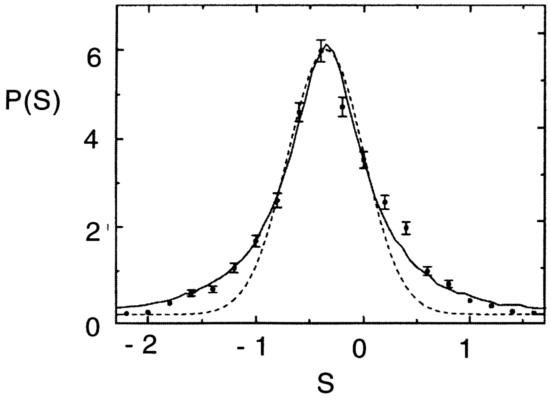

Figure 1-5. Distribution of the thermopower (arbitrary units) of a ballistic quantum dot. Datapoints represent the measured distribution; full curve is the result of a random matrix simulation. Dotted curve is an attempt to fit the measured distribution with a Gaussian. (From Ref. [7].)

The correlator of the current fluctuations $\Delta I(t) = I(t) - \bar{I}$ has the spectral density

$$P(\omega) = 2\int_{-\infty}^{\infty} dt\, \mathrm{e}^{i\omega t}\overline{\Delta I(t_0)\Delta I(t_0 + t)}, \tag{1.1.15}$$

where the bar $\overline{\cdots}$ indicates an average over the initial time t_0. The spectral density (1.1.15) can be related to the scattering matrix. In the zero-temperature, zero-frequency limit, the result is [2]

$$P(0) = \frac{2e^2}{h} 2eV \,\mathrm{Tr}\, \left[tt^\dagger \left(1 - tt^\dagger\right)\right]. \tag{1.1.16}$$

If all the eigenvalues of $tt^\dagger$ are $\ll 1$ (for example in a tunnel barrier) then the factor $1 - tt^\dagger$ can be omitted, and the noise power is proportional to the conductance. In this case the noise power is given by the Poisson formula,

$$P_{\mathrm{Poisson}} = 2eVG = 2eI, \tag{1.1.17}$$

corresponding to uncorrelated transmission events. If one of the eigenvalues of $tt^\dagger$ becomes of order unity, the shot noise is suppressed below P_{Poisson}, due to correlations between transmission events. One speaks of sub-Poissonian shot noise.

In Fig. 1-6 the measured noise power of a quantum point contact is plotted. The shot noise is strongly suppressed below the Poisson value on the conductance plateaux.

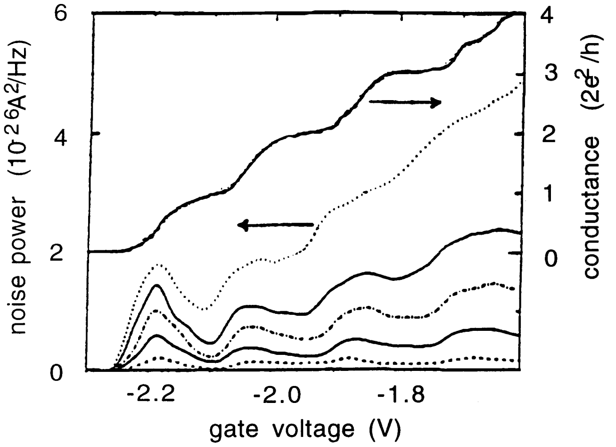

Figure 1-6. Shot noise power of a quantum point contact as a function of gate voltage. The current-driving voltage is 0.5, 1, 1.5, 2, and 3 mV, starting from the bottom curve. The upper curve shows the conductance. (From Ref. [9].)

1.1.4 Optical speckle

Laser light reflected by a rough surface produces a speckle pattern on a screen, a random pattern of dark and bright spots. The spatial distribution of the intensity I on the screen has the exponential form,

$$P(I) = \frac{1}{\langle I\rangle}\exp\left(-\frac{I}{\langle I\rangle}\right), \tag{1.1.18}$$

where $\langle I\rangle$ is the spatial average of the intensity. This so-called Rayleigh distribution arises because the local field amplitude ψ is the sum of many uncorrelated contributions from light scattered in different ways. Thus its real and imaginary parts are independent Gaussian random numbers of zero average, yielding Eq. (1.1.18) for the intensity $I = |\psi|^2$.

Speckle also occurs if light is transmitted through a disordered medium. Consider for instance the transmission of a laser beam through the disordered waveguide of Fig. 1-7 (top panel). The fraction of the light transmitted to mode m is given by $T_{mn} = |t_{mn}|^2$, where n labels the mode in which the light is injected. When the transmitted light is collected on a screen, the spatial intensity distribution corresponds to the distribution of T_{mn} over outgoing modes m. By collecting all the outgoing modes (as in Fig. 1-7, bottom panel) one measures the total transmitted intensity. It is a fraction $T_n = \sum_m T_{mn}$ of the incident intensity in mode n. This fraction fluctuates as a function of n and also for fixed n from one sample to another. For short waveguides in which the propagation of light is diffusive, T_{mn} has a Rayleigh distribution for moderate values, and the distri-

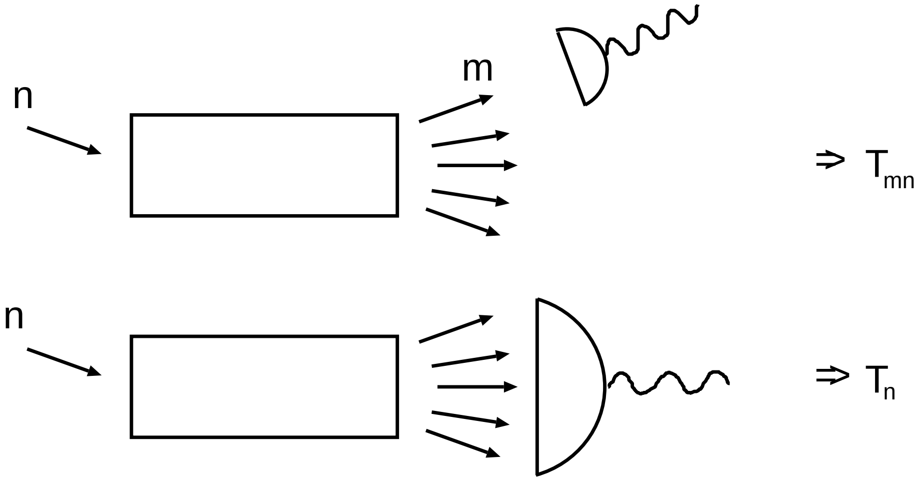

Figure 1-7. Schematic picture of a measurement of the optical transmittances T_{mn} and T_n. Only mode n is incident; the photodetector measures either the light transmitted in mode m (top diagram) or the light transmitted in all modes (bottom diagram).

bution of T_n is approximately Gaussian with a variance much smaller than the mean. Deviations are found in the tails of the distributions. This is due to the effects of (weak) localization, discussed in the next section.

1.2 Disordered waveguides

So far we discussed the scattering formalism and its application to electrical and optical systems in general. The theory was illustrated for a simple ballistic geometry, the quantum point contact. This thesis is about two types of systems with more complicated, chaotic scattering. First we discuss scattering caused by randomly placed impurities, which make the motion diffusive. In Sec. 1.3 chaotic ballistic systems are introduced. In such systems chaotic scattering arises not due to impurities, but due to a complicated geometry.

Disorder can turn propagating waves into localized states which fall off exponentially. This phenomenon, known as Anderson localization, is the result of interference between multiply scattered waves. The effect on electrical conduction is drastic: it turns a conductor into an insulator. Below we discuss three techniques used to describe disordered systems.

1.2.1 Semiclassical theory of weak localization

The conductance of a diffusive metal is given by Ohm's law, with a small negative correction. This correction is a precursor of Anderson localization, which goes under the name of *weak localization.* Whereas the theory of Anderson localization is complicated, weak localization can be understood in a simple

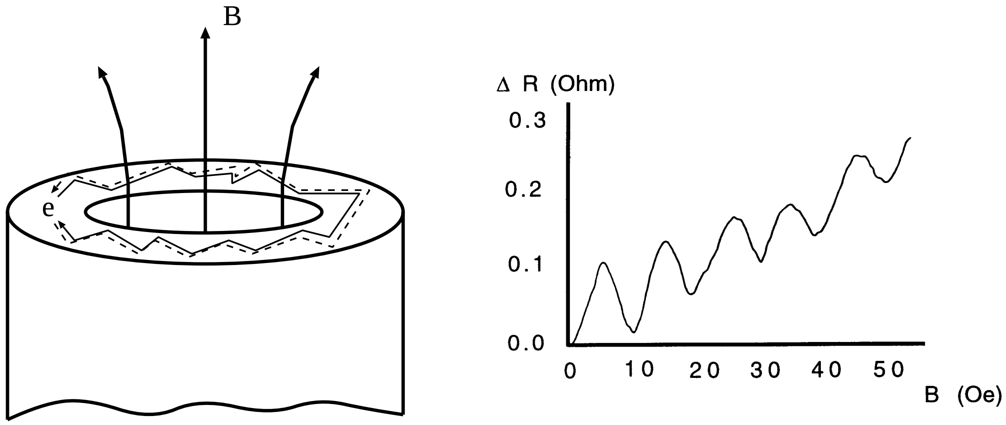

Figure 1-8. Observation of weak localization in a hollow metal cylinder. The resistance oscillates as a function of the flux due the Aharonov-Bohm effect. A cylinder is effectively an ensemble of rings, and therefore one measures the weak-localization correction to the conductivity. Weak localization is due to the interference of paths with their time-reversed partners, like the two shown. (From Ref. [10].)

semiclassical picture, based on the constructive interference of paths with their time-reversed partners. A magnetic field breaks the symmetry between these pairs of paths, and therefore destroys the weak-localization correction. Thus the experimental signature of weak localization is a negative magnetoresistance.

A similar phenomenon occurs in multiply-connected samples threaded by a magnetic flux. In that case the ensemble-averaged conductance shows oscillations on top of the classical value as a function of the flux, with period $h/2e$ (Fig. 1-8). This is the realization of the Aharonov-Bohm effect for electrons in a solid.

Weak localization is understood in a simple way by combining the notion of Feynman paths with random walks [11, 12]. In the Feynman picture, the probability $P(\mathbf{r},\mathbf{r}',t)$ of a particle to propagate from $\mathbf{r}$ to $\mathbf{r}'$ in a time t is the squared modulus of the sum of the amplitudes A_i of all paths i connecting the two points,

$$P(\mathbf{r},\mathbf{r}',t) = \left|\sum_i A_i\right|^2 = \sum_i |A_i|^2 + \sum_{i\neq j} A_i A_j^*. \tag{1.2.1}$$

The first term is the classical probability, which does not depend on the phases of A_i. The second term is due to quantum-mechanical interference. It oscillates as a function of the phases, which depend sensitively on the precise geometry of the paths. Therefore, the second term vanishes on averaging over all impurity configurations, but not completely. What remains is a particular set of terms when $\mathbf{r} = \mathbf{r}'$, consisting of all pairs of paths i and j which are time-reversed partners. These terms yield a contribution doubling the classical result. Thus, the probability of the particle to return to its starting point is enhanced by a factor of two.

It was shown by Chakravarty and Schmid [13] that the weak-localization correction $\Delta\sigma$ to the conductivity σ is given by

$$\frac{\Delta\sigma}{\sigma} = -\frac{2\hbar}{m}\int_0^\infty dt\, P(\mathbf{r},\mathbf{r},t)\mathrm{e}^{-t/\tau_\phi}, \tag{1.2.2}$$

(for dimension $d = 2$) where τ_ϕ is the time after which a particle looses its phase coherence, for instance by electron-electron scattering. In the absence of a magnetic field one can compute the return probability classically from the diffusion equation

$$\left[\frac{\partial}{\partial t} - D\frac{\partial^2}{\partial \mathbf{r}^2}\right] P(\mathbf{r},\mathbf{r}',t) = \delta(t)\delta(\mathbf{r}-\mathbf{r}'). \tag{1.2.3}$$

The influence of a magnetic field on $\Delta\sigma$ can be found by generalizing P to a “quasi-probability” $\tilde{P}$, where each classical return path is weighted with the complex factor

$$\exp\left[\frac{2ie}{\hbar c}\oint \mathbf{A}(\mathbf{r})\cdot d\mathbf{r}\right]. \tag{1.2.4}$$

In the diffusion equation (1.2.3), this phase factor is taken into account by making the substitution

$$\frac{\partial}{\partial \mathbf{r}} \to \frac{\partial}{\partial \mathbf{r}} - \frac{2ie}{\hbar c}\mathbf{A}(\mathbf{r}). \tag{1.2.5}$$

This accounts for the coupling of a magnetic field to the charge of the particle. The Zeeman coupling of a non-uniform field to the spin has a similar effect on weak localization, which we discuss next.

The adiabatic theorem of quantum mechanics implies that the final state of a spin moving slowly along a closed path in a non-uniform field $\mathbf{B}(\mathbf{r})$ is identical to the initial eigenstate — up to a phase factor. The Berry phase is a time-independent contribution to this phase. Like the Aharonov-Bohm phase, it depends on the geometry of the path [14]. For a spin-1/2 particle, the Berry phase

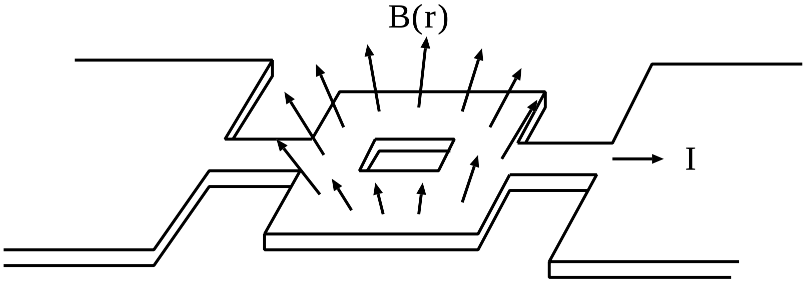

Figure 1-9. Schematic view of an experiment proposed to observe the Berry phase of a spin via the conductance of a metal ring. If the non-uniform magnetic field is strong enough, the particle picks up a path-independent geometric phase (or Berry phase) which is different for both arms, yielding interference oscillations in the average conductance.

equals half the solid angle traced out by **B** along the path. It was proposed to observe the Berry phase in the conductance of a solid ring with a non-uniform magnetic field applied in the sample (Fig. 1-9), such that paths along the left or right arm pick up different phases before interfering [15, 16]. A difference between the Berry and Aharonov-Bohm phases is that the former requires a sufficiently strong field in order to have slow, "adiabatic" dynamics, whereas the latter is present for arbitrary field strength.

1.2.2 Herbert-Jones-Thouless formula

In one-dimensional disordered systems all eigenstates are localized. The localization length $\xi(E)$ is defined as the spatial scale on which an eigenstate at energy E falls off exponentially. If E is not precisely equal to an eigenvalue, one can still define $\xi(E)$ for an open sample as the rate at which the transmission probability $T(E)$ falls off,

$$\lim_{L\to\infty} L^{-1} \ln T(E) = -2/\xi(E). \tag{1.2.6}$$

The Herbert-Jones-Thouless formula [17, 18] relates ξ to the density of states ρ, both evaluated at the energy E,

$$\frac{L}{\xi(E)} = \int dE' \rho(E') \ln|E - E'| + \text{constant}. \tag{1.2.7}$$

The additive constant is energy-independent on the scale of the level spacing.

Eq. (1.2.7) has been derived formally for different models in Refs. [17] and [18]. We repeat here the general argument of Thouless [18]. Consider a wave function at energy E, $\psi(x) \sim e^{ikx}$ with a complex wave number $k(E)$. The real part of k gives rise to oscillations in ψ. It is a basic theorem of quantum mechanics that the number of nodes, $\mathrm{Re}\, kL/\pi$, equals the integrated density of states $N(E) = \int^E dE' \rho(E')$. On the other hand, the imaginary part of k gives rise to the exponential decay of the wave function, and $1/\xi(E) = \mathrm{Im}\, k$. The Kramers-Kronig relation for the analytic function $k(E)$ reads

$$\frac{L}{\xi(E)} = P \int dE' \frac{N(E')}{E - E'} \tag{1.2.8}$$

Partial integration of the right hand side yields Eq. (1.2.7).

1.2.3 Dorokhov-Mello-Pereyra-Kumar equation

The Herbert-Jones-Thouless formula applies to single-mode waveguides. We now discuss a technique to study localization in multi-mode waveguides. Consider an N-channel waveguide of length L. The transmission eigenvalues $\tau_1, \ldots, \tau_N$ are numbers between 0 and 1, defined as the eigenvalues of the matrix

$tt^\dagger$. The Dorokhov-Mello-Pereyra-Kumar (DMPK) equation [19] is a Fokker-Planck equation for the evolution as a function of L of the probability density $P(x_1, x_2, \ldots, x_N, L)$, where x_k is defined by $\tau_k = \cosh^{-2} x_k$,

$$\begin{aligned} \ell \frac{\partial P}{\partial L} &= \frac{1}{2(\beta N + 2 - \beta)} \sum_{k=1}^{N} \frac{\partial}{\partial x_k} \left(\frac{\partial P}{\partial x_k} + \beta P \frac{\partial \Omega}{\partial x_k} \right), && (1.2.9) \\ \Omega &= -\sum_{i=1}^{N} \sum_{j=i+1}^{N} \ln|\sinh^2 x_j - \sinh^2 x_i| - \frac{1}{\beta} \sum_{i=1}^{N} \ln|\sinh 2x_i|. && (1.2.10) \end{aligned}$$

The integer β equals 1 (2) when time-reversal symmetry is present (broken). Eq. (1.2.9) is derived by computing the change in the scattering matrix S if the length of the wire is increased from L to $L + \delta L$, under the condition that the mean free path ℓ exceeds the wavelength λ. Another essential assumption in the derivation is the statistical equivalence of scattering from any channel to any other channel. This isotropy assumption is correct if the waveguide is much longer than wide, such that the time for transverse diffusion can be neglected.

Eq. (1.2.9) was solved exactly for $\beta = 2$ [20]. As an illustration of the solution we show the result for the eigenvalue density ρ, obtained by integrating the joint distribution P over all but one arguments,

$$\rho(x, L) = N \int_0^\infty dx_2 \cdots \int_0^\infty dx_N P(x, x_2, \ldots, x_N, L). \qquad (1.2.11)$$

It determines the average of a transport quantity $A = \sum_{k=1}^{N} a(\tau_k)$, where $a(\tau)$ is an arbitrary function of the transmission eigenvalues. Like the exact joint distribution, the density is a complicated expression in terms of Legendre functions [21]. The result is plotted in Fig. 1-10, for $N = 5$ and values of L/ℓ in the diffusive, localized, and crossover regime. In the diffusive regime $L \ll N\ell$, the density of x_k's is uniform,

$$\rho(x, L) = \frac{N\ell}{L} \theta(L/\ell - x). \qquad (1.2.12)$$

This result holds for $\beta = 1$ as well, and describes the regime of classical diffusion. For the average of the conductance $G = (2e^2/h) \sum_k \tau_k$ one recovers from Eq. (1.2.12) Ohm's law, $\langle G \rangle = (2e^2/h) N\ell/L$. In the transition towards the localized regime $L \sim N\ell$, the density starts to develop peaks, indicating a "crystallization" of the eigenvalues. In the localized regime $L \gg N\ell$, the x_k's are fixed at positions spaced by $L/N\ell$. All transmittances T, T_n, and T_{mn} are then dominated by the largest transmission eigenvalue $\tau_1 = \cosh^{-2} x_1$. Its distribution is log-normal, with

$$\mathrm{Var}\,(\ln \tau_1) = -2\langle \ln \tau_1 \rangle = \frac{4L}{\beta N \ell}. \qquad (1.2.13)$$

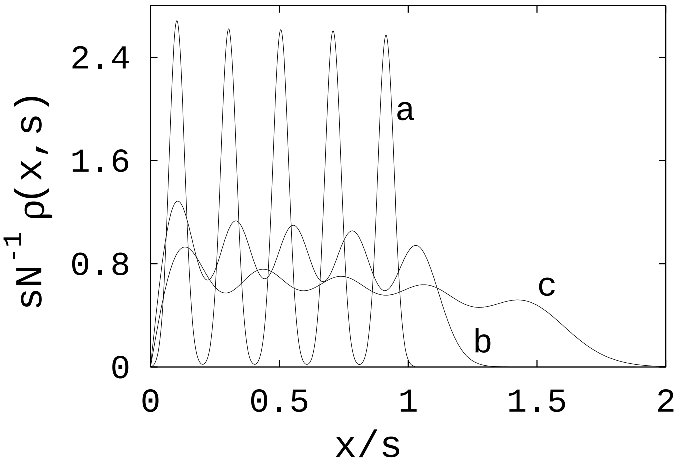

Figure 1-10. Exact eigenvalue density for $N = 5$ and $s = L/\ell = 100$, 10 and 2, respectively, for curves a, b, and c. The x_k's are uniformly distributed in the metallic regime (the wiggles in curve c are due to the relatively small channel number N), and form a "crystal" with lattice spacing $L/N\ell$ in the localized regime. (From Ref. [21].)

1.3 Chaotic cavities

In disordered systems the motion is chaotic as a result of multiple scattering by impurities. Disorder is not required for chaoticity, as is illustrated in Fig. 1-11. It shows a particle bouncing in a circular and a stadium billiard. These are examples of systems whose classical dynamics is integrable respectively non-integrable. Integrable systems are characterized by conserved quantities other than the energy. Non-integrable systems, in contrast, have only the energy as a conserved quantity. Chaotic systems form a subset of non-integrable systems. Two main characteristics of a chaotic system are the exponential separation of initially nearby trajectories and their ergodic exploration of phase space.

The integrability determines also in quantum mechanics whether an explicit solution for the dynamics can be written down or not. The quantum-mechanical description of a classically chaotic system is central in the field of "quantum chaos" [22, 23]. Exponential separation of trajectories is a purely classical concept, and can not be used as a signature of chaotic quantum mechanics. The obvious quantities to study for a quantum system are the energy levels and wavefunctions if the system is closed, or scattering states if the system is open. The basic theoretical tool that we use to describe these quantities is random-matrix theory (RMT) [24]. We introduce it separately for closed and open cavities.

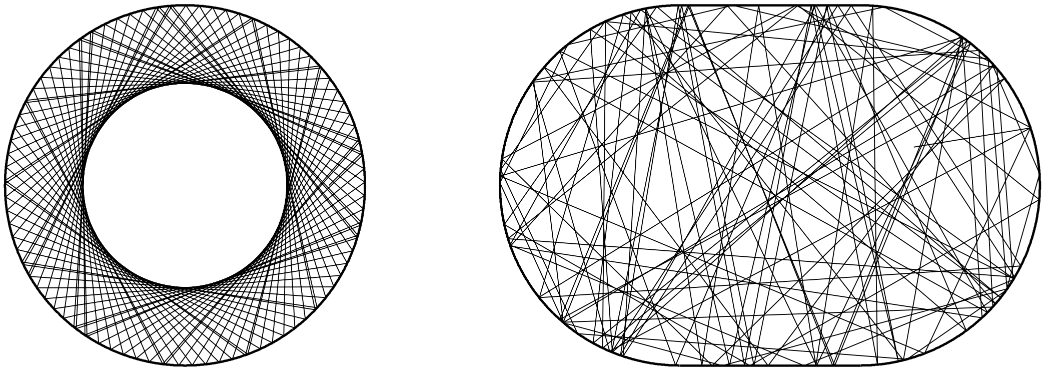

Figure 1-11. Billiards in the form of a circle (left) and a stadium (right). The lines inside the billiard are trajectories followed by a particle or light ray. Motion in the circle is integrable, while in the stadium it is non-integrable and chaotic.

1.3.1 Random-matrix theory of a closed cavity

In 1980 it was conjectured [25] that the spectrum of a classically chaotic system is statistically described by RMT. RMT was originally developed to describe resonances in nuclear scattering, with the underlying idea that a system of strongly interacting nucleons is so complex that a statistical description works well. The realization of chaos in mesoscopic systems has stimulated many applications of RMT to quantum transport problems [26,27].

The basic assumption of RMT is that the distribution of the Hamiltonian $\mathcal{H}$ is of the simple form

$$P(\mathcal{H}) \propto \exp\left[-\sum_n V(E_n)\right]. \tag{1.3.1}$$

The function $V(E)$ of the eigenvalues is usually taken quadratic, $V(E) = cE^2$. Eq. (1.3.1) then defines the Gaussian Ensemble. The parameter c determines the average spacing Δ between the levels. Depending on the absence or presence of time-reversal symmetry we speak of the Gaussian Unitary Ensemble (GUE) or the Gaussian Orthogonal Ensemble (GOE), respectively. In the first case $\mathcal{H}$ is a complex Hermitian matrix, in the second case a real symmetric matrix. There exists also a third symmetry class, the symplectic ensemble, describing systems with strong spin-orbit coupling in zero magnetic field.

Eq. (1.3.1) implies for the distribution of the eigenvalues

$$P(\{E_k\}) \propto \prod_{i>j} |E_i - E_j|^\beta \exp\left[-\sum_n V(E_n)\right]. \tag{1.3.2}$$

The term multiplying the exponent is the Jacobian due to the change of variables from matrix elements to eigenvalues. The Jacobian yields an effective repulsion

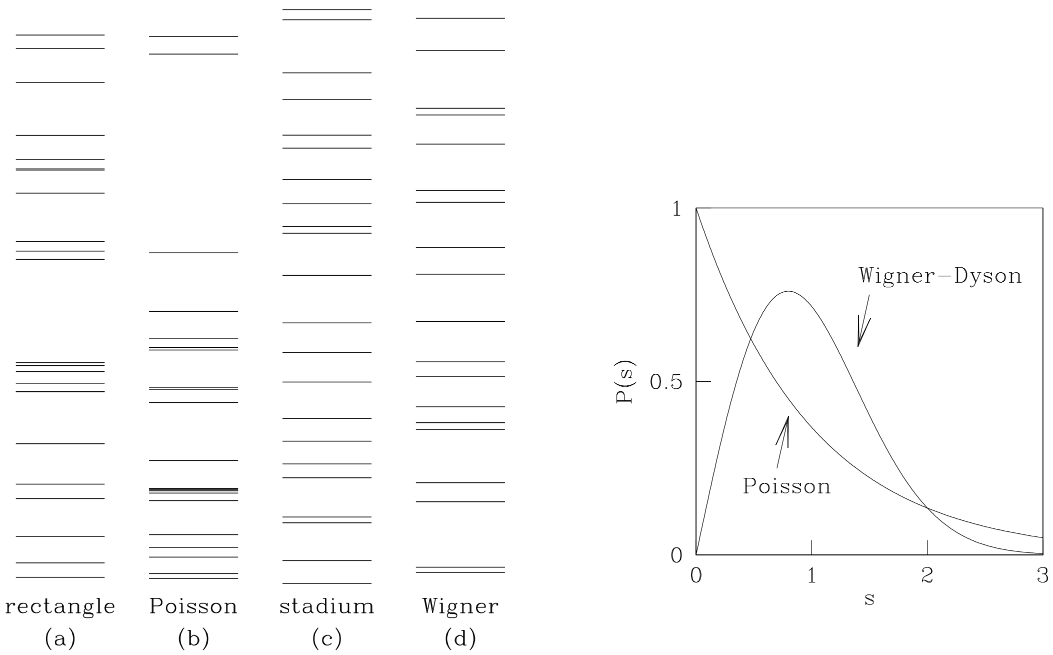

Figure 1-12. Highly excited levels of a rectangular and a stadium billiard, compared with a set of independently chosen random energy levels (Poisson) and a part of a spectrum of a random matrix choosen from the GOE (Wigner). All spectra are normalized to the same average level spacing. Spectra (a) and (b) have identical statistical properties, as well as (c) and (d). This is expressed e. g. in the distribution of spacings s between neighbouring levels (normalized to unit mean spacing). This is an exponential or Poisson distribution $P(s) = \mathrm{e}^{-s}$ for (a) and (b), and a Wigner-Dyson distribution $P(s) = \frac{\pi}{2} s \mathrm{e}^{-\frac{\pi}{4}s^2}$ for (c) and (d).

between neighbouring levels. Such level repulsion was found in numerical studies of quantum chaotic systems, in clear contrast with the uncorrelated spectra of integrable systems (see Fig. 1-12). This observation led to the conjecture that RMT applies to quantum chaotic systems [25]. Recently, the conjecture has found analytical support as well [28].

Signatures of chaotic motion can also be found in the eigenstates (Fig. 1-13). The statistical properties follow from the fact that Eq. (1.3.1) depends only on the eigenvalues and not on the eigenvectors. The matrix of eigenvectors is uniformly distributed on the orthogonal (unitary) group. For orthogonal matrices O with dimension $M \gg 1$, the matrix elements O_{ij} are independent Gaussian variables, with average zero, and variance $1/M$. Thus, wave-function intensities $V|\psi_j(\mathbf{r}_i)|^2 = M|U_{ij}|^2$ at different sites are uncorrelated, and have the distribution

$$P\left(x = V|\psi_j(\mathbf{r}_i)|^2\right) = \frac{1}{\sqrt{2\pi x}} \mathrm{e}^{-x/2} \qquad (1.3.3)$$

(V is the volume of the system). Eq. (1.3.3) is called the Porter-Thomas distribu-

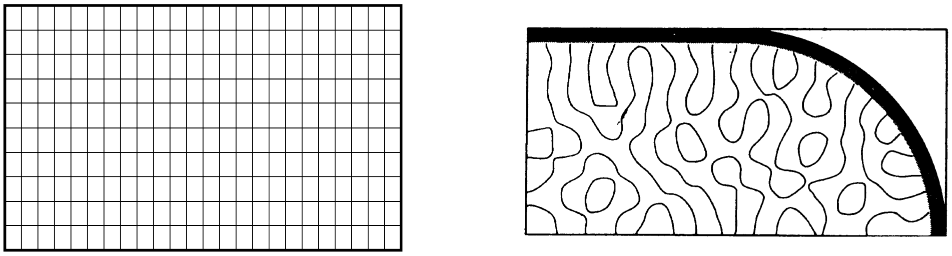

Figure 1-13. Highly excited eigenstate of a chaotic quartered stadium billiard and an integrable, rectangular billiard. Plotted are the nodal lines of the wavefunctions. (From Ref. [29].)

tion [30]. Similarly, for the unitary ensemble, the real and imaginary parts of U_{ij} are independent and Gaussian, yielding again vanishing spatial correlations and an exponential intensity distribution,

$$P(x) = \mathrm{e}^{-x}. \tag{1.3.4}$$

These wave-function distributions from RMT are consistent with a study by Berry [31] of chaotic systems in the semiclassical limit $\hbar \to 0$. He conjectured that a high-energy eigenfunction is effectively an infinite sum of plane waves with random phases and amplitudes, and with wavevectors isotropically distributed on a sphere. (The waves are taken real or complex, depending on the presence or absence of time-reversal symmetry.) Spatial correlations decay to zero algebraically at the scale of the wavelength. This conjecture has been verified theoretically [32] and experimentally [33].

So far we discussed systems where discrete symmetries are either present or fully broken. A symmetry can also be partially broken, for instance time-reversal symmetry by a weak magnetic field. A random matrix ensemble that interpolates between the GOE and the GUE is given by [34]

$$H = S + i\gamma A, \tag{1.3.5}$$

where S is real symmetric, A is real and antisymmetric, and both matrices have the same distribution Eq. (1.3.1). For $\gamma = 0$ one has the GOE; for $\gamma = 1$ the GUE. We will study the wavefunction statistics of this ensemble later on.

1.3.2 Random-matrix theory of an open cavity

In order to study transport through a cavity, one has to couple it to the outside world via leads. The Hamiltonian $\mathcal{H}_{\text{open}}$ of the open system (cavity plus leads) is

$$\mathcal{H}_{\text{open}} = \sum_{\alpha} |\alpha\rangle E \langle\alpha| + \sum_{ij} |i\rangle \mathcal{H}_{ij} \langle j| + \sum_{\alpha i} \left[|i\rangle W_{i\alpha} \langle\alpha| + |\alpha\rangle W^{*}_{i\alpha} \langle i| \right], \tag{1.3.6}$$

where $\mathcal{H}$ is the Hamiltonian of the (closed) cavity as studied in Sec. 1.3.1, and a rectangular matrix W describes the coupling of the M states $|i\rangle$ in the cavity to

N scattering states $|\alpha\rangle$ at energy E. The scattering matrix is expressed in terms of $\mathcal{H}$ and W as [35]

$$S(E) = 1 - 2\pi i W^\dagger \left(E - \mathcal{H} + i\pi W W^\dagger\right)^{-1} W. \tag{1.3.7}$$

The choice $W = \frac{\sqrt{M\Delta}}{\pi}\delta_{i\alpha}$ corresponds to ideal, non-reflective coupling. In that case the distribution of the scattering matrix is Dyson's Circular Ensemble [36],

$$P(S) = \text{constant}. \tag{1.3.8}$$

One can again distinguish between a unitary and orthogonal ensemble, consisting of unitary, respectively unitary symmetric matrices. As a simple application, one finds that, in the many-channel limit $N \gg 1$, the distribution of a transmittance $T_{mn} = |S_{mn}|^2$ is given by the Rayleigh distribution (1.1.18), with average $\langle T_{mn}\rangle = 1/N$.

In Eq. (1.3.8) we have lost all information about the energy dependence, which is still contained in Eq. (1.3.7). If we are interested in the thermopower for instance, we need the energy derivative of S, as shown in Sec. 1.1.2. Recently the distribution of

$$Q = -i\hbar S^{-1/2}\frac{\partial S}{\partial E}S^{-1/2} \tag{1.3.9}$$

has been computed for a chaotic cavity [37]. The matrix Q is called the Wigner-Smith time-delay matrix. It determines also the density of states of the open system at the Fermi level, $\rho = h^{-1}\mathrm{Tr}\, Q$. The reciprocal eigenvalues of Q are distributed according to the Laguerre ensemble, defined by Eq. (1.3.2) with $V(E) \propto E$.

1.4 This thesis

Non-perturbative calculation of the probability distribution of plane-wave transmission through a disordered waveguide

In Sec. 1.1.4 we mentioned that weak localization influences the distribution of the speckle intensity I transmitted through a disordered medium. The distributions of the transmittances T_{mn} and T_n were computed in Refs. [38] and [39], using perturbation theory in $\langle\sum_n T_n\rangle^{-1}$. These theories apply to the diffusive regime of large total transmittance $\sum_n T_n = \mathrm{Tr}\, tt^\dagger$. The results for $P(T_{mn})$ show a Rayleigh distribution with a non-exponential asymptote, in agreement with experiments in the diffusive regime.

In the mean time, experimentalists have entered the localized regime (Fig. 1-14). In Chapter 2, we present non-perturbative results for $P(T_{mn})$ and $P(T_n)$ for a waveguide, which were obtained from the solution of the DMPK-equation described in Sec. 1.2.3. The distribution shows the crossover from exponential respectively Gaussian statistics in the diffusive regime to lognormal statistics in the localized regime. Our calculation is for broken time-reversal symmetry. We also present perturbative results which indicate that the difference between broken and unbroken time-reversal symmetry is quantitative rather than qualitative.

A qualitatively different crossover occurs if the disordered region is replaced by a chaotic cavity. The transmittance distributions follow then from the circular ensemble (1.3.8) for the scattering matrix.

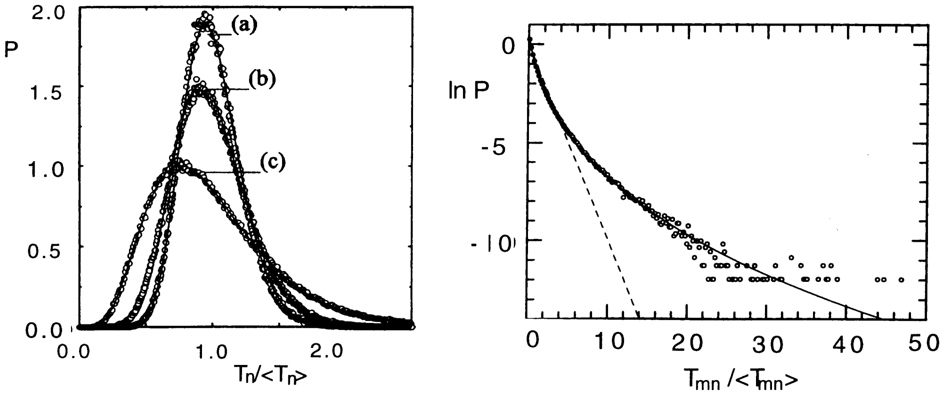

Figure 1-14. Left: Distribution of the transmittance T_n, measured for a copper tube filled with random pieces of dielectric material. Plotted are the results for three different lengths, corresponding to $N\ell/L = 15.0$ (a), 9.0 (b), and 2.25 (c). The distribution becomes markedly non-Gaussian as one approaches the localized regime. Right: similar for T_{mn} with $N\ell/L = 1.1$. The dashed curve is the Rayleigh distribution. [From Ref. [40].]

Fluctuating phase rigidity for a quantum chaotic system with partially broken time-reversal symmetry

In Chapter 3 we consider two anomalous properties of a closed chaotic system which were found in the crossover regime between unbroken and fully broken time-reversal symmetry [41, 42]. We show that both anomalies are due to the fluctuations of what we call the phase rigidity ρ of an eigenstate $\psi(\mathbf{r})$, defined by

$$\rho = \left| \int d\mathbf{r}\, \psi(\mathbf{r})^2 \right|^2 . \tag{1.4.1}$$

When going from the orthogonal to the unitary symmetry class following Eq. (1.3.5), the distribution of ρ crosses over from a delta peak at one to a delta peak at zero. The distribution is broadened in between.

The first property explained by the fluctuations in ρ is the existence of long-range spatial correlations in eigenstates. As we mentioned in Sec. (1.3.1), the eigenstate amplitudes at different points in a closed chaotic cavity are uncorrelated, except for correlations on the scale of the wavelength. Therefore, it came as a surprise that spatial correlations do exist in the crossover regime between the orthogonal and unitary ensemble [41]. These correlations are of order unity, and do not decay with distance (as long as there is no localization).

Although in electronic systems a direct measurement of wave-functions is difficult, several quantities can be used as an indirect probe. As an example we mention the conductance peak heights in the Coulomb-blockade regime. The conductance of a quantum dot closed by tunnel barriers shows sharp peaks as a function of the gate voltage, spaced by the electrostatic charging energy. For temperatures T larger than the level broadening the peak heights are given by

$$G_{\max} = \frac{2e^2}{h}\frac{1}{4\pi T}\frac{\Gamma_{\mathrm{L}}\Gamma_{\mathrm{R}}}{\Gamma_{\mathrm{L}}+\Gamma_{\mathrm{R}}}. \tag{1.4.2}$$

The contribution Γ_{L} (Γ_{R}) to the level width due to tunneling through the left (right) lead is proportional to the squared modulus of the resonant wave function at the point $\mathbf{r}_{\mathrm{L}}$ ($\mathbf{r}_{\mathrm{R}}$) where the lead is attached, $\Gamma_{\mathrm{L}} \propto |\psi(\mathbf{r}_{\mathrm{L}})|^2$. In optical experiments one can directly measure wave intensities. Several experiments were done for instance on microwave cavities (Fig. 1-15). Here breaking of time-reversal symmetry is not as easy as in electronic systems.

The second property that we consider in this chapter concerns the response of the energy levels E_n to an external perturbation of the system. In particular we study the "level velocities", defined as $v_n = dE_n/dX$. Here X is a parameter that governs the perturbation, which is for instance an applied field or the shape of the system. In the orthogonal and unitary ensemble, the level velocities have Gaussian distributions, but not in the crossover between the symmetry classes [42]. We show that this is due to the fluctuations of the phase rigidity ρ. We finally demonstrate that the responses of a single level to different, independent perturbations are correlated in the regime of partially broken time-reversal symmetry.

Figure 1-15. Experimentally obtained wavefunction. Plotted is a two-dimensional scan of the intensity in a microwave cavity shaped like a quarter stadium. (From Ref. [43].)

Quantum-statistical current correlations in multi-lead chaotic cavities

In Sec. 1.1.3 we discussed fluctuations in the current due to the discreteness of the charge, and the suppression of this shot noise due to correlated transmission events. In chapter 4 we will consider a conductor coupled to four reservoirs instead of two. The currents in such multi-terminal conductors do not only fluctuate, but are also mutually correlated. The shot noise power (1.1.15) is easily generalized to the power spectrum of the current correlations,

$$P_{ab}(\omega) = 2\int_{-\infty}^{\infty} dt\, e^{i\omega t}\overline{\Delta I_a(t)\Delta I_b(t_0+t)}, \tag{1.4.3}$$

where $\Delta I_k(t) = I_k(t) - \bar{I}_k$ is the fluctuation of the current through lead k. Eq. (1.4.3) can be related to the scattering matrix [2]. Recently the current correlators P_{ab} have been measured for an "electronic beam splitter", formed by four quantum points contacts and a thin barrier in a two-dimensional electron gas [44]; see Fig. 1-16.

We computed the average zero-frequency power $P_{ab}(0)$ for a chaotic quantum dot with open, many-channel leads, using the circular ensemble (1.3.8) for the scattering matrix. Like the two-terminal shot noise, the current correlations are of the order of the channel number, and are insensitive to dephasing. We also consider the situation where the leads are closed by tunnel barriers with transmission probability Γ. Finally, we compare the results with a classical resistor network, were the currents are correlated due to charge conservation.

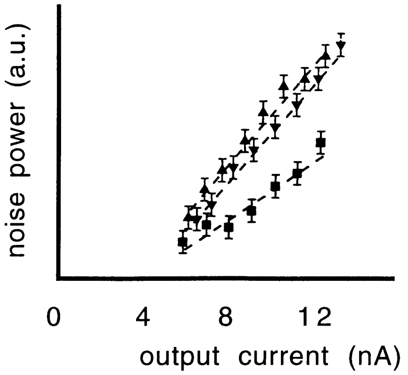

Figure 1-16. Left: Mesoscopic conductor with four contacts. A thin barrier in the middle serves as an electronic analogue of a half-silvered mirror. Right: noise power versus average current, both measured at the right-hand output contact. The transport noise is the part proportional to the current. Results are given for three experiments: either current is incident in the left or right input channel only (downward and upward triangles), or in both input channels (squares). In the last case the noise power is reduced due to Pauli repulsion. [From Ref. [44].]

Thermopower of single-channel disordered and chaotic conductors

In Sec. (1.1.2) we showed that the thermopower at low temperatures T is proportional to the logarithmic energy derivative at the Fermi level of the transmission probability $T(E) = \mathrm{Tr}\, tt^{\dagger}$. For few-channel quantum-mechanical scattering, the fluctuations in $T(E)$ can be of the order of its average. As an illustration we show in Fig. 1-17 typical plots of the transmission versus E for simulations of a one-dimensional disordered wire much longer than the mean free path, and a chaotic cavity coupled to single-channel leads. The transmittance of the wire shows well separated resonances (note the logarithmic scale) due to tunneling through localized states, with peak positions reflecting the Poisson statistics of the energy spectrum. In the cavity, the typical width of the resonances is of the order of the average spacing Δ, and the overlap leads to strong correlations in $T(E)$.

In Chapter 5 we compute the distribution of the thermopower S for these two types of systems. For the wire, we show that $P(S)$ in the zero-temperature limit is a Lorentzian with a disorder-independent width $4\pi^3 k_B^2 T/3e\Delta$. This follows from the Herbert-Jones-Thouless formula (1.2.7). Upon raising the temperature one finds a crossover to an exponential form $\propto \exp(-2|S|eT/\Delta)$. For the chaotic quantum dot we find a distribution with a cusp at $S = 0$ and a tail $\propto |S|^{-1-\beta} \ln|S|$ for large $|S|$ (with $\beta = 1, 2$ depending on the presence or absence of time-reversal symmetry). This result is obtained from the distribution of the Wigner-Smith time-delay matrix Eq. (1.3.9).

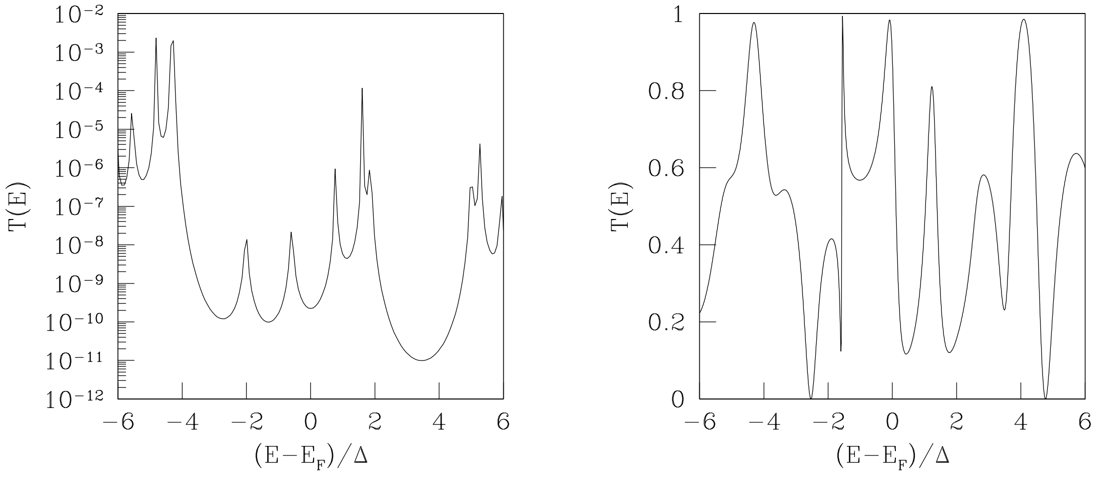

Figure 1-17. Transmission $T(E)$ versus energy E for a one-dimensional wire in the localized regime (left) and a chaotic cavity with single-mode point contacts (right). The thermopower is proportional to $d \ln T(E)/dE$.

Berry phase and adiabaticity of a spin diffusing in a non-uniform magnetic field

In Sec. 1.2.1 we discussed the Aharonov-Bohm oscillations in the conductance of a metal ring, and the proposed variation on this experiment based on the Berry phase of a spin. In order to observe the Berry phase, one needs a sufficiently large non-uniform magnetic field, such that the spin remains parallel to the field during its motion. To estimate the minimal necessary field strength, one should compare the spin-precession time $\tau_{\rm s} = \hbar/g\mu_{\rm B}B$ (g = Landé factor; $\mu_{\rm B}$ = Bohr magneton) with the typical timescale at which the field changes direction. For ballistic motion of the electron, this timescale is unambiguously $L_B/v_{\rm F}$, where L_B is the length scale at which the direction varies and $v_{\rm F}$ the Fermi velocity, and thus the criterion for adiabatic dynamics is

$$\tau_{\rm s} \ll L_B/v_{\rm F}. \tag{1.4.4}$$

If the electron motion is diffusive, it is not a priori clear which timescale of the motion is the relevant one. In the literature, two widely different criteria are presented, based on either the elastic scattering time τ or the diffusive transit time $\tau(L/\ell)^2$, where L is the system size and $\ell = v_{\rm F}\tau$ the mean free path.

Stern [16] proposed that

$$\tau_{\rm s} \ll \tau L_B/L \tag{1.4.5}$$

is necessary for adiabatic dynamics. For typical parameter values one finds a required field strength which is out of reach experimentally. Moreover, in the regime defined by Eq. (1.4.5), the picture of diffusing electrons breaks down due to quantization of the orbital motion. For these reasons we call Eq. (1.4.5) the “pessimistic criterion”.

Loss, Schoeller, and Goldbart [45] argued that a much weaker magnetic field is sufficient for adiabatic motion. Their calculation gives

$$\tau_{\rm s} \ll \tau L_B L/\ell^2. \tag{1.4.6}$$

The right hand side differs from Eq. (1.4.5) by a large factor $(L/\ell)^2$, and magnetic fields satisfying Eq. (1.4.6) for typical parameters are in the experimentally accessible regime. We call Eq. (1.4.6) the “optimistic” criterion.

In Chapter 6 we resolve this controversy by computing the spin polarization of transmitted particles from the Boltzmann equation. In a similar way we solve the Boltzmann equation for the “quasi-probability” of return, to obtain the weak-localization correction in the presence of a non-uniform field. Both results confirm the pessimistic criterion Eq. (1.4.5), which severely complicates the observation of the Berry phase in a disordered system.

References

[1] Y. Imry, *Introduction to Mesoscopic Physics* (Oxford University, Oxford, 1997).

[2] M. Büttiker, Phys. Rev. B **46**, 12485 (1992); Phys. Rev. Lett. **65**, 2901 (1990); *ibid.* **68**, 843 (1992).

[3] P. N. Butcher, J. Phys. C **2**, 4869 (1990).

[4] C. W. J. Beenakker and H. van Houten, Solid State Phys. **44**, 1 (1991).

[5] B. J. van Wees, H. van Houten, C. W. J. Beenakker, J. G. Williamson, L. P. Kouwenhoven, D. van der Marel, and C. T. Foxon, Phys. Rev. Lett. **60**, 848 (1988).

[6] L. W. Molenkamp, H. van Houten, C. W. J. Beenakker, R. Eppenga, and C. T. Foxon, Phys. Rev. Lett. **65**, 1052 (1990).

[7] S. F. Godijn et al., unpublished.

[8] For recent reviews, see M. J. M. de Jong and C. W. J. Beenakker, in *Mesoscopic Electron Transport*, eds. L. L. Sohn, L. P. Kouwenhoven, and G. Schön, NATO ASI Series Vol. 345 (Kluwer, Dordrecht, 1997); M. Reznikov, R. de Picciotto, M. Heiblum, D. C. Glattli, A. Kumar, and L. Saminadayar, Superlattices and Microstructures **23**, 901 (1998).

[9] M. Reznikov, M. Heiblum, H. Shtrikman, and D. Mahalu, Phys. Rev. Lett. **75**, 3340 (1995).

[10] D. Yu. Sharvin and Yu. V. Sharvin, Pis'ma Zh. Eksp. Teor. Fiz. **34**, 285 (1981) [JETP Lett. **34**, 272 (1981)].

[11] G. Bergmann, Phys. Rep. **107**, 1 (1984); Phys. Rev. B **28**, 2914 (1983).

[12] D. E. Khmel'nitskiĭ, Physica B **126**, 235 (1984).

[13] S. Chakravarty and A. Schmid, Phys. Rep. **140**, 193 (1986).

[14] M. V. Berry, Proc. R. Soc. London A **392**, 45 (1984).

[15] D. Loss, P. Goldbart, and A. V. Balatsky, Phys. Rev. Lett. **65**, 1655 (1990).

[16] A. Stern, Phys. Rev. Lett. **68**, 1022 (1992).

[17] D. C. Herbert and R. Jones, J. Phys. C **4**, 1145 (1971).

[18] D. J. Thouless, J. Phys. C **5**, 77 (1972).

[19] O. N. Dorokhov, Pis'ma Zh. Eksp. Teor. Fiz. **36**, 259 (1982) [JETP Lett. **36**, 318 (1982)]; P. A. Mello, P. Pereyra, and N. Kumar, Ann. Phys. (N.Y.) **181**, 290 (1988).

[20] C. W. J. Beenakker and B. Rejaei, Phys. Rev. Lett. **71**, 3689 (1993); Phys. Rev. B **49**, 7499 (1994).

[21] K. M. Frahm, Phys. Rev. Lett. **74**, 4706 (1995).

[22] F. Haake, *Quantum signatures of chaos* (Springer, Berlin, 1991).

[23] M. C. Gutzwiller, *Chaos in classical and quantum mechanics* (Springer, New York, 1990).

[24] M. L. Mehta, *Random Matrices* (Academic, New York, 1991).

[25] O. Bohigas, M. J. Giannoni, and C. Schmitt, Phys. Rev. Lett. **52**, 1 (1984).

[26] C. W. J. Beenakker, Rev. Mod. Phys. **69**, 731 (1997).

[27] T. Guhr, A. Müller-Groeling, and H. A. Weidenmüller, cond-mat/9707301 (Phys. Rep. , to be published).

[28] A. V. Andreev, O. Agam, B. D. Simons, and B. L. Altshuler, Phys. Rev. Lett. **76**, 3947 (1996).

[29] S. W. McDonald and A. N. Kaufman, Phys. Rev. Lett. **42**, 1189 (1979).

[30] C. E. Porter, *Statistical theory of spectra: Fluctuations* (Academic, New York, 1965).

[31] M. V. Berry, Proc. R. Soc. Lond. A **10**, 2083 (1977).

[32] V. N. Prigodin, Phys. Rev. Lett. **74**, 1566 (1995).

[33] V. N. Prigodin, N. Taniguchi, A. Kudrolli, V. Kidambi, and S. Sridhar, Phys. Rev. Lett. **75**, 2392 (1995).

[34] A. Pandey and M. L. Mehta, Commun. Math. Phys. **87**, 449 (1983).

[35] J. J. M. Verbaarschot, H. A. Weidenmuller, and M. R. Zirnbauer, Phys. Rep. **129**, 367 (1985).

[36] F. J. Dyson, J. Math. Phys. **3**, 140 (1962); *ibid.* **3**, 157 (1962).

[37] P. W. Brouwer, K. M. Frahm, and C. W. J. Beenakker, Phys. Rev. Lett. **78**, 4737 (1997).

[38] Th. M. Nieuwenhuizen and M. C. W. van Rossum, Phys. Rev. Lett. **74**, 2674 (1995).

[39] E. Kogan and M. Kaveh, Phys. Rev. B **52**, 3813 (1995).

[40] M. Stoytchev and A. Z. Genack, Phys. Rev. Lett. **79**, 309 (1997); cond-mat/9805223.

[41] V. Fal'ko and K. B. Efetov, Phys. Rev. Lett. **77**, 912 (1996).

[42] N. Taniguchi, A. Hashimoto, B. D. Simons, and B. L. Altshuler, Europhys. Lett. **27**, 335 (1994).

[43] J. Stein, H.-J. Stöckmann, and U. Stoffregen, Phys. Rev. Lett. **75**, 53 (1995).

[44] R. C. Liu, B. Odom, Y. Yamamoto, and S. Tarucha, Nature **391**, 263 (1998); see also M. Büttiker, Physics World **11**, 30 (1998).

[45] D. Loss, H. Schoeller, and P. M. Goldbart, Phys. Rev. B **48**, 15218 (1993).

2 Nonperturbative calculation of the probability distribution of plane-wave transmission through a disordered waveguide

The statistical properties of transmission through a disordered waveguide have been extensively studied since 1959, when Gertsenshtein and Vasil'ev [1] computed the probability distribution $P(T)$ of the transmittance T of a single-mode waveguide. It turned out to be remarkably difficult to extend this result to the N-mode case. Instead of a single transmission amplitude t and transmittance $T = |t|^2$, one then has an $N \times N$ transmission matrix t_{mn} and three types of transmittances

$$T_{mn} = |t_{mn}|^2, \; T_n = \sum_{m=1}^{N} |t_{mn}|^2, \; T = \sum_{n,m=1}^{N} |t_{mn}|^2. \tag{2.1}$$

All three transmittances have different probability distributions, which can be measured in different types of experiments: If the waveguide is illuminated through a diffusor, the ratio of transmitted and incident power equals T/N, because the incident power is equally distributed among all N modes. (For electrons, T is the conductance in units of $2e^2/h$.) If the incident power is entirely in mode n, then the ratio of transmitted and incident power equals T_n. For $N \gg 1$ this corresponds to illumination by a plane wave. Finally, T_{mn} measures the speckle pattern (the fraction of the power incident in mode n which is transmitted into mode m).

The complexity of the multi-mode case is due to the strong coupling of the modes by multiple scattering. While in the single-mode case the localization length ξ is of the same order of magnitude as the mean free path l, the mode coupling increases ξ by a factor of N. If $N \gg 1$, a waveguide of length L can be in two distinct regimes: the diffusive regime $l \ll L \ll Nl$ and the localized regime $L \gg Nl$. The average of each of the three transmittances decays linearly with L in the diffusive regime and exponentially in the localized regime. In an important development, Nieuwenhuizen and Van Rossum [2] (and more recently Kogan and Kaveh [3]) succeeded in computing the probability distributions $P(T_{mn})$ and $P(T_n)$ for plane-wave illumination in the diffusive regime. The former is exponential (Rayleigh's law) with non-exponential tails, while the latter is Gaussian with non-Gaussian tails. The existence of such anomalous tails has been observed in optical experiments [4, 5] and in numerical simulations [6]. From the simulations, one expects a crossover to a lognormal distribution on entering the localized regime. Since the theory of Refs. [2, 3] is based on a perturbation expansion in the small parameter L/Nl, it cannot describe this crossover which occurs when $L/Nl \simeq 1$.

It is the purpose of the present paper to provide a non-perturbative calculation of $P(T_{mn})$ and $P(T_n)$, which is valid all the way from the diffusive into the localized regime, and which shows how the Rayleigh and Gaussian distributions of T_{mn} and T_n evolve into the same lognormal distribution as L increases beyond the localization length $\xi \simeq Nl$. We expect that $P(T)$ also evolves from a Gaussian to a lognormal distribution, but our calculation applies only to the plane-wave transmittances T_{mn} and T_n, and not to the transmittance T for diffuse illumination. For technical reasons, we need to assume that time-reversal symmetry is broken by some magneto-optical effect. Similar results are expected in the presence of time-reversal symmetry, but then a non-perturbative calculation becomes much more involved. We make essential use of the quasi-one-dimensionality of the waveguide (length L much greater than width W) and assume weak disorder (mean free path l much greater than wavelength λ). The localization which occurs in unbounded media when $l \lesssim \lambda$ requires a very different non-perturbative approach [7].

A related problem of experimental interest is the transmittance of a cavity coupled to two N-mode waveguides without disorder. If the cavity has an irregular shape, it has a complicated "chaotic" spectrum of eigenmodes. At the end of the paper we compute $P(T_{mn})$ and $P(T_n)$ for such a chaotic cavity and contrast the results with the disordered waveguide, which we consider first.

Our calculation applies results from random-matrix theory for the statistics of the transmission matrix. This matrix $t = u\sqrt{\tau}v$ is the product of two unitary matrices u and v, and a matrix $\tau = \mathrm{diag}(\tau_1, \tau_2, \ldots \tau_N)$ containing the transmission eigenvalues. It describes the transmission of electrons or electromagnetic radiation, to the extent that the effects of electron-electron interaction or polarization can be disregarded. The two plane-wave transmittances which we consider are

$$T_{mn} = \sum_{k,l} u_{mk} u^*_{ml} v_{kn} v^*_{ln} \sqrt{\tau_k \tau_l}, \quad T_n = \sum_k |v_{kn}|^2 \tau_k. \tag{2.2}$$

We seek the probability distributions

$$P(\mathcal{T}_{mn}) = \langle \delta(\mathcal{T}_{mn} - N^2 T_{mn}) \rangle, \tag{2.3}$$

$$P(\mathcal{T}_n) = \langle \delta(\mathcal{T}_n - N T_n) \rangle, \tag{2.4}$$

of the normalized transmittances $\mathcal{T}_{mn} = N^2 T_{mn}$ and $\mathcal{T}_n = N T_n$. (These conventions differ by a factor l/L with Refs. [2, 3].) The brackets $\langle \cdots \rangle$ denote an average over the disorder. In the quasi-one-dimensional limit of a waveguide which is much longer than wide, the matrices u and v are uniformly distributed in the unitary group [8]. The joint probability distribution of the transmission eigenvalues evolves with increasing L according to the Dorokhov-Mello-Pereyra-Kumar (DMPK) equation [9]. The average can be performed in two steps, first over u and v, and then over the transmission eigenvalues τ_k.

The first step was done by Kogan and Kaveh [3]. The result is an expression for the Laplace transform of $P(\mathcal{T}_n)$,

$$F(s) = \int_0^\infty d\mathcal{T}_n \, \exp\left(-s\mathcal{T}_n\right) P(\mathcal{T}_n), \tag{2.5}$$

which in the thick-waveguide limit ($N \to \infty, L/l \to \infty$, fixed Nl/L) is exactly given by

$$F(s) = \left\langle \textstyle\prod_k (1 + s\tau_k)^{-1} \right\rangle . \tag{2.6}$$

The same function $F(s)$ also determines $P(\mathcal{T}_{mn})$, which in the same limit is related to $P(\mathcal{T}_n)$ by [3]

$$P(\mathcal{T}_{mn}) = \int_0^\infty d\mathcal{T}_n \, \mathcal{T}_n^{-1} \exp\left(-\mathcal{T}_{mn}/\mathcal{T}_n\right) P(\mathcal{T}_n). \tag{2.7}$$

The next step, which is the most difficult one, is to average over the transmission eigenvalues in Eq. (2.6). The result depends on whether time-reversal symmetry is present or not (indicated by $\beta = 1$ or 2, respectively). In Refs. [2, 3], $\ln F$ was evaluated to leading order in L/Nl, under the assumption that the waveguide length L is much less than the localization length $\xi \simeq Nl$. Here we relax this assumption.

We consider the case of broken time-reversal symmetry ($\beta = 2$). Then the probability distribution of the τ_k's is known exactly, in the form of a determinant of Legendre functions P_ν [10]. Still, to compute expectation values with this distribution is in general a formidable problem. It is a lucky coincidence that the average (2.6) which we need can be evaluated exactly. This was shown by Rejaei [11], using a field-theoretic approach which leads to a supersymmetric non-linear σ model [12]. It was recently proven [13] that this supersymmetric theory is equivalent to the DMPK-equation used in Ref. [10]. From Rejaei's general expressions we find

$$F(s) = 1 - 2s \sum_{p=0}^{\infty} \int_0^\infty dk \, f_p(k) \tanh(\tfrac{1}{2}\pi k) P_{\frac{1}{2}(ik-1)}(1+2s), \tag{2.8}$$

$$f_p(k) = \frac{(2p+1)k}{(2p+1)^2 + k^2} \exp\left(-\frac{L\left[(2p+1)^2 + k^2\right]}{4Nl}\right). \tag{2.9}$$

Inversion of the Laplace transform (2.5) yields $P(\mathcal{T}_n)$,

$$P(\mathcal{T}_n) = \sum_{p=0}^{\infty} \int_0^\infty dk \, f_p(k) \sinh(\tfrac{1}{2}\pi k) \frac{\partial}{\partial \mathcal{T}_n} \frac{2K_{\frac{1}{2}ik}(\frac{1}{2}\mathcal{T}_n)}{(\pi^3 \mathcal{T}_n \mathrm{e}^{\mathcal{T}_n})^{1/2}}, \tag{2.10}$$

where K_ν is the Macdonald function. One further integration gives $P(\mathcal{T}_{mn})$, in view of Eq. (2.7). Results are plotted in Fig. 2-1. The large $\mathcal{T}_n$ and $\mathcal{T}_{mn}$ tails are

$$P(\mathcal{T}_{mn}) \propto \mathcal{T}_{mn}^{-3/4} \mathrm{e}^{-2\sqrt{\mathcal{T}_{mn}}}, \qquad \mathcal{T}_{mn} \gg 1, (Nl/L)^2, \tag{2.11}$$

$$P(\mathcal{T}_n) \propto \mathcal{T}_n^{-1} \mathrm{e}^{-\mathcal{T}_n}, \qquad \mathcal{T}_n \gg 1, Nl/L. \tag{2.12}$$

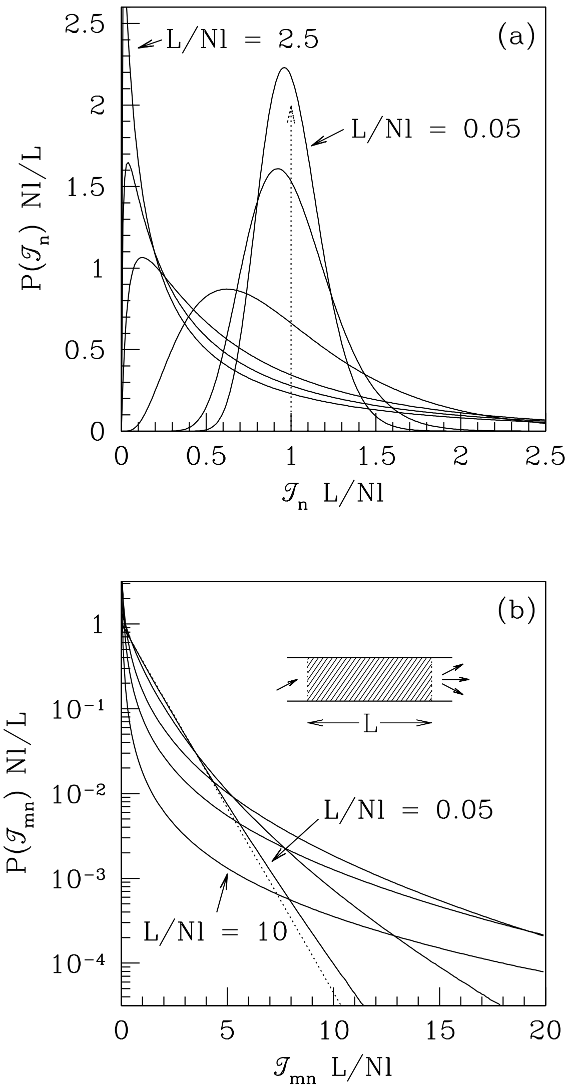

Figure 2-1. Distributions of (a) $\mathcal{T}_n \equiv NT_n$ for L/Nl = 0.05, 0.1, 0.5, 1.5, 2.0, and 2.5, and (b) $\mathcal{T}_{mn} \equiv N^2 T_{mn}$ for L/Nl = 0.05, 0.5, 2.5, 5, and 10. Computed from the exact $\beta = 2$ expressions (2.7) and (2.10). The dotted curves are the limits $L/Nl \to 0$ of an infinitely narrow Gaussian in (a) and an exponential distribution in (b) (note the logarithmic scale). The inset in (b) shows the waveguide geometry considered (disordered region is shaded).

It is worth noting that Fyodorov and Mirlin [14] found the same tail as Eq. (2.11) for the distribution of the local density of electronic states in a closed disordered wire. It is not clear to us whether this coincidence is accidental.

The diffusive and localized limits can be computed from Eq. (2.6) by using the known asymptotic form of the distribution of the τ_k's. In contrast to the full

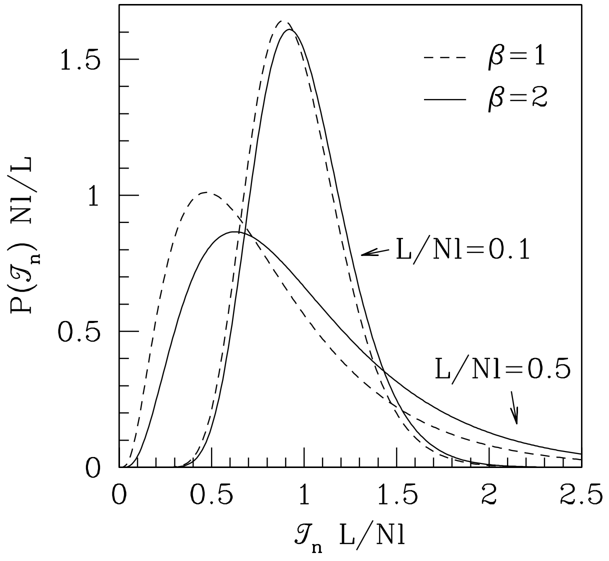

Figure 2-2. Distribution of $\mathcal{T}_n$ calculated from the perturbation expansion (2.13), (2.14), and (2.15), for $\beta = 1, 2$ and $L/Nl = 0.1, 0.5$.

result (2.10), which holds for $\beta = 2$ only, the following asymptotic expressions hold for any β. In the diffusive regime, for $L \ll Nl$, we may expand $\ln F$ in cumulants of the linear statistic $A = \sum_k \ln(1 + s\tau_k)$:

$$\ln F(s) \equiv \ln \left\langle \mathrm{e}^{-A} \right\rangle = -\langle A \rangle + \tfrac{1}{2}\mathrm{Var}\, A + \mathcal{O}(L/Nl). \qquad (2.13)$$

The mean and variance of A can be computed from the general formulas of Refs. [10, 15, 16]:

$$\langle A \rangle = \frac{Nl}{L}\,\mathrm{asinh}^2\sqrt{s} + \frac{2-\beta}{4\beta}\ln\left[\frac{\mathrm{asinh}^2\sqrt{s}}{s(1+s)}\right], \qquad (2.14)$$

$$\mathrm{Var}\, A = -\frac{1}{\beta}\left[\ln(1+s) + 6\ln\left(\frac{\mathrm{asinh}\sqrt{s}}{\sqrt{s}}\right)\right], \qquad (2.15)$$

valid up to corrections of order L/Nl. To leading order in L/Nl one has the β-independent result of Refs. [2, 3], yielding Gaussian and Rayleigh statistics for $L/Nl \to 0$. The β-dependent terms in Eqs. (2.14) and (2.15) are the first corrections due to localization effects. In Fig. 2-2 we plot $P(\mathcal{T}_n)$ resulting from Eqs. (2.13), (2.14), and (2.15). The β-independent result of Refs. [2,3] (not shown) is very close to the $\beta = 2$ curve. This figure indicates that the β-dependence is essentially quantitative rather than qualitative.

In the opposite, localized regime ($L \gg Nl$), only a single transmission eigenvalue contributes significantly to Eq. (2.6). This largest eigenvalue τ has the

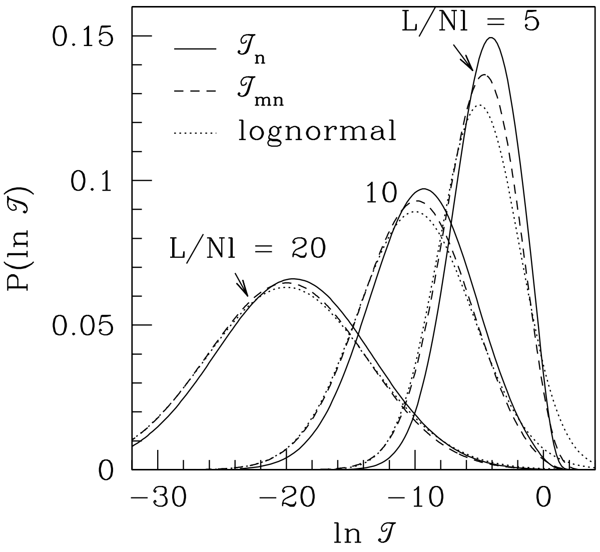

Figure 2-3. Distributions of $\mathcal{T}_n$ and $\mathcal{T}_{mn}$ for $\beta = 2$ and $L/Nl = 5, 10, 20$, computed from Eqs. (2.7) and (2.10). The dotted curve is the lognormal distribution (2.16) which is approached as $L/Nl \to \infty$.

lognormal distribution [17]

$$P(\ln\tau) = \left(\tfrac{\beta Nl}{8\pi L}\right)^{1/2} \exp\left[-\tfrac{\beta Nl}{8L}\left(\tfrac{2L}{\beta Nl} + \ln\tau\right)^2\right]. \tag{2.16}$$

It follows that $\ln\mathcal{T}_{mn}$ and $\ln\mathcal{T}_n$ are also distributed according to Eq. (2.16) in the localized regime. The approach to a common lognormal distribution as L/Nl increases is illustrated in Fig. 2-3, using the exact $\beta = 2$ result of Eq. (2.10).

We contrast these results for a disordered waveguide with those for a chaotic cavity, attached to two N-mode leads without disorder. Following Ref. [18] we assume that the $2N \times 2N$ scattering matrix of the cavity is distributed uniformly in the unitary group if $\beta = 2$ or in the subset of unitary and symmetric matrices if $\beta = 1$. Then $P(T_{mn})$ and $P(T_n)$ follow from general formulas [19] for the distribution of matrix elements in these socalled "circular" ensembles. For $\beta = 2$ the result is

$$P(T_{mn}) = (2N-1)\,(1-T_{mn})^{2N-2}\,, \tag{2.17}$$

$$P(T_n) = \tfrac{1}{2}N\binom{2N}{N}\,[T_n(1-T_n)]^{N-1}\,. \tag{2.18}$$

For $\beta = 1$ Eq. (2.17) should be multiplied by $\frac{1}{2}F(N-\frac{1}{2}, 1; 2N-1; 1-T_{mn})$ and Eq. (2.18) by $\frac{1}{2}F(N-\frac{1}{2}, 1; N; 1-T_n)$, where F is the hypergeometric function. These

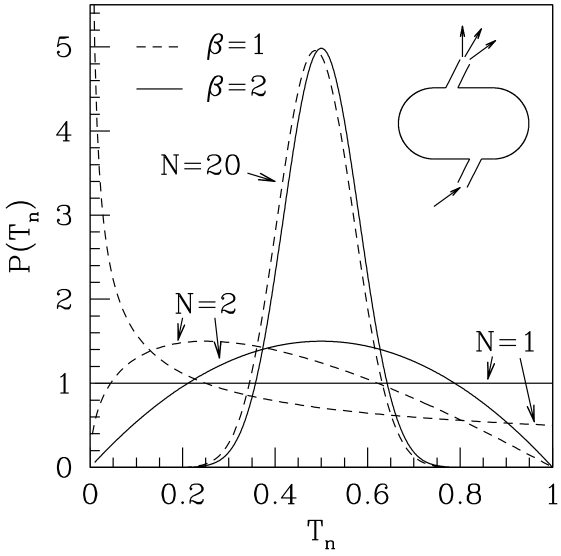

Figure 2-4. Distribution of T_n for a chaotic cavity attached to two N-mode leads (inset). The curves are computed from Eq. (2.18), for β = 1, 2 and N = 1, 2, 20.

are exact results for any N. If $N \to \infty$, $P(T_{mn})$ is an exponential distribution with mean $1/2N$, and $P(T_n)$ is a Gaussian with mean $1/2$ and variance $1/8N$. This is similar to the disordered waveguide, with N playing the role of Nl/L. As shown in Fig. 2-4, the distributions for N of order unity are quite different from those in a disordered waveguide with Nl/L of order unity. For $N = 1$ the distinction between T_{mn}, T_n, and T disappears and we recover the results of Ref. [18].

In conclusion, we have presented a non-perturbative calculation of the distributions of the plane-wave transmittances T_{mn} and T_n through a disordered waveguide without time-reversal symmetry, which shows how the distributions cross over from Rayleigh and Gaussian statistics in the diffusive regime, to a common lognormal distribution in the localized regime. Qualitatively different distributions are obtained if the disordered region is replaced by a chaotic cavity. Existing experiments have been mainly in the regime $L \ll Nl$ where the perturbation theory of Refs. [2, 3] applies. If the absorption of light in the waveguide can be reduced sufficiently, it should be possible to enter the regime $L \simeq Nl$ where perturbation theory breaks down and the crossover to lognormal statistics is expected.

References

[1] M. E. Gertsenshtein and V. B. Vasil'ev, Teor. Veroyatn. Primen. **4**, 424 (1959); **5**, 3(E) (1960) [Theor. Probab. Appl. **4**, 391 (1959); **5**, 340(E) (1960)].

[2] Th. M. Nieuwenhuizen and M. C. W. van Rossum, Phys. Rev. Lett. **74**, 2674 (1995).

[3] E. Kogan and M. Kaveh, Phys. Rev. B **52**, 3813 (1995).

[4] A. Z. Genack and N. Garcia, Europhys. Lett. **21**, 753 (1993).

[5] J. F. de Boer, M. C. W. van Rossum, M. P. van Albada, Th. M. Nieuwenhuizen, and A. Lagendijk, Phys. Rev. Lett. **73**, 2567 (1994).

[6] I. Edrei, M. Kaveh, and B. Shapiro, Phys. Rev. Lett. **62**, 2120 (1989).

[7] B. L. Al'tshuler, V. E. Kravtsov, and I. V. Lerner, in *Mesoscopic Phenomena in Solids*, edited by B. L. Al'tshuler, P. A. Lee, and R. A. Webb (North-Holland, Amsterdam, 1991); B. A. Muzykantskiĭ and D. E. Khmel'nitskiĭ, Phys. Rev. B **51**, 5480 (1995); V. I. Fal'ko and K. B. Efetov, Phys. Rev. B **52**, 17413 (1995); preprint (cond-mat/9503096); A. D. Mirlin, JETP Lett. **62**, 603 (1995); Phys. Rev. B **53**, 1186 (1996).

[8] P. A. Mello, E. Akkermans, and B. Shapiro, Phys. Rev. Lett. **61**, 459 (1988).

[9] O. N. Dorokhov, Pis'ma Zh. Eksp. Teor. Fiz. **36**, 259 (1982) [JETP Lett. **36**, 318 (1982)]; P. A. Mello, P. Pereyra, and N. Kumar, Ann. Phys. (N.Y.) **181**, 290 (1988).

[10] C. W. J. Beenakker and B. Rejaei, Phys. Rev. Lett. **71**, 3689 (1993); Phys. Rev. B **49**, 7499 (1994).

[11] B. Rejaei, Phys. Rev. B **53**, R13235 (1996).

[12] K. B. Efetov, Adv. Phys. **32**, 53 (1983).

[13] P. W. Brouwer and K. Frahm, Phys. Rev. B **53**, 1490 (1996).

[14] Y. V. Fyodorov and A. D. Mirlin, Int. J. Mod. Phys. B **27**, 3795 (1994).

[15] C. W. J. Beenakker, Phys. Rev. B **49**, 2205 (1994).

[16] J. T. Chalker and A. M. S. Macêdo, Phys. Rev. Lett. **71**, 3693 (1993); Phys. Rev. B **49**, 4695 (1994).

[17] A. D. Stone, P. A. Mello, K. A. Muttalib, and J.-L. Pichard, in *Mesoscopic Phenomena in Solids*, edited by B. L. Al'tshuler, P. A. Lee, and R. A. Webb (North-Holland, Amsterdam, 1991).

[18] H. U. Baranger and P. A. Mello, Phys. Rev. Lett. **73**, 142 (1994); R. A. Jalabert, J.-L. Pichard, and C. W. J. Beenakker, Europhys. Lett. **27**, 255 (1994).

[19] P. Pereyra and P. A. Mello, J. Phys. A **16**, 237 (1983).

3 Fluctuating phase rigidity for a quantum chaotic system with partially broken time-reversal symmetry

Wave functions of billiards with a chaotic classical dynamics have been measured both for classical [1, 2] and quantum mechanical waves [3, 4]. The experiments are consistent with a χ^2_β distribution of the squared modulus $|\psi(\vec{r})|^2$ of a wave function at point $\vec{r}$, the index $\beta = 1$ or 2 depending on whether time-reversal symmetry is present or completely broken. These two symmetry classes are the orthogonal and unitary ensembles of random-matrix theory [5]. For a complete description of the experiments one also needs to know what spatial correlations exist between $|\psi(\vec{r}_1)|^2$ and $|\psi(\vec{r}_2)|^2$ at two different points and how these correlations are affected by breaking of time-reversal symmetry. In the orthogonal and unitary ensembles it is known that the correlations decay to zero if the distance $|\vec{r}_2 - \vec{r}_1|$ greatly exceeds the wavelength λ [6].

Recently, Fal'ko and Efetov [7] managed to compute the two-point distribution $P_2(p_1, p_2)$ in the crossover regime between the orthogonal and unitary ensembles. (We abbreviate $p_i \equiv V|\psi(\vec{r}_i)|^2$, with V the volume of the system.) They found that the two-point distribution does not factorize into one-point distributions, $P_2(p_1, p_2) \neq P_1(p_1)P_1(p_2)$, even if $|\vec{r}_2 - \vec{r}_1| \gg \lambda$. The existence of long-range correlations in a chaotic wave function came as a surprise.

Two years earlier, in an apparently unrelated paper, Taniguchi, Hashimoto, Simons, and Altshuler [8] had studied the response of an energy level $E(X)$ to a small perturbation of the Hamiltonian (parameterized by the variable X). They discovered a non-Gaussian distribution of the level "velocity" dE/dX in the orthogonal to unitary crossover. This was remarkable, since the distribution is Gaussian in the orthogonal and unitary ensembles.

It is the purpose of the present paper to show that these two crossover effects are two different manifestations of one fundamental phenomenon, which we identify as *phase-rigidity fluctuations.* The phase rigidity is the real number $\rho = |\int d\vec{r}\, \psi^2|^2$ in the interval $[0, 1]$, which equals 1 (0) in the orthogonal (unitary) ensemble. The possibility of fluctuations in ρ was first noticed by French, Kota, Pandey, and Tomsovic [9], but the distribution $P(\rho)$ was not known. We have computed $P(\rho)$ in the crossover regime, building on work by Sommers and Iida [10], and find a broad distribution. Previous theories for the crossover by Życzkowski and Lenz [11], by Kogan and Kaveh [12], and most recently by Kanzieper and Freilikher [13] amount to a neglect of fluctuations in ρ, and thus imply the absence of long-range correlations in $\psi(\vec{r})$ and a Gaussian distribution of dE/dX. Conversely, once the fluctuations of the phase rigidity are properly accounted for, we recover the distant correlations and non-Gaussian distribution of Refs. [7, 8], and find a novel correlation between level velocities for independent perturbations of the Hamiltonian.

We start from the Pandey-Mehta Hamiltonian [5, 14] for a system with partially broken time-reversal symmetry,

$$H = S + i\alpha\,(2N)^{-1/2}\,A, \tag{3.1}$$

where α is a positive number, and S (A) is a symmetric (anti-symmetric) real $N \times N$ matrix. The matrix S has the Gaussian distribution

$$P(S) \propto \exp\left(-\tfrac{1}{4}Nc^{-2}\mathrm{Tr}\,SS^{\dagger}\right), \tag{3.2}$$

and the distribution of A is the same. The real parameter c determines the mean level spacing Δ at the center of the spectrum for $N \gg 1$, by $c = N\Delta/\pi$. The distribution of H crosses over from the orthogonal to the unitary ensemble at $\alpha \simeq 1$. The wave function ψ_k of the k-th energy level at widely separated points ($|\vec{r}_i - \vec{r}_j| \gg \lambda$) is represented by the unitary matrix U that diagonalizes H:

$$V^{1/2}\psi_k(\vec{r}_i) \to N^{1/2}U_{ik}. \tag{3.3}$$

Consider now an eigenvector $|u\rangle = (U_{1k}, U_{2k}, \ldots, U_{Nk})$. (Since we deal with a single eigenstate, we suppress the level index k.) Following Ref. [9] we decompose $|u\rangle$ in the form

$$|u\rangle = \mathrm{e}^{i\phi}\left(t|R\rangle + i\sqrt{1-t^2}|I\rangle\right), \tag{3.4}$$

where $|R\rangle$ and $|I\rangle$ are real orthonormal N-component vectors, and $\phi \in [0, \pi/2)$ and $t \in [0, 1]$ are real numbers. This decomposition exists for any normalized vector $|u\rangle$ and is unique for $t \neq 0, 1$. The phase rigidity ρ is related to the parameter t by

$$\rho = \left|\int d\vec{r}\,\psi_k^2\right|^2 \to \left|\sum_i U_{ik}^2\right|^2 = (2t^2-1)^2. \tag{3.5}$$

In the orthogonal ensemble $t = 0$ or 1, hence $\rho = 1$, while in the unitary ensemble $t = \sqrt{1/2}$ hence $\rho = 0$. In the crossover between these two ensembles the parameter ρ does not take on a single value but fluctuates.

To compute the distribution $P(\rho)$ we use a result of Sommers and Iida [10], for the joint probability distribution of an eigenvalue E and the corresponding eigenvector $|u\rangle$ of the Hamiltonian (3.1). Substitution of the decomposition (3.4), and inclusion of the Jacobian for the change of variables from $|u\rangle$ to ρ, gives the expression

$$\begin{aligned} P(\rho) &\propto \frac{(1-\rho)^{N/2-3/2}}{D^{N/2-1}\sqrt{\Lambda}}\Bigg[\frac{c^2}{N\Lambda} \\ &\quad +\rho\left(\frac{2b_-}{D}\right)^2\frac{\partial}{\partial b_-}+\left(\frac{2b_+}{D}\right)^2\left(\frac{1}{2}\frac{\partial^2}{\partial E^2}+\frac{\partial}{\partial b_+}\right)\Bigg] Z_{N-2}(E)\Bigg|_{E=0}, \qquad (3.6) \\ b_\pm &= \frac{c^2}{N}\left(1\pm\frac{\alpha^2}{2N}\right), \quad D=4+\frac{2N}{\alpha^2}(1-\rho)\left(1-\frac{\alpha^2}{2N}\right)^2, \qquad (3.7) \\ \Lambda &= 2+(1-\rho)\left(\frac{2N}{\alpha^2}-1\right), \qquad (3.8) \\ Z_N(E) &= \frac{1}{N!}\left(b_+\frac{\partial}{\partial\omega}\right)^N \\ &\quad \times\left(1-\omega b_-/b_+\right)^{-1}(1-\omega)^{-\frac{3}{2}}(1+\omega)^{-\frac{1}{2}}\exp\left(\frac{-\omega E^2}{(1+\omega)b_+}\right)\Bigg|_{\omega=0} \qquad (3.9) \end{aligned}$$

We have set $E=0$, corresponding to the center of the spectrum. We still have to take the limit $N\to\infty$. Expansion of $Z_N(0)$ in a series,

$$Z_N(0)=b_+^N\sum_{k=0}^{N}a_k\left(\frac{b_-}{b_+}\right)^{N-k}, \qquad (3.10)$$

$$a_k=\frac{1}{k!}\frac{\partial^k}{\partial\omega^k}(1-\omega)^{-\frac{3}{2}}(1+\omega)^{-\frac{1}{2}}\Bigg|_{\omega=0}\xrightarrow{k\gg 1}\sqrt{\frac{2k}{\pi}}, \qquad (3.11)$$

and replacement of the summation by an integration, yields

$$Z_N(0) = \frac{c^{2N}\sqrt{2/\pi}}{\alpha^2 N^{N-3/2}}\left(e^{\alpha^2/2}+\frac{ie^{-\alpha^2/2}\sqrt{\pi}}{2\alpha}\mathrm{erf}(i\alpha)\right) \qquad (3.12)$$

for $N\gg 1$. Here $\mathrm{erf}(i\alpha)\equiv 2i\pi^{-1/2}\int_0^\alpha e^{y^2}dy$. The double energy derivative of $Z_N(E)$ is computed similarly, but turns out to be smaller by a factor N and can thus be neglected. The derivatives with respect to $b_\pm$ can be found by differentiation of Eq. (3.12). Collecting all terms, we find

$$\begin{aligned} &P(\rho)=(1-\rho)^{-2}\exp\left(\frac{\alpha^2}{\rho-1}\right) \\ &\times\left[\frac{\alpha^2-1+\rho}{1-\rho}\left(e^{\alpha^2}+\frac{i\pi^{\frac{1}{2}}}{2\alpha}\mathrm{erf}(i\alpha)\right)-\frac{i\alpha\pi^{\frac{1}{2}}}{2}\mathrm{erf}(i\alpha)\right]. \qquad (3.13) \end{aligned}$$

In Fig. 3-1 the distribution of ρ is plotted for three values of the crossover parameter α. It is very broad for $\alpha=1$, and narrows to a delta function at 1 (0) for $\alpha\to 0$ ($\alpha\to\infty$).

It remains to show that the long-range wave-function correlations and non-Gaussian level-velocity distributions of Refs. [7, 8] follow from the distribution

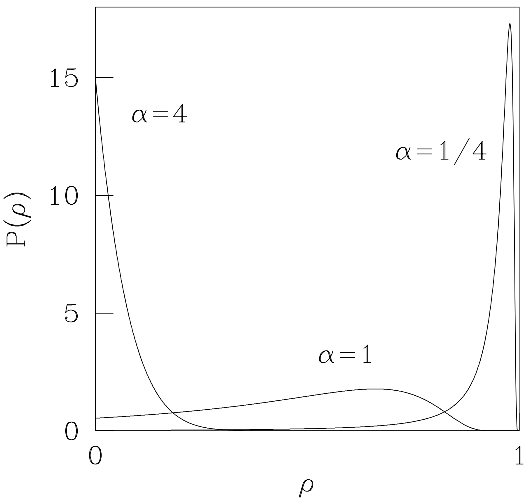

Figure 3-1. Distribution of the phase rigidity ρ for $\alpha = 1/4$, 1, and 4, computed from Eq. (3.13). The crossover from the orthogonal to unitary ensemble occurs when $\alpha \approx 1$, and is associated with large fluctuations in ρ around its ensemble average.

$P(\rho)$ which we have computed. We begin with the wave-function correlations, and consider the n-point distribution function

$$P_n(p_1, p_2, \ldots, p_n) = \left\langle \prod_{i=1}^{n} \delta(p_i - N|U_{ik}|^2) \right\rangle. \tag{3.14}$$

We substitute the decomposition (3.4) and do the average in two steps: First over $|R\rangle$ and $|I\rangle$, and then over t. Due to the invariance of $P(H)$ under orthogonal transformations of H, the vectors $|R\rangle$ and $|I\rangle$ can be integrated out immediately. In the limit $N \to \infty$, the components of the two vectors are $2N$ independent real Gaussian variables with zero mean and variance $1/N$. Doing the Gaussian integrals we find a generalization of results in Refs. [9, 11] to $n > 1$:

$$P_n(p_1, p_2, \ldots, p_n) = \int_0^1 d\rho\, P(\rho) \prod_{i=1}^{n} F(p_i, \rho), \tag{3.15}$$

$$F(p, \rho) = (1-\rho)^{-\frac{1}{2}} \exp\left(\frac{p}{\rho - 1}\right) I_0\left(\frac{p\sqrt{\rho}}{1-\rho}\right). \tag{3.16}$$

Here I_0 is a Bessel function. We see that long-range spatial correlations exist only if the distribution $P(\rho)$ of ρ has a finite width. For example, the two-point correlator $\langle p_1^2 p_2^2\rangle - \langle p_1^2\rangle\langle p_2^2\rangle$ equals the variance of ρ. The approximation of Ref. [11] (implicit in Refs. [12, 13]) was to take ρ fixed at each α. If ρ is fixed,

$P_n(p_1,\ldots,p_n) \to P_1(p_1)\cdots P_1(p_n)$ factorizes, and hence spatial correlations are absent. If instead we substitute for $P(\rho)$ our result (3.13), we recover exactly the results of Fal'ko and Efetov [7,15].

We now turn to the level-velocity distributions. We consider perturbations of the Hamiltonian (3.1) by a real symmetric (anti-symmetric) matrix S' (A'),

$$H' = H + x_{\mathrm{o}}S' + x_{\mathrm{u}}iA'. \tag{3.17}$$

Here x_{u}, x_{o} are real infinitesimals, which parameterize, respectively, a perturbation that breaks or does not break time-reversal symmetry. The corresponding level velocities

$$\nu_{\mathrm{o}} = \frac{\partial E_k}{\partial x_{\mathrm{o}}}, \quad \nu_{\mathrm{u}} = \frac{\partial E_k}{\partial x_{\mathrm{u}}}, \tag{3.18}$$

have distributions

$$\begin{aligned} P(\nu_{\mathrm{o}}) &= \left\langle \delta(\nu_{\mathrm{o}} - \sum_{i,j} U_{ik}U^*_{jk}S'_{ji}) \right\rangle, & (3.19)\\ P(\nu_{\mathrm{u}}) &= \left\langle \delta(\nu_{\mathrm{u}} - \sum_{i,j} U_{ik}U^*_{jk}iA'_{ji}) \right\rangle. & (3.20)\end{aligned}$$

We substitute the decomposition (3.4) for the eigenvector U_{ik} of H and average first over S' and A', assuming a Gaussian distribution for these perturbation matrices. After averaging over S' and A', the eigenvector enters only via the parameter ρ. One finds

$$\begin{aligned} P(\nu_{\mathrm{o}}) &= \int_0^1 d\rho\, P(\rho)G_{1+\rho}(\nu_{\mathrm{o}}), & (3.21)\\ P(\nu_{\mathrm{u}}) &= \int_0^1 d\rho\, P(\rho)G_{1-\rho}(\nu_{\mathrm{u}}), & (3.22)\end{aligned}$$

where $G_{1\pm\rho}$ is a Gaussian distribution with zero mean and variance $1 \pm \rho$. We have normalized the velocities such that $\overline{\nu_{\mathrm{o}}^2} = \overline{\nu_{\mathrm{u}}^2} = 1$ in the unitary ensemble. Substitution of Eq. (3.13) for $P(\rho)$ shows that the distribution of ν_{o} coincides with the result of Ref. [8]. However, our $P(\nu_{\mathrm{u}})$ is different. This is because we have chosen A and A' to be independent random matrices, whereas they are identical in Ref. [8]. Independent matrices A and A' are appropriate for a system with a perturbing magnetic field in a random direction; Identical A and A' correspond to a system in which only the magnitude but not the direction of the field is varied. Eq. (3.21-3.22) demonstrates that $P(\nu_{\mathrm{o}})$ and $P(\nu_{\mathrm{u}})$ are Gaussians in the orthogonal and unitary ensembles, since then $P(\rho)$ is a delta function. In the crossover regime the distributions are non-Gaussian, because of the finite width of $P(\rho)$. The relation (3.21-3.22) between the distributions of ν and ρ for the GOE–GUE transition is reminiscent of a relation obtained by Fyodorov and Mirlin for the metal–insulator transition [16]. The role of the parameter ρ is then played by the so-called inverse participation ratio $I = \int d\vec{r}\, |\psi|^4$. In our system $NI \to \rho + 2$ for $N \to \infty$. A difference with Ref. [16] is that our perturbation matrices are drawn from orthogonally invariant ensembles, whereas their perturbation is band-diagonal.

As a final example of the importance of the phase-rigidity fluctuations in the crossover regime, we consider the response of the system to two or more independent perturbations,

$$H' = H + \sum_{i=1}^{m} x_{\mathrm{o}i} S_i' + \sum_{j=1}^{n} x_{\mathrm{u}j} iA_j'. \tag{3.23}$$

For example, one may think of the displacement of m different scatterers, or the application of a localized magnetic field at n different sites. Proceeding as before, we obtain the joint probability distribution of the level velocities $v_{\mathrm{o}i} = \partial E_k / \partial x_{\mathrm{o}i}$ and $v_{\mathrm{u}j} = \partial E_k / \partial x_{\mathrm{u}j}$,

$$\begin{aligned} &P(v_{\mathrm{o}1}, v_{\mathrm{o}2}, \ldots, v_{\mathrm{o}m}, v_{\mathrm{u}1}, v_{\mathrm{u}2}, \ldots, v_{\mathrm{u}n}) \\ &\quad = \int_0^1 d\rho\, P(\rho) \prod_{i=1}^{m} G_{1+\rho}(v_{\mathrm{o}i}) \prod_{j=1}^{n} G_{1-\rho}(v_{\mathrm{u}j}). \end{aligned} \tag{3.24}$$

We see that as a result of the finite width of $P(\rho)$, the joint distribution of level velocities does not factorize into the individual distributions (3.21-3.22), implying that the response of an energy level to independent perturbations of the Hamiltonian is correlated.

To summarize, we have introduced the phase rigidity, defined as the squared modulus of the spatial average of the wave function squared, and computed its distribution for a chaotic system with partially broken time-reversal symmetry. Fluctuations of the phase rigidity from one wave function to another exist if time-reversal symmetry is partially broken. We have shown that these fluctuations imply long-range wave-function correlations and non-Gaussian eigenvalue perturbations, thereby unifying two previously unrelated discoveries [7, 8]. A novel manifestation of the phase-rigidity fluctuations is the existence of level-velocity correlations for independent perturbations of the system.

References

[1] J. Stein, H.-J. Stöckmann, and U. Stoffregen, Phys. Rev. Lett. **75**, 53 (1995).

[2] V. N. Prigodin, N. Taniguchi, A. Kudrolli, V. Kidambi, and S. Sridhar, Phys. Rev. Lett. **75**, 2392 (1995).

[3] A. M. Chang, H. U. Baranger, L. N. Pfeiffer, K. W. West, and T. Y. Chang, Phys. Rev. Lett. **76**, 1695 (1996).

[4] J. A. Folk, S. R. Patel, S. F. Godijn, A. G. Huibers, S. M. Cronenwett, C. M. Marcus, K. Campman, and A. C. Gossard, Phys. Rev. Lett. **76**, 1699 (1996).

[5] M. L. Mehta, *Random Matrices* (Academic, New York, 1991).

[6] V. N. Prigodin and N. Taniguchi, Mod. Phys. Lett. B **10**, 69 (1996).

[7] V. I. Fal'ko and K. B. Efetov, Phys. Rev. Lett. **77**, 912 (1996).

[8] N. Taniguchi, A. Hashimoto, B. D. Simons, and B. L. Altshuler, Europhys. Lett. **27**, 335 (1994).

[9] J. B. French, V. K. B. Kota, A. Pandey, and S. Tomsovic, Ann. Phys. (N. Y.) **181**, 198 (1988).

[10] H.-J. Sommers and S. Iida, Phys. Rev. E **49**, R2513 (1994).

[11] K. Życzkowski and G. Lenz, Z. Phys. B **82**, 299 (1991).

[12] E. Kogan and M. Kaveh, Phys. Rev. B **51**, 16400 (1995).

[13] E. Kanzieper and V. Freilikher, Phys. Rev. B **54**, 8737 (1996).

[14] A. Pandey and M. L. Mehta, Commun. Math. Phys. **87**, 449 (1983).

[15] V. I. Fal'ko and K. B. Efetov, Phys. Rev. B **50**, 11267 (1994).

[16] Y. V. Fyodorov and A. D. Mirlin, Phys. Rev. B **51**, 13403 (1995).

4 Quantum-statistical current correlations in multi-lead chaotic cavities

Quantum theory requires that identical particles are treated as indistinguishable. In particular, the wave function has to remain invariant up to a sign under the exchange of any pair of particles. A well known consequence of this symmetry is the exchange hole in the equal time density-density correlation of an electron gas [1]. It is the purpose of this paper to investigate exchange effects in current-current correlations of a mesoscopic chaotic cavity connected to four leads. A four-lead geometry is the simplest structure which allows an unambiguous identification of exchange effects. While a similar experiment has already been proposed and analyzed under conditions where electron motion is along one-dimensional edge channels [2], the investigation presented here is the first for a non-trivial many-channel conductor. One might expect from the former analysis that exchange effects are washed out in an ensemble of chaotic conductors, and can thus be observed at best in the fluctuations away from the average. The most important result of our discussion is that this is not the case: exchange effects survive ensemble averaging and are even of the same order of magnitude as the direct terms.

The general existence of exchange effects in a scattering process with two detectors and two mutually incoherent sources has been pointed out already by Goldberger et al. [3], following the seminal experiments of Hanbury-Brown and Twiss [4] with a stellar interferometer based on this principle. A clear account of two-particle interference of bosons and fermions has been given by Loudon [5]. In electronic conductors we deal with a Fermi sea, instead of only two particles. Nevertheless, for electrons moving in a fixed Hartree potential the current-current correlations can be expressed via two-particle exchange amplitudes in terms of the single-particle scattering matrix [2]. The resulting correlations are negative, except in the case of normal-superconductor hybrid structures [6]. Our work is closely related to recent theoretical [7, 8] and experimental [9] efforts to understand shot noise in mesoscopic conductors. Most of this effort has concentrated on conductors which are effectively two-terminal, and has focused on the suppression of the shot-noise power below the uncorrelated Poisson limit $2e|I|$. The situation is potentially richer in multi-lead conductors, where there is the possibility of investigating correlations between current fluctuations at different leads.

We compute the current correlations for a chaotic quantum dot [10]. During the last few years, there has been an increasing activity of experimentalists in tailoring electronic confinement potentials, and characterizing the conductive properties of such cavities [11, 12]. If the classical dynamics of the dot is fully chaotic, the quantum transport properties are well described by a relatively simple statistical ensemble for the scattering matrix [13–15]. Using this approach, we find that both the direct and exchange contributions to the correlations are of the order of the channel number N, and that they are insensitive to dephasing. This is remarkable, since in single-channel scattering geometries the exchange terms depend sensitively on phases, in contrast with the direct terms [2, 5]. Furthermore, we find that the sign of the averaged exchange contribution reverses if the cavity is closed up by tunnel barriers. The particular dependence of our results on the barrier transparency offers a possibility to distinguish these correlations from other effects. In the end we compare with a purely classical resistor network.

The quantity that we study, is the zero-frequency spectral density of current correlations,

$$P_{\alpha\beta} = 2\int_{-\infty}^{\infty} dt\, \overline{\Delta I_\alpha(t+t_0)\Delta I_\beta(t_0)}, \tag{4.1}$$

where $\Delta I_\alpha = I_\alpha - \overline{I_\alpha}$ is the fluctuation of the current in lead α away from the time-average. It is shown in Ref. [2] that

$$P_{\alpha\beta} = 2\frac{e^2}{h}\sum_{\gamma,\delta}\int dE\, f_\gamma(1-f_\delta)\mathrm{Tr}\,[A_{\gamma\delta}(\alpha)A_{\delta\gamma}(\beta)] \tag{4.2}$$

where $f_\alpha(E)$ is the distribution of reservoir α, and

$$A_{\beta\gamma}(\alpha) = 1_\alpha\delta_{\alpha\beta}\delta_{\alpha\gamma} - s^\dagger_{\alpha\beta}(E)s_{\alpha\gamma}(E). \tag{4.3}$$

Here $s_{\alpha\beta}(E)$ is the sub-block of the scattering matrix S for scattering from lead β (N_β channels) to lead α at energy E, and 1_α is the $N_\alpha \times N_\alpha$-unit matrix. If all reservoirs are at zero-temperature equilibrium, $f_\alpha(E) = \theta(E - eV_\alpha)$, the summation in Eq. (4.2) is over $\gamma \neq \delta$, and the trace becomes a noise conductance

$$C_{\gamma\delta}(\alpha\beta) = \mathrm{Tr}(s^\dagger_{\alpha\gamma}s_{\alpha\delta}s^\dagger_{\beta\delta}s_{\beta\gamma}). \tag{4.4}$$

To be specific we introduce the correlator P_{34} for three experiments [2] A, B, and C: In experiment A (B) a small voltage V is applied only to lead 1 (2), whereas in experiment C a voltage V is applied to both reservoir 1 and 2. It follows from Eq. (4.2) that the result of experiment C is not identical to the sum of the results from experiments A and B. We identify the difference as the exchange correlation:

$$P^{\mathrm{ex}}_{34} \equiv P^{\mathrm{C}}_{34} - P^{\mathrm{A}}_{34} - P^{\mathrm{B}}_{34} = -2P_0\mathrm{Re}\, C_{12}(34), \tag{4.5}$$

where $P_0 = 2e|V|e^2/h$. Although $P_{\alpha\beta} \leq 0$ in every experiment for $\alpha \neq \beta$, the difference can still have both signs.

We first consider ideal coupling of the four N-channel leads to the cavity (Fig. 4-1). If time-reversal symmetry is (un)broken, the $4N \times 4N$-scattering matrix S is uniformly distributed on the set of unitary (unitary symmetric) matrices

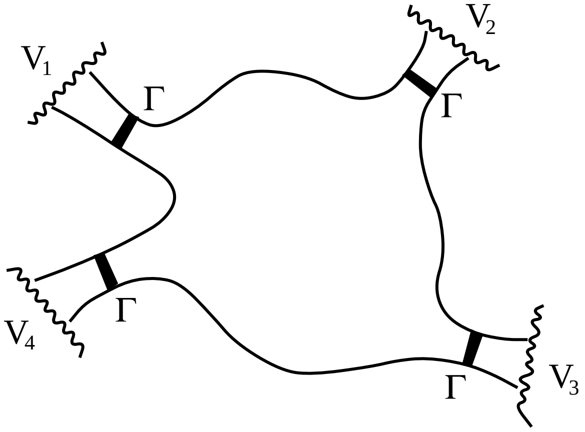

Figure 4-1. Chaotic cavity connected to four reservoirs via N-channel leads. Tunnel barriers of transparency Γ model non-ideal coupling of the leads to the cavity.

[13, 14]. This is the circular unitary (orthogonal) ensemble of random matrix theory. Since our results for both ensembles differ only to order N^{-2}, we will focus on the simpler unitary ensemble, thus assuming that there is a sufficiently large magnetic field in the cavity. From the general formula of Ref. [16] one finds the exact ensemble average $\langle \cdots \rangle$ of the noise conductances:

$$\langle C_{\gamma\delta}(\alpha\beta)\rangle = (\delta_{\alpha\beta} + \delta_{\gamma\delta} - 1/4) \times N^3/(16N^2 - 1). \tag{4.6}$$

Fluctuations are of order one. Thus we find

$$\langle P_{\alpha\beta}\rangle = \frac{e^3}{h}(\delta_{\alpha\beta} - 1/4)\frac{N^3}{16N^2 - 1}\sum_{i,j=1}^{4} |V_i - V_j|. \tag{4.7}$$

The average exchange correlation $\langle P_{34}^{\text{ex}}\rangle = \frac{1}{2}P_0\ N^3/(16N^2 - 1)$ is positive and, just as the direct terms, of order N. This is remarkable, given the fact that the sign of the noise conductance $C_{12}(34) = \text{Tr}(s_{31}^\dagger s_{32} s_{42}^\dagger s_{41})$ can vary from sample to sample. *The large average is essentially due to correlations between scattering matrix elements imposed by unitarity.*

The size of the exchange effect, and the important role played by unitarity, makes it more robust than a normal wave-interference effect. We next show that the current correlations are the same even under conditions where phase-coherent transfer through the sample is completely destroyed, but energy is conserved in the dephasing process. We model dephasing by connecting the sample to an additional fictitious reservoir. Attaching an equilibrium reservoir, like a voltage probe, causes inelastic scattering [17], which reduces shot noise far below the value in phase-coherent transport [18]. Following De Jong and Beenakker [7, 19], we rather consider dephasing by a reservoir with a fluctuating non-equilibrium distribution $f_\phi(E,t)$ such that no current is drawn *at every energy and instant of time.* Such quasi-elastic scattering does not change the shot noise of a chaotic cavity with wide leads [7]. Below we generalize this result to the current correlations in a multi-terminal geometry.

The total current through lead α at time t and energy E is [2]

$$I_\alpha(E,t) = \frac{e}{h}\sum_\beta (N_\alpha \delta_{\alpha\beta} - G_{\alpha\beta}) f_\beta + \delta I_\alpha(E,t), \tag{4.8}$$

where $G_{\alpha\beta} = \operatorname{Tr} s^\dagger_{\alpha\beta} s_{\alpha\beta}$ and the indices run over all five leads. Apart from the intrinsic fluctuations defined by $\delta I_\alpha(E,t)$, there is now also a time-dependence due to the fluctuating $f_\phi(E,t)$. The requirement $I_\phi(E,t) = 0$ determines $f_\phi(E,t)$ which, by substitution back into Eq. (4.8) yields the total fluctuation ΔI_k at a real lead k,

$$\Delta I_k = \delta I_k + G_{k\phi} \delta I_\phi / \sum_{m=1}^{4} G_{\phi m}. \tag{4.9}$$

The correlations of the intrinsic fluctuations $\delta I_\alpha = \int dE\, \delta I_\alpha(E,t)$ satisfy Eq. (4.2) with the time-averaged distribution

$$f_\phi(E) = \sum_{k=1}^{4} G_{\phi k} f(E - eV_k) / \sum_{k=1}^{4} G_{\phi k}. \tag{4.10}$$

We assume homogeneous and complete dephasing, which implies that the extra lead has $N_\phi \gg N$ channels, and is coupled ideally to the dot [20]. In this limit, the only non-vanishing transport coefficients are

$$G_{k\phi} = G_{\phi k} = N, \quad G_{\phi\phi} = N_\phi - 4N, \tag{4.11}$$

$$C_{kk}(\phi\phi) = N, \quad C_{\phi\phi}(\phi\phi) = N_\phi - 4N, \tag{4.12}$$

independent of the magnetic field, for all N, and without fluctuations. Thus

$$P_{kl} = 2\frac{e^2}{h}(\delta_{kl} - 1/4) N \int dE\, f_\phi(E)(1 - f_\phi(E)). \tag{4.13}$$

For $N \gg 1$ Eq. (4.13) coincides exactly with Eq. (4.7). It shows a striking similarity with a semi-classical expression for the shot-noise power first obtained by Nagaev [21]. However, it should be noted that for geometries with non-ideal leads, discussed below, the correlations are not determined by the distribution function of the dephasing reservoir only.

We have now shown that exchange effects do survive changes in the elastic scattering potential as well as phase-breaking scattering. This finding sheds new light on the actual issue of shot-noise suppression in two-terminal many-channel geometries [22]. Universal suppression factors were found in both quantum mechanical [18, 23] and semi-classical [19, 21, 24] approaches. In fact, the two-terminal shot noise contains direct and exchange terms corresponding to pairs of particles coming from different *channels*. The reduction below the Poisson noise is partly due to such channel-exchange terms.

The analysis of the cavity connected to open leads is not sufficient for an unambigious identification of exchange correlations in practice. Current correlations could be established by any other process, and there is no general reason why the results of experiments A, B, and C should be additive. Indeed, in the end we will briefly discuss a classical network where currents are correlated by fluctuations of the self-consistent electrostatic potential inside the "dot", and where experiment C is not the sum of experiment A and B. To facilitate identification of the exchange effect, we now make specific predictions for the correlations in the case of non-ideal leads, as a function of the probability Γ of transmission through the contact region. We focus on the many-channel limit $N \gg 1$, where one cannot distinguish isolated resonances of the system, except if the coupling is so weak that $\Gamma \ll 1/N$. Below, we discuss this weak coupling limit before turning to the main result of the paper: the correlations in the regime $1/N \ll \Gamma \leq 1$.

We first assume that the contacts are so poorly transmitting that transport is dominated by a single state at the Fermi energy E_F. The scattering amplitude from a point b to a point a takes the form

$$S_{ab} = \delta_{ab} - \frac{i\alpha\Delta}{\pi} \frac{\psi_\nu^*(a)\psi_\nu(b)}{E_F - E_\nu + i\gamma_\nu/2}. \tag{4.14}$$

where ψ_ν is the resonant eigenstate with energy E_ν, Δ is the mean level spacing, $\alpha \ll 1$ is a dimensionless coupling parameter, and $\gamma_\nu = \alpha\Delta/\pi \sum_r |\psi_\nu(r)|^2$ is the width of the resonant level. The sum is over positions in the four coupling regions. We assume that each lead contributes equally to the width, which is automatically satisfied for a chaotic cavity with leads of the same width, due to self-averaging of the overlaps with the eigenstate. Then, at small bias $V \ll \gamma_\nu$, the current correlations are

$$P^{\mathrm{A,B}}_{\alpha\beta} = P_0(4\delta_{\alpha\beta} - 1)/16, \tag{4.15}$$

$$P^{\mathrm{C}}_{\alpha\alpha} = -P^{\mathrm{C}}_{34} = -P^{\mathrm{C}}_{12} = P_0/4, \tag{4.16}$$

$$P^{\mathrm{C}}_{13} = P^{\mathrm{C}}_{14} = P^{\mathrm{C}}_{23} = P^{\mathrm{C}}_{24} = 0. \tag{4.17}$$

The result of experiment C is easily understood. For resonant tunneling through a two-terminal symmetric barrier, the shot noise vanishes. Indeed, in experiment C the total current from lead 1 and 2 to lead 3 and 4 is noiseless. All fluctuations and correlations are due to 'unification' of the currents from 1 and 2, and 'partition' of the total current into 3 and 4. The vanishing of the correlations between incoming and outgoing currents shows that these two choices are made independently. The exchange correlation $P^{\mathrm{ex}}_{34} = -P_0/8$ has a sign opposite to that of the ideally coupled cavity.

We now compute the ensemble averaged correlations for the cavity with tunnel barriers in the regime $N \gg 1$, $N\Gamma \gg 1$. The scattering matrix of the combined system is [25]

$$S = R + T'(1 - UR')^{-1}UT, \tag{4.18}$$

where we assume without loss of generality that the reflection and transmission matrices of the barriers are proportional to the $4N \times 4N$ unit matrix I: $R = R' = (1-\Gamma)^{1/2} I$, $T = -T' = \Gamma^{1/2} I$. The distribution of the scattering matrix U of the cavity is the circular unitary ensemble, as before. The average noise conductances are computed by series expansion of the four fractions $(1 - UR')^{-1}$, collecting the order N contributions to each term with the diagrammatic technique of Ref. [25], and resumming. Thus one finds

$$\begin{aligned}\langle C_{\gamma\delta}(\alpha\beta)\rangle = \Big[&\Gamma(2-3\Gamma) + 4\Gamma^2(\delta_{\alpha\beta} + \delta_{\gamma\delta})\\ &-4\Gamma(1-\Gamma)(\delta_{\alpha\gamma} + \delta_{\alpha\delta} + \delta_{\beta\gamma} + \delta_{\beta\delta})\\ &+16\Gamma(1-\Gamma)(\delta_{\alpha\beta}\delta_{\beta\gamma} + \delta_{\alpha\beta}\delta_{\beta\delta} + \delta_{\alpha\gamma}\delta_{\gamma\delta} + \delta_{\beta\gamma}\delta_{\gamma\delta})\\ &+64(1-\Gamma)^2\delta_{\alpha\beta}\delta_{\beta\gamma}\delta_{\gamma\delta}\Big] \times N/64 + \mathcal{O}(1),\end{aligned} \tag{4.19}$$

which for $\Gamma = 1$ reduces to the large-N limit of Eq. (4.6). The correlators for the experiments A and C are

$$\langle P^{\mathrm{C}}_{\alpha\beta}\rangle = P_0 N\Gamma(2-\Gamma)(4\delta_{\alpha\beta} - 1)/16, \tag{4.20}$$

$$\langle P^{\mathrm{A}}_{\alpha 1}\rangle = P_0 N\Gamma(10-7\Gamma)(4\delta_{\alpha 1} - 1)/64, \tag{4.21}$$

$$\langle P^{\mathrm{A}}_{\alpha\alpha}\rangle = P_0 N\Gamma(14-5\Gamma)/64 \quad (\alpha \neq 1), \tag{4.22}$$

$$\langle P^{\mathrm{A}}_{\alpha\beta}\rangle = -P_0 N\Gamma(\Gamma+2)/64 \quad (\alpha, \beta \neq 1, \alpha \neq \beta). \tag{4.23}$$

Experiment B is identical to experiment A with all indices 1 replaced by indices 2. The functional dependence of these results provides a fingerprint for an experimental identification of the correlations. The exchange correlation $\langle P^{\mathrm{ex}}_{34}\rangle = P_0 N\Gamma(3\Gamma - 2)/32$ reverses sign at $\Gamma = 2/3$. An observation of this sign change would be a clear indication that measured correlations are due to exchange. One easily checks that in experiment C the shot noise of the total current from lead 1 and 2 to lead 3 and 4 crosses over from one quarter times the Poisson noise at $\Gamma = 1$ to one half of the Poisson noise if Γ is small, both in correspondence with the literature [14, 23, 24].

We now compare these results with a classical circuit, where current conservation induces correlations, which are also non-additive for the experiments A, B, and C. Four resistors R are connected to four voltage sources as in Fig. 4-2. Parallel to the resistors there are independent sources of Poisson noise. Temporal fluctuations of the central potential around $U = \sum_k V_k/4$ are necessary to conserve the instantaneous total current. These voltage fluctuations yield the following current correlations:

$$P_{kl} = e\sum_{m=1}^{4}\left[1 + 4(2\delta_{kl} - 1)(\delta_{mk} + \delta_{ml})\right]\frac{|V_m - U|}{8R}. \tag{4.24}$$

For experiment A, B and C, Eq. (4.24) gives the same result as Eqs. (4.20-4.23) with $\Gamma \ll 1$ and $N\Gamma e^2/h = 1/R$. For other values of the voltages and Γ the correlations

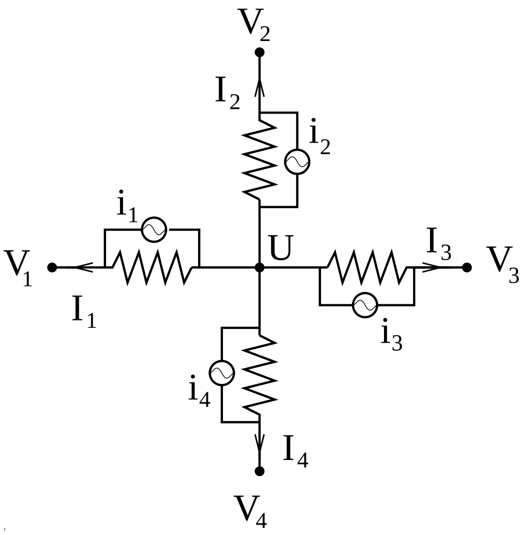

Figure 4-2. Classical network consisting of resistors and noise sources. The outgoing currents are correlated, due to fluctuations of the “dot” potential preventing temporal accumulations of charge.

differ. This example demonstrates the need to investigate the correlations as a function of a parameter like the barrier strength Γ in order to understand the source of the correlations.

In conclusion, we have evaluated the exchange contributions to current-current correlations in a multilead chaotic cavity. We found that these correlations, instead of being a small interference effect, are of the order of the channel number N, and that they persist in the presence of dephasing. We have made specific predictions for the dependence of the correlations on the transparency of non-ideal leads. Finding such a direct signature of exchange in experiments is likely a challenging task, but would clearly be a fundamental contribution to our understanding of noise in electrical conductors.

References

[1] L. D. Landau and E. M. Lifshitz, *Statistical Physics* (Pergamon, Oxford, 1959), p. 354.

[2] M. Büttiker, Phys. Rev. B 46, 12485 (1992); Phys. Rev. Lett. **65**, 2901 (1990); *ibid.* **68**, 843 (1992).

[3] M. L. Goldberger, H. W. Lewis, and K. M. Watson, Phys. Rev. **132**, 2764 (1963).

[4] R. Hanbury-Brown and R. Q. Twiss, Phil. Mag. **45**, 663 (1954).

[5] R. Loudon, in *Disorder in Condensed Matter Physics*, eds. J. A. Blackman and J. Taguena (Clarendon Press, Oxford, 1991), p. 441.

[6] M. P. Anantram and S. Datta, Phys. Rev. B **53**, 16390 (1996); Th. Martin, Phys. Lett. **A** 220, 137 (1996).

[7] For a recent review, see M. J. M. de Jong and C. W. J. Beenakker, in *Mesoscopic Electron Transport*, eds. L. P. Kouwenhoven et al., NATO ASI Series E (Kluwer Academic Publishing, Dordrecht).

[8] L. S. Levitov, H. Lee, and G. B. Lesovik, J. Math. Phys. **37**, 4845 (1996).

[9] H. Birk, M. J. M. de Jong, and C. Schönenberger, Phys. Rev. Lett. **75**, 1610 (1995); M. Reznikov, M. Heiblum, H. Shtrikman, and D. Mahalu, Phys. Rev. Lett. **75**, 3340 (1995); A. Kumar, L. Saminadayar, D. C. Glattli, Y. Jin and B. Etienne, Phys. Rev. Lett. **76**, 2778 (1996); A. H. Steinbach, J. M. Martinis, and M. H. Devoret, Phys. Rev. Lett. **76**, 3806 (1996).

[10] A similar calculation for diffusive metallic conductors has recently been reported in Ya. M. Blanter and M. Büttiker, Phys. Rev. B **56**, 2127 (1997).

[11] A. M. Chang et al. Phys. Rev. Lett. **76**, 1695 (1996).

[12] J. A. Folk et al. Phys. Rev. Lett. **76**, 1699 (1996).

[13] H. A. Baranger and P. A. Mello, Phys. Rev. Lett. **73**, 142 (1994).

[14] R. A. Jalabert, J.-L. Pichard, and C. W. J. Beenakker, Europhys. Lett. **27**, 255 (1994).

[15] For a comprehensive review of random matrix theory applied to quantum transport, see C. W. J. Beenakker, Rev. Mod. Phys. **69**, 731 (1997).

[16] M. Creutz, J. Math. Phys. **19**, 2043 (1978).

[17] M. Büttiker, IBM J. Res. Dev. **32**, 63 (1988).

[18] C. W. J. Beenakker and M. Büttiker, Phys. Rev. B **46**, 1889 (1992).

[19] M. J. M. de Jong and C. W. J. Beenakker, Physica A **230**, 219 (1996).

[20] P. W. Brouwer and C. W. J. Beenakker, Phys. Rev. B **55**, 4695 (1997).

[21] K. E. Nagaev, Phys. Lett. A **169**, 103 (1992).

[22] R. Landauer, Ann. NY Acad. Sci. 755, 417 (1995).

[23] L. Y. Chen and C. S. Ting, Phys. Rev. B **43**, 4534 (1991).

[24] L. Y. Chen and C. S. Ting, Phys. Rev. B **46**, 4717 (1992); J. H. Davies et al., Phys. Rev. B **46**, 9620 (1992).

[25] P. W. Brouwer and C. W. J. Beenakker, J. Math. Phys. **37**, 4904 (1996).

5 Thermopower of single-channel disordered and chaotic conductors

5.1 Introduction

Thermo-electric transport properties of conductors probe the energy dependence of the scattering processes limiting conduction. At low temperatures and in small (mesoscopic) systems, elastic impurity scattering is the dominant scattering process. The energy dependence of the conductance is then a quantum interference effect [1]. The derivative dG/dE of the conductance with respect to the Fermi energy is measured by the thermopower S, defined as the ratio $-\Delta V/\Delta T$ of a (small) voltage and temperature difference applied over the sample at zero electrical current. Experimental and theoretical studies of the thermopower exist for several mesoscopic devices. One finds a series of sharp peaks in the thermopower of quantum point contacts [2], aperiodic fluctuations in diffusive conductors [3], sawtooth oscillations in quantum dots in the Coulomb blockade regime [4], and Aharonov-Bohm oscillations in metal rings [5].

Here we study the statistical distribution of the thermopower in two different systems, not considered previously: A disordered wire in the localized regime and a chaotic quantum dot with ballistic point contacts. A single transmitted mode is assumed in both cases. In the disordered wire, conduction takes place by resonant tunneling through localized states. The resonances are very narrow and appear at uncorrelated energies. The distributions of the thermopower and the conductance are both broad, but otherwise quite different: Instead of the log-normal distribution of the conductance [1] we find a Lorentzian distribution for the thermopower. In the quantum dot, the resonances are correlated and the widths are of the same order as the spacings. The correlations are described by random-matrix theory [6, 7], under the assumption that the classical dynamics in the dot is chaotic. The thermopower distribution in this case follows from the distribution of the time-delay matrix found recently [8].

The thermopower (at temperature T and Fermi energy E_{F}) is given by the Cutler-Mott formula [9, 10]

$$S = -\frac{1}{eT}\frac{\int dE\,(E-E_{\mathrm{F}})G(E)df/dE}{\int dE\,G(E)df/dE}, \tag{5.1.1}$$

where G is the zero-temperature conductance and f is the Fermi-Dirac distribution function. In the limit $T \to 0$ Eq. (5.1.1) simplifies to

$$S = -\frac{\pi^2}{3}\frac{k_{\mathrm{B}}^2 T}{eG}\frac{dG}{dE}, \tag{5.1.2}$$

where G and dG/dE are to be evaluated at $E = E_{\mathrm{F}}$. We consider mainly the zero-temperature limit of the thermopower, by studying the dimensionless quantity

$$\sigma = \frac{\Delta}{2\pi G}\frac{dG}{dE}. \tag{5.1.3}$$

Here Δ is the mean level spacing near the Fermi energy. Since we are dealing with single-channel conduction, the conductance is related to the transmission probability $T(E)$ by the Landauer formula [1, 11]

$$G(E) = \frac{2e^2}{h}T(E). \tag{5.1.4}$$

The problem of the distribution of the thermopower is therefore a problem of the distribution of the logarithmic derivative of the transmission probability.

5.2 Disordered wire

In this section we study a disordered single-mode wire of length L much greater than the mean free path l. This is the localized regime. We compute the thermopower distribution in the zero-temperature limit. The analytical theory is tested by comparing with a numerical simulation. The effect of a finite temperature is considered at the end of the section. Electron-electron interactions play an important role in one-dimensional conduction, but we do not take these into account here.

5.2.1 Analytical theory

The localization length $\xi(E)$ [which is of order l and is defined by $\lim_{L\to\infty} L^{-1} \ln T(E) = -2/\xi(E)$] and the density of states $\rho(E)$ [per unit of length in the limit $L \to \infty$] are related by the Herbert-Jones-Thouless formula [12]

$$\frac{1}{\xi(E)} = \int dE'\,\rho(E')\ln|E - E'| + \text{constant}. \tag{5.2.1}$$

The additive constant is energy-independent on the scale of the level spacing. Eq. (5.2.1) follows from the Kramers-Kronig relation between the real and imaginary parts of the wave number (the real part determining ρ, the imaginary part ξ). Neglecting the width of the resonances in the large-L limit, the density of states $\rho(E) = L^{-1}\sum_i \delta(E - E_i)$ is a sum of delta functions, and thus

$$\sigma = -\frac{L\Delta}{\pi}\frac{d}{dE}\frac{1}{\xi(E)} = \frac{\Delta}{\pi}\sum_i \frac{1}{E_i - E_{\mathrm{F}}}. \tag{5.2.2}$$

In the localized regime the energy levels E_i are uncorrelated, and we assume that they are uniformly distributed in a band of width B around $E_{\rm F}$. To obtain the distribution of σ,

$$P(\sigma) = \prod_i \int_{-B/2}^{B/2} \frac{dE_i}{B}\,\delta\left(\sigma - \frac{\Delta}{\pi}\sum_j \frac{1}{E_j}\right), \tag{5.2.3}$$

we first compute the Fourier transform

$$P(k) = \int_{-\infty}^{\infty} d\sigma\, {\rm e}^{{\rm i}k\sigma} P(\sigma) = \left[\frac{1}{B}\int_{-B/2}^{B/2} dE\, {\rm e}^{{\rm i}k\Delta/\pi E}\right]^{B/\Delta} = {\rm e}^{-|k|}, \tag{5.2.4}$$

where the limit $B/\Delta \to \infty$ is taken in the last step. Inverting the Fourier transform, we find that the thermopower distribution is a Lorentzian,

$$P(\sigma) = \frac{1/\pi}{1+\sigma^2}. \tag{5.2.5}$$

The "full width at half maximum" of $P(\sigma)$ is equal to 2, hence it is equal to $4\pi^3 k_{\rm B}^2 T/3e\Delta$ for $P(S)$. This width depends on the length L of the system (through $\Delta \propto 1/L$), but it does not depend on the mean free path l (as long as $l \ll L$, so that the system remains in the localized regime).

5.2.2 Numerical simulation

In order to check the analytical theory, we performed a numerical simulation using the tight-binding Hamiltonian

$$\mathcal{H} = -\frac{w}{2}\sum_j \left(c_{j+1}^\dagger c_j + c_j^\dagger c_{j+1}\right) + \sum_j V_j c_j^\dagger c_j. \tag{5.2.6}$$

The disordered wire was modeled by a chain of lattice constant a, with a random impurity potential V_j at each site drawn from a Gaussian distribution of mean zero and variance u^2. The localization length of the wire is given by [13] $\xi = 2(a/u^2)(w^2 - E_{\rm F}^2)$. We have chosen $u = 0.075\,w$, $E_{\rm F} = -0.55\,w$, such that $\xi = 248\,a$, much smaller than $L = 8000\,a$. From the scattering matrix we obtained the conductance via the Landauer formula (5.1.4), and then the (dimensionless) thermopower via Eq. (5.1.3) (with $\Delta = 3.3 \cdot 10^{-4}\,w$). The differentiation with respect to energy was done numerically, by repeating the calculation at two closely spaced values of $E_{\rm F}$. As shown in Fig. 5-1, the agreement with the analytical result is good without any adjustable parameters.

5.2.3 Finite temperatures

Our derivation of the Lorentzian distribution of the thermopower holds if the temperature is so low that $k_{\rm B}T$ is small compared to the typical width γ of the

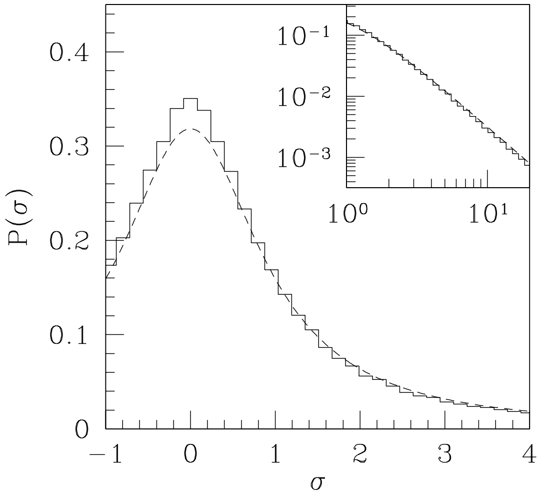

Figure 5-1. Distribution of the dimensionless thermopower $\sigma = (\Delta/2\pi)d\ln T(E)/dE$ for a one-dimensional wire in the localized regime. The histogram is obtained from a numerical simulation, for a sample length $L = 32.3\,\xi$. The dashed curve is the Lorentzian (5.2.5), being the analytical result for $L \gg \xi$. The inset shows the algebraic tail of the distribution on a logarithmic scale. The thermopower S, in the zero-temperature limit, is related to σ by $S = -(2\pi^3/3)(k_B^2T/e\Delta)\sigma$.

transmission resonances. What if $k_BT > \gamma$, but still $k_BT \ll \Delta$ (so that the discreteness of the spectrum remains resolved)? We will show that the distribution crosses over to an exponential, but in a highly non-uniform way.

Consider arbitrary γ and k_BT, both $\ll \Delta$. The Cutler-Mott formula (5.1.1) is dominated by two contributions, one from a peak in df/dE of width k_BT around E_F and one from a peak in $G(E)$ of width γ_0 around E_0. Here γ_0 and E_0 are the width and position of the level closest to E_F. If $|E_F - E_0| \gg \max(k_BT, \gamma_0)$, the two peaks do not overlap and one can estimate the thermopower as

$$\begin{aligned} S &= \frac{1}{eT}\left[\frac{\pi\gamma_0(k_BT)^2}{3(E_F-E_0)^3} + \frac{E_F-E_0}{k_BT}\mathrm{e}^{-|E_F-E_0|/k_BT}\right] \\ &\quad\times\left[\frac{\gamma_0}{2\pi(E_F-E_0)^2} + \frac{1}{k_BT}\mathrm{e}^{-|E_F-E_0|/k_BT}\right]^{-1}. \end{aligned} \tag{5.2.7}$$

If $k_BT \ll \gamma_0$, the first terms in numerator and denominator dominate over the second terms. This is the regime that the Lorentzian distribution (5.2.5) holds for all S.

We now turn to the regime $k_BT > \gamma_0$. The first terms dominate if $|E_F - E_0| \gg k_BT\ln k_BT/\gamma_0$ Hence $P(S)$ is a Lorentzian for $|S| \ll (k_B/e)\,(\ln k_BT/\gamma_0)^{-1}$.

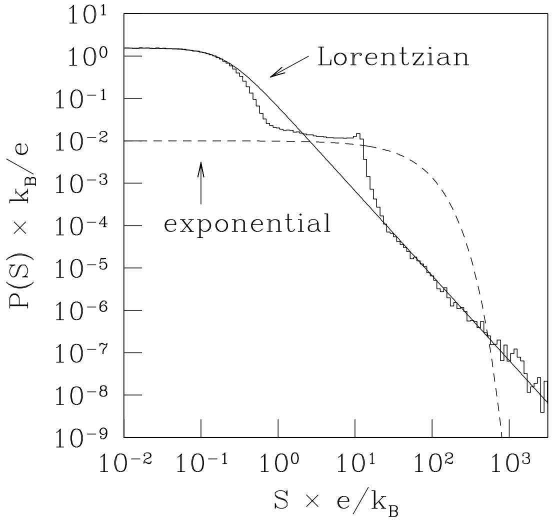

Figure 5-2. Thermopower distribution of a one-dimensional wire in the localized regime at finite temperature. The histogram is obtained from Eqs. (5.1.1) and (5.2.10), by numerical integration for a set of randomly chosen energy levels E_i, all having the same width $\gamma_i = \gamma = 10^{-6}\Delta$. The temperature is $k_B T/\Delta = 0.01$, such that $\gamma \ll k_B T \ll \Delta$. The distribution follows the Lorentzian (5.2.5) (solid curve) for small and large S, but it follows the exponential (5.2.8) (dashed curve) in an intermediate region.

The logarithm of $k_B T/\gamma_0$ can be quite large, because the width of the levels is exponentially small in the system size, $\gamma \sim \mathrm{e}^{-L/\xi}$. The Lorentzian persists in an interval larger than its width, provided $k_B T < \Delta\,(\ln k_B T/\gamma_0)^{-1}$. The second terms in Eq. (5.2.7) dominate if $k_B T \ll |E_F - E_0| \ll k_B T \ln k_B T/\gamma_0$. In this case the thermopower is simply $S = (E_F - E_0)/eT$, with exponential distribution

$$P(S) = \frac{eT}{\Delta}\mathrm{e}^{-2|S|eT/\Delta}. \tag{5.2.8}$$

The distribution (5.2.8) follows because the energy levels are uncorrelated, so that the spacing $|E_F - E_0|$ has an exponential distribution with a mean of $\Delta/2$.

We conclude that the thermopower distribution for $\gamma < k_B T \ll \Delta$ contains both Lorentzian and exponential contributions. The peak region $|S| \ll (k_B/e)\,(\ln k_B T/\gamma)^{-1}$ is the Lorentzian (5.2.5). The intermediate region $(k_B/e)\,(\ln k_B T/\gamma)^{-1} \ll |S| \ll (k_B/e) \ln k_B T/\gamma$ is the exponential (5.2.8). The far tails $|S| \gg (k_B/e) \ln k_B T/\gamma$ can not be explained by Eq. (5.2.7). With increasing temperature, the Lorentzian peak region shrinks, and ultimately the exponential region starts right at $S = 0$. This applies to the temperature range $\Delta\,(\ln k_B T/\gamma)^{-1} < k_B T \ll \Delta$.

To illustrate these various regimes, we computed $P(S)$ numerically from Eq.

(5.1.1). We took the density of states

$$\rho(E) = L^{-1} \sum_i \frac{\gamma_i/2\pi}{(E - E_i)^2 + \gamma_i^2/4}, \tag{5.2.9}$$

so that the conductance according to Eq. (5.2.1) has the energy dependence

$$G(E) \propto \prod_i \left[(E - E_i)^2 + \gamma_i^2/4 \right]^{-1}. \tag{5.2.10}$$

The levels E_i were chosen uniformly and independently (mean spacing Δ), but the fluctuations of the widths γ_i were ignored ($\gamma_i \equiv \gamma$ for all i). Such fluctuations are irrelevant in the low-temperature limit $k_B T \ll \gamma$, but not for $\gamma < k_B T \ll \Delta$. We believe that ignoring fluctuations in γ_i should still be a reasonable approximation, because γ_0 appears only in logarithms. The resulting $P(S)$ is plotted in Fig. 5-2. We see the expected crossover from a Lorentzian to an exponential. The exponential region appears as a plateau. Beyond the exponential region, the distribution appears to return to the Lorentzian form. We have no explanation for this far tail.

5.3 Chaotic quantum dot

In this section we consider a chaotic quantum dot with single-channel ballistic point contacts (see Fig. 5-3, inset). Because there are no tunnel barriers in the point contacts, the effects of the Coulomb blockade are small and here we ignore them altogether. For this system, the distribution of dT/dE was computed recently from random-matrix theory [8]. The energy derivative of the transmission probability has the parametrization

$$\frac{dT}{dE} = \frac{c}{\hbar}(\tau_1 - \tau_2)\sqrt{T(1-T)}, \tag{5.3.1}$$

with independent distributions

$$P(c) \propto (1 - c^2)^{-1+\beta/2}, \quad |c| < 1, \tag{5.3.2}$$

$$P(\tau_1, \tau_2) \propto |\tau_1 - \tau_2|^\beta (\tau_1 \tau_2)^{-2(\beta+1)} \mathrm{e}^{-(1/\tau_1 + 1/\tau_2)\pi\beta\hbar/\Delta}, \quad \tau_1, \tau_2 > 0, \tag{5.3.3}$$

$$P(T) \propto T^{-1+\beta/2}, \quad 0 < T < 1. \tag{5.3.4}$$

The integer β equals 1 or 2, depending on whether time-reversal symmetry is present or not. The times τ_1, τ_2 are the eigenvalues of the Wigner-Smith time-delay matrix (see Refs. [8] and [14]). Their sum $\tau_1 + \tau_2$ is the density of states (multiplied by $2\pi\hbar$). The thermopower distribution follows from

$$\begin{aligned} P(\sigma) \quad \propto & \quad \int_{-1}^{1} dc\, P(c) \int_0^\infty d\tau_1 \int_0^\infty d\tau_2\, P(\tau_1, \tau_2) \int_0^1 dT\, P(T) \\ & \times (\tau_1 + \tau_2) \delta\left(\sigma - (\Delta/2\pi\hbar) c (\tau_1 - \tau_2) \sqrt{1/T - 1}\right). \end{aligned} \tag{5.3.5}$$

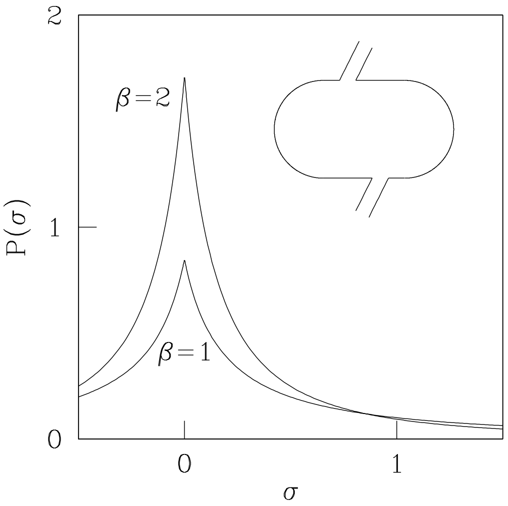

Figure 5-3. Distribution of the dimensionless thermopower of a chaotic cavity with two single-channel ballistic point contacts (inset), computed from Eq. (5.3.5) for the case of broken ($\beta = 2$) and unbroken ($\beta = 1$) time-reversal symmetry.

As in Refs. [8] and [15], the density of states appears as a weight factor $\tau_1 + \tau_2$ in the ensemble average (5.3.5), because the ensemble is generated by uniformly varying the charge on the quantum dot rather than its Fermi energy. This is the correct thing to do in the Hartree (self-consistent potential) approximation. A more sophisticated treatment of the electron-electron interactions (as advocated in Ref. [16]) does not yet exist for this problem. The resulting distributions are plotted in Fig. 5-3. The curves have a cusp at $\sigma = 0$, and asymptotes $P(\sigma) \propto |\sigma|^{-1-\beta} \ln |\sigma|$ for $|\sigma| \gg 1$.

5.4 Conclusion

The results we have reported hold for single-channel conductors. The generalization to multi-channel conductors is of interest. Multi-channel diffusive conductors were studied in Ref. [3]. For a chaotic cavity with ballistic point contacts having a large number of modes (N modes per point contact), the distribution of the thermopower is Gaussian. The mean is zero and the variance is

$$\operatorname{Var} S = \frac{k_{\mathrm{B}}^4 T^2 \pi^6}{9 e^2 N^4 \Delta^2 \beta}. \tag{5.4.1}$$

(We have used the results of Ref. [17].) Analogously to universal conductance fluctuations, the variance of the thermopower is reduced by a factor of 2 upon breaking time-reversal symmetry ($\beta = 1 \to \beta = 2$).

For an N-mode wire in the localized regime, our derivation of the exponential distribution of the thermopower remains valid. This is not true for the Lorentzian distribution. The reason is that the Herbert-Jones-Thouless formula for $N > 1$ relates the density of states to the sum of the inverse localization lengths [18], and there is no simple relation between this sum and the thermopower. We expect that the tail of the distribution remains quadratic, $P(S) \propto S^{-2}$ — because of the argument of Sec. 5.2.3, which is still valid for $N > 1$. It remains a challenge to determine analytically the entire thermopower distribution of a multi-channel disordered wire.

References

[1] Y. Imry, *Introduction to Mesoscopic Physics* (Oxford University, Oxford, 1997).

[2] P. Středa, J. Phys. C **1**, 1025 (1989); L. W. Molenkamp, Th. Gravier, H. van Houten, O. J. A. Buijk, M. A. A. Mabesoone, and C. T. Foxon, Phys. Rev. Lett. **65**, 1052 (1990); C. R. Proetto, Phys. Rev. B **44**, 9096 (1991); R. A. Wyss, C. C. Eugster, J. A. del Alamo, Q. Hu, M. J. Rooks, and M. R. Melloch, Appl. Phys. Lett. **66**, 1144 (1995).

[3] A. V. Anisovich, B. L. Alt'shuler, A. G. Aronov, and A. Yu. Zyuzin, Pis'ma Zh. Eksp. Teor. Fiz. **45**, 237 (1987) [JETP Lett. **45**, 295 (1987)]; G. B. Lesovik and D. E. Khmel'nitskiĭ, Zh. Eksp. Teor. Fiz. **94**, 164 (1988) [Sov. Phys. JETP **67**, 957 (1988)]; R. A. Serota, M. Ma, and B. Goodman, Phys. Rev. B **37**, 6540 (1988); G. M. Gusev, Z. D. Kvon, and A. G. Pogosov, Pis'ma Zh. Eksp. Teor. Fiz. **51**, 151 (1990) [JETP Lett. **51**, 171 (1990)]; B. L. Gallagher, T. Galloway, P. Beton, J. P. Oxley, S. P. Beaumont, S. Thoms, and C. D. W. Wilkinson, Phys. Rev. Lett. **64**, 2058 (1990); D. P. DiVincenzo, Phys. Rev. B **48**, 1404 (1993).

[4] C. W. J. Beenakker and A. A. M. Staring, Phys. Rev. B **46**, 9667 (1992); A. S. Dzurak, C. G. Smith, M. Pepper, D. A. Ritchie, J. E. F. Frost, G. A. C. Jones, and D. G. Hasko, Sol. State Comm. **87**, 1145 (1993); A. A. M. Staring, L. W. Molenkamp, B. W. Alphenaar, H. van Houten, O. J. A. Buijk, M. A. A. Mabesoone, C. W. J. Beenakker, and C. T. Foxon, Europhys. Lett. **22**, 57 (1993); A. S. Dzurak, C. G. Smith, C. H. W. Barnes, M. Pepper, L. Martin-Moreno, C. T. Liang, D. A. Ritchie, and G. A. C. Jones, Phys. Rev. B **55**, R10197 (1997).

[5] Ya. M. Blanter, C. Bruder, R. Fazio, and H. Schoeller, Phys. Rev. B **55**, 4069 (1997).

[6] C. W. J. Beenakker, Rev. Mod. Phys. **69**, 731 (1997).

[7] T. Guhr, A. Müller-Groeling, and H. A. Weidenmüller, Phys. Rep. (to be published).

[8] P. W. Brouwer, S. A. van Langen, K. M. Frahm, M. Büttiker, and C. W. J. Beenakker, Phys. Rev. Lett. **79**, 913 (1997).

[9] M. Cutler and N. F. Mott, Phys. Rev. **181**, 1336 (1969).

[10] U. Sivan and Y. Imry, Phys. Rev. B **33**, 551 (1986).

[11] R. Landauer, IBM J. Res. Dev. **1**, 223 (1957).

[12] D. C. Herbert and R. Jones, J. Phys. C **4**, 1145 (1971); D. J. Thouless, J. Phys. C **5**, 77 (1972).

[13] O. N. Dorokhov, Zh. Eksp. Teor. Fiz. **101**, 966 (1992) [Sov. Phys. JETP **74**, 518 (1992)].

[14] Y. V. Fyodorov and H.-J. Sommers, J. Math. Phys. **38**, 1918 (1997).

[15] M. H. Pedersen, S. A. van Langen, and M. Büttiker, Phys. Rev. B **57**, 1838 (1998).

[16] I. L. Aleiner and L. I. Glazman, Phys. Rev. B **57**, 9608 (1998); preprint (cond-mat/9612138).

[17] K. B. Efetov, Phys. Rev. Lett. **74**, 2299 (1995); K. Frahm, Europhys. Lett. **30**, 457 (1995).

[18] W. Craig and B. Simon, Comm. Math. Phys. **90**, 207 (1983).

6 Berry phase and adiabaticity of a spin diffusing in a non-uniform magnetic field

6.1 Introduction

The adiabatic theorem of quantum mechanics implies that the final state of a particle that moves slowly along a closed path is identical to the initial eigenstate — up to a phase factor. The Berry phase is a time-independent contribution to this phase, depending only on the geometry of the path [1]. A simple example is a spin-1/2 in a rotating magnetic field **B**, where the Berry phase equals half the solid angle swept by **B**. It was proposed by Stern [2] to measure the Berry phase in the conductance G of a mesoscopic ring in a spatially rotating magnetic field. Oscillations of G as a function of the swept solid angle were predicted, similar to the Aharonov-Bohm oscillations as a function of the enclosed flux [3].

An important practical difference between the two effects is that the Aharonov-Bohm oscillations exist at arbitrarily small magnetic fields, whereas for the oscillations due to the Berry phase the magnetic field should be sufficiently strong to allow the spin to adiabatically follow the changing direction. Generally speaking, adiabaticity requires that the precession frequency ω_B is large compared to the reciprocal of the characteristic timescale t_c on which **B** changes direction. We know that $\omega_\mathrm{B} = g\mu_\mathrm{B}B/2\hbar$, with g the Landé-factor and μ_B the Bohr magneton. The question is, what is t_c? In a ballistic ring there is only one candidate, the circumference L of the ring divided by the Fermi velocity v. (For simplicity we assume that L is also the scale on which the field direction changes.) In a diffusive ring there are two candidates: the elastic scattering time τ and the diffusion time τ_d around the ring. They differ by a factor $\tau_\mathrm{d}/\tau \simeq (L/\ell)^2$, where $\ell = v\tau$ is the mean free path. Since, by definition, $L \gg \ell$ in a diffusive system, the two time scales are far apart. Which of the two time scales is the relevant one is still under debate [4].

Stern's original proposal [2] was that

$$\omega_\mathrm{B} \gg \frac{1}{\tau} \tag{6.1.1}$$

is necessary to observe the Berry-phase oscillations. For realistic values of g this requires magnetic fields in the quantum Hall regime, outside the range of validity of the semiclassical theory. We call Eq. (6.1.1) the "pessimistic criterion". In a later work [5], Loss, Schoeller, and Goldbart (LSG) concluded that adiabaticity is reached already at much weaker magnetic fields, when

$$\omega_\mathrm{B} \gg \frac{1}{\tau_\mathrm{d}} \simeq \frac{1}{\tau}\left(\frac{\ell}{L}\right)^2 . \tag{6.1.2}$$

This “optimistic criterion” has motivated experimentalists to search for the Berry-phase oscillations in disordered conductors [6], and was invoked in a recent study of the conductivity of mesoscopic ferromagnets [7]. In this paper, we re-examine the semiclassical theory of LSG to resolve the controversy.

The Berry-phase oscillations in the conductance result from a periodic modulation of the weak-localization correction, and require the solution of a diffusion equation for the Cooperon propagator. To solve this problem we need to consider the coupled dynamics of four spin-degrees of freedom. (The Cooperon has four spin indices.) To gain insight we first examine in Sec. 6.2 the simpler problem of the dynamics of a single spin variable, by studying the randomization of a spin-polarized electron gas by a non-uniform magnetic field. We start at the level of the Boltzmann equation and then make the diffusion approximation. We show how the diffusion equation can be solved exactly for the first two moments of the polarization. The same procedure is used in Sec. 6.3 to arrive at a diffusion equation for the Cooperon. This equation coincides with the equation derived by LSG in the weak-field regime $\omega_{\mathrm{B}}\tau \ll 1$, but is different in the strong-field regime $\omega_{\mathrm{B}}\tau \gtrsim 1$. We present an exact solution for the weak-localization correction and compare with the findings of LSG.

Our conclusion both for the polarization and for the weak-localization correction is that adiabaticity requires $\omega_{\mathrm{B}}\tau \gg 1$. Regrettably, the pessimistic criterion (6.1.1) is correct, in agreement with Stern’s original conclusion. The optimistic criterion (6.1.2) advocated by LSG turns out to be the criterion for maximal randomization of the spin by the magnetic field, and not the criterion for adiabaticity.

6.2 Spin-resolved transmission

6.2.1 Formulation of the problem

Consider a conductor in a magnetic field $\mathbf{B}$, containing a disordered segment (length L, mean free path ℓ at Fermi velocity v) in which the magnetic field changes its direction. An electron at the Fermi level with spin up (relative to the local magnetic field) is injected at one end and reaches the other end. What is the probability that its spin is up?

For simplicity we take for the conductor a two-dimensional electron gas (in the x-y plane, with the disordered region between $x = 0$ and $x = L$), and we ignore the curvature of the electron trajectories by the Lorentz force. The problem becomes effectively one-dimensional by assuming that $\mathbf{B}$ depends on x only. We choose a rotation of $\mathbf{B}$ in the x-y-plane, according to

$$\mathbf{B}(x, y, z = 0) = \left(B \sin\eta \cos\tfrac{2\pi f x}{L}, B \sin\eta \sin\tfrac{2\pi f x}{L}, B\cos\eta\right), \qquad (6.2.1)$$

with η and f arbitrary parameters. The geometry is sketched in Fig. 6-1. We treat the orbital motion semiclassically, within the framework of the Boltzmann

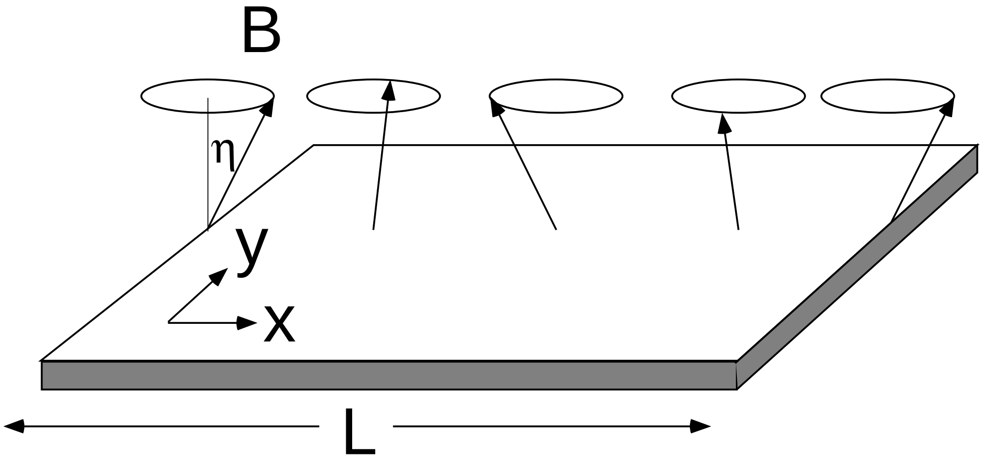

Figure 6-1. Schematic drawing of a two-dimensional electron gas in the spatially rotating magnetic field of Eq. (6.2.1), with $f = 1$.

equation. (This is justified if the Fermi wavelength is much smaller than ℓ.) The spin dynamics requires a fully quantum mechanical treatment. We assume that the Zeeman energy $g\mu_B B$ is much smaller than the Fermi energy $\frac{1}{2}mv^2$, so that the orbital motion is independent of the spin.

We introduce the probability density $P(x, \phi, \xi, t)$ for the electron to be at time t at position x with velocity $\mathbf{v} = (v \cos\phi, v \sin\phi, 0)$, in the spin state with spinor $\xi = (\xi_1, \xi_2)$. The dynamics of ξ depends on the local magnetic field according to

$$\frac{d\xi}{dt} = \frac{ig\mu_B}{2\hbar}\mathbf{B} \cdot \boldsymbol{\sigma}\,\xi, \tag{6.2.2}$$

where $\boldsymbol{\sigma} = (\sigma_x, \sigma_y, \sigma_z)$ is the vector of Pauli matrices. It is convenient to decompose $\xi = \chi_1\xi_\uparrow + \chi_2\xi_\downarrow$ into the local eigenstates $\xi_\uparrow, \xi_\downarrow$ of $\mathbf{B} \cdot \boldsymbol{\sigma}$,

$$\xi_\uparrow = \begin{pmatrix} \cos\frac{\eta}{2}\,\mathrm{e}^{-i\pi f x/L} \\ \sin\frac{\eta}{2}\,\mathrm{e}^{i\pi f x/L} \end{pmatrix}, \quad \xi_\downarrow = \begin{pmatrix} -\sin\frac{\eta}{2}\,\mathrm{e}^{-i\pi f x/L} \\ \cos\frac{\eta}{2}\,\mathrm{e}^{i\pi f x/L} \end{pmatrix}, \tag{6.2.3}$$

$$\mathbf{B} \cdot \boldsymbol{\sigma}\,\xi_\uparrow = B\xi_\uparrow, \quad \mathbf{B} \cdot \boldsymbol{\sigma}\,\xi_\downarrow = -B\xi_\downarrow, \tag{6.2.4}$$

and use the real and imaginary parts of the coefficients χ_1, χ_2 as variables in the Boltzmann equation. The dynamics of the vector of coefficients $c = (c_1, c_2, c_3, c_4) = (\mathrm{Re}\,\chi_1, \mathrm{Im}\,\chi_1, \mathrm{Re}\,\chi_2, \mathrm{Im}\,\chi_2)$ is given by

$$\frac{dc}{dt} = \frac{1}{\tau}Mc, \quad M = M_0 + M_1 \cos\phi, \tag{6.2.5}$$

$$M_0 = \omega_B\tau \begin{pmatrix} 0 & -1 & 0 & 0 \\ 1 & 0 & 0 & 0 \\ 0 & 0 & 0 & 1 \\ 0 & 0 & -1 & 0 \end{pmatrix}, \tag{6.2.6}$$

$$M_1 = \frac{\pi f \ell}{L} \begin{pmatrix} 0 & -\cos\eta & 0 & \sin\eta \\ \cos\eta & 0 & -\sin\eta & 0 \\ 0 & \sin\eta & 0 & \cos\eta \\ -\sin\eta & 0 & -\cos\eta & 0 \end{pmatrix}, \tag{6.2.7}$$

where $\omega_{\rm B} = g\mu_{\rm B}B/2\hbar$ is the precession frequency of the spin. The Boltzmann equation takes the form

$$\tau\frac{\partial}{\partial t}P(x,\phi,c,t) = -\ell\cos\phi\frac{\partial P}{\partial x} - \sum_{i,j}\frac{\partial}{\partial c_i}(M_{ij}c_jP) - P + \int_0^{2\pi}\frac{d\phi'}{2\pi}P(x,\phi',c,t), \tag{6.2.8}$$

where we have assumed isotropic scattering (rate $1/\tau = v/\ell$).

We look for a stationary solution to the Boltzmann equation, so the left-hand-side of Eq. (6.2.8) is zero and we omit the argument t of P. A stationary flux of particles with an isotropic velocity distribution is injected at $x = 0$, their spins all aligned with the local magnetic field (so $\chi_2 = 0$ at $x = 0$). Without loss of generality we may assume that $\chi_1 = 1$ at $x = 0$. No particles are incident from the other end, at $x = L$. Thus the boundary conditions are

$$P(x=0,\phi,c) = \delta(c_1-1)\delta(c_2)\delta(c_3)\delta(c_4) \text{ if } \cos\phi > 0, \tag{6.2.9}$$

$$P(x=L,\phi,c) = 0 \text{ if } \cos\phi < 0. \tag{6.2.10}$$

This completes the formulation of the problem. We compare two methods of solution. The first is an exact numerical solution of the Boltzmann equation using the Monte Carlo method. The second is an approximate analytical solution using the diffusion approximation, valid for $L \gg \ell$. We begin with the latter.

6.2.2 Diffusion approximation

The diffusion approximation amounts to the assumption that P has a simple cosine-dependence on ϕ,

$$P(x,\phi,c) = N(x,c) + J(x,c)\cos\phi. \tag{6.2.11}$$

To determine the density N and current J we substitute Eq. (6.2.11) into Eq. (6.2.8) and integrate over ϕ. This gives

$$\ell\frac{\partial J}{\partial x} = -\frac{\partial}{\partial c}(2M_0cN + M_1cJ). \tag{6.2.12}$$

Similarly, multiplication with $\cos\phi$ before integration gives

$$\ell\frac{\partial N}{\partial x} = -\frac{\partial}{\partial c}(M_0cJ + M_1cN) - J. \tag{6.2.13}$$

Thus we have a closed set of partial differential equations for the unknown functions $N(x,c)$ and $J(x,c)$. Boundary conditions are obtained by multiplying

Eq. (6.2.9-6.2.10) with $\cos\phi$ and integrating over ϕ:

$$N(x=0,c)+\frac{\pi}{4}J(x=0,c)=\delta(c_1-1)\delta(c_2)\delta(c_3)\delta(c_4), \tag{6.2.14}$$

$$N(x=L,c)-\frac{\pi}{4}J(x=L,c)=0. \tag{6.2.15}$$

We seek the spin polarization $p=c_1^2+c_2^2-c_3^2-c_4^2$ of the transmitted electrons, characterized by the distribution

$$P(p)=\frac{\int dc\, J(x=L,c)\delta(c_1^2+c_2^2-c_3^2-c_4^2-p)}{\int dc\, J(x=L,c)}. \tag{6.2.16}$$

(The notation $\int dc \equiv \int dc_1 \int dc_2 \int dc_3 \int dc_4$ indicates an integration over the spin variables.) We compute the first two moments of $P(p)$. The first moment $\overline{p}$ is the fraction of transmitted electrons with spin up minus the fraction with spin down, averaged quantum mechanically over the spin state and statistically over the disorder. The variance $\mathrm{Var}\, p=\overline{p^2}-\overline{p}^2$ gives an indication of the magnitude of the statistical fluctuations.

Integration of Eqs. (6.2.12)–(6.2.15) over the spin variables yields the equations and boundary conditions for the functions $N(x)=\int dc\, N(x,c)$ and $J(x)=\int dc\, J(x,c)$:

$$\ell\frac{dN}{dx}=-J,\quad \frac{dJ}{dx}=0, \tag{6.2.17}$$

$$N(0)+\frac{\pi}{4}J(0)=1,\quad N(L)-\frac{\pi}{4}J(L)=0. \tag{6.2.18}$$

The solution

$$J(x)=\left(\frac{\pi}{2}+\frac{L}{\ell}\right)^{-1} \tag{6.2.19}$$

determines the denominator of Eq. (6.2.16).

To determine $\overline{p}$ we multiply Eqs. (6.2.12) and (6.2.13) with $\chi_\alpha\chi_\beta^*$ and integrate over c. (Recall that $\chi_1=c_1+ic_2, \chi_2=c_3+ic_4$.) It follows upon partial integration that

$$\int dc\, \chi_\alpha\chi_\beta^*\frac{\partial}{\partial c}(M_0 c f)=-\sum_{\rho,\sigma}(S_{\alpha\rho}\delta_{\beta\sigma}-\delta_{\alpha\rho}S_{\beta\sigma})\int dc\, \chi_\rho\chi_\sigma^* f, \tag{6.2.20}$$

$$\int dc\, \chi_\alpha\chi_\beta^*\frac{\partial}{\partial c}(M_1 c f)=-\sum_{\rho,\sigma}(T_{\alpha\rho}\delta_{\beta\sigma}-\delta_{\alpha\rho}T_{\beta\sigma})\int dc\, \chi_\rho\chi_\sigma^* f, \tag{6.2.21}$$

for arbitrary functions $f(x,c)$. The 2×2 matrices S, T are defined by

$$S=i\omega_{\mathrm{B}}\tau\sigma_z,\quad T=\frac{i\pi f\ell}{L}(\sigma_z\cos\eta-\sigma_x\sin\eta). \tag{6.2.22}$$

In this way we find that the moments

$$\begin{aligned} N_{\alpha\beta}(x) &= \int dc\,\chi_\alpha\chi_\beta^* N(x,c), && (6.2.23)\\ J_{\alpha\beta}(x) &= \int dc\,\chi_\alpha\chi_\beta^* J(x,c), && (6.2.24)\end{aligned}$$

satisfy the ordinary differential equations

$$\begin{aligned} \ell\frac{dN_{\alpha\beta}}{dx} &= \sum_{\rho,\sigma}\left(T_{\alpha\rho}\delta_{\beta\sigma}-\delta_{\alpha\rho}T_{\beta\sigma}\right)N_{\rho\sigma}\\ &\quad+\sum_{\rho,\sigma}\left(S_{\alpha\rho}\delta_{\beta\sigma}-\delta_{\alpha\rho}S_{\beta\sigma}\right)J_{\rho\sigma}-J_{\alpha\beta}, && (6.2.25)\\ \ell\frac{dJ_{\alpha\beta}}{dx} &= 2\sum_{\rho,\sigma}\left(S_{\alpha\rho}\delta_{\beta\sigma}-\delta_{\alpha\rho}S_{\beta\sigma}\right)N_{\rho\sigma}\\ &\quad+\sum_{\rho,\sigma}\left(T_{\alpha\rho}\delta_{\beta\sigma}-\delta_{\alpha\rho}T_{\beta\sigma}\right)J_{\rho\sigma}, && (6.2.26)\end{aligned}$$

with boundary conditions

$$\begin{aligned} N_{\alpha\beta}(x=0)+\frac{\pi}{4}J_{\alpha\beta}(x=0) &= \delta_{\alpha 1}\delta_{\beta 1}, && (6.2.27)\\ N_{\alpha\beta}(x=L)-\frac{\pi}{4}J_{\alpha\beta}(x=L) &= 0. && (6.2.28)\end{aligned}$$

The mean polarization $\overline{p}$ is determined by $J_{\alpha\beta}$ according to

$$\overline{p}=\frac{J_{11}(L)-J_{22}(L)}{J(L)}=\left(\frac{\pi}{2}+\frac{L}{\ell}\right)\left[J_{11}(L)-J_{22}(L)\right]. \qquad (6.2.29)$$

Since Eq. (6.2.25-6.2.26) is linear in the 8 functions $N_{\alpha\beta}(x), J_{\alpha\beta}(x)$ ($\alpha,\beta = 1,2$), a solution requires the eigenvalues and right eigenvectors of the 8×8 matrix of coefficients. These can be readily computed numerically for any values of L/ℓ and $\omega_B\tau$. We have found an analytic asymptotic solution for $L/\ell \gg 1$ and $\omega_B\tau \gg (f\ell/L)^2$, given by

$$\overline{p}=\frac{k}{\sinh k},\quad k=\frac{2\pi f\sin\eta}{\sqrt{1+(2\omega_B\tau)^2}}. \qquad (6.2.30)$$

In Fig. 6-2 we compare the numerical solution (solid curve) with Eq. (6.2.30) (dashed curve) for $L/\ell = 25$ and $\eta = \pi/3, f = 1$. The two curves are almost indistinguishable, except for the smallest values of $\omega_B\tau$.

In a similar way, we compute the second moment of $P(p)$ by multiplying Eqs. (6.2.12) and (6.2.13) with $\chi_\alpha\chi_\beta^*\chi_\gamma\chi_\delta^*$ and integrating over c. The result is a closed set of equations

$$\ell\frac{d}{dx}N_{\alpha\beta\gamma\delta}=\sum_{\mu,\nu,\rho,\sigma}\left(L^{\mu\nu\rho\sigma}_{\alpha\beta\gamma\delta}N_{\mu\nu\rho\sigma}+K^{\mu\nu\rho\sigma}_{\alpha\beta\gamma\delta}J_{\mu\nu\rho\sigma}\right)-J_{\alpha\beta\gamma\delta}, \qquad (6.2.31)$$

$$\ell\frac{d}{dx}J_{\alpha\beta\gamma\delta}=\sum_{\mu,\nu,\rho,\sigma}\left(2K^{\mu\nu\rho\sigma}_{\alpha\beta\gamma\delta}N_{\mu\nu\rho\sigma}+L^{\mu\nu\rho\sigma}_{\alpha\beta\gamma\delta}J_{\mu\nu\rho\sigma}\right), \qquad (6.2.32)$$

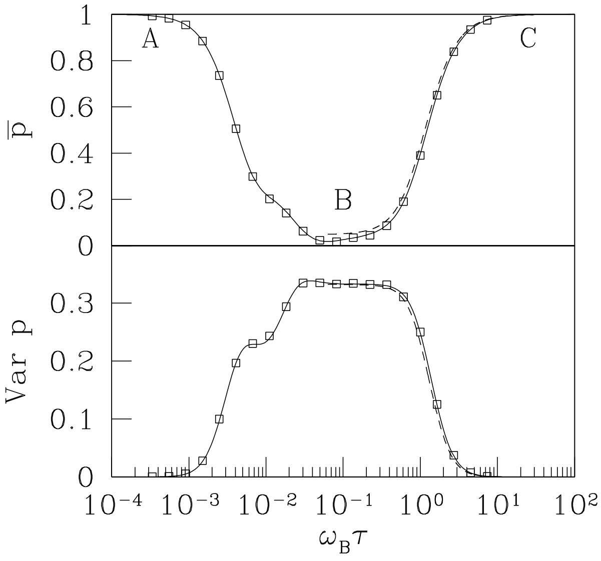

Figure 6-2. Average and variance of the spin polarization p of the current transmitted through a two-dimensional region of length $L = 25\,\ell$, as a function of $\omega_B\tau$, for a magnetic field given by Eq. (6.2.1) with $\eta = \pi/3$ and $f = 1$. The data points result from Monte Carlo simulations of the Boltzmann equation (6.2.8), the solid curves result from the diffusion approximation (6.2.11), and the dashed curves are the asymptotic formulas (6.2.30) and (6.2.40). Notice the transient regime (A), the randomized regime (B), and the adiabatic regime (C).

where we have defined

$$\begin{aligned} K^{\mu\nu\rho\sigma}_{\alpha\beta\gamma\delta} &= S_{\alpha\mu}\delta_{\beta\nu}\delta_{\gamma\rho}\delta_{\delta\sigma} - \delta_{\alpha\mu}S_{\beta\nu}\delta_{\gamma\rho}\delta_{\delta\sigma} \\ &\quad +\delta_{\alpha\mu}\delta_{\beta\nu}S_{\gamma\rho}\delta_{\delta\sigma} - \delta_{\alpha\mu}\delta_{\beta\nu}\delta_{\gamma\rho}S_{\delta\sigma}, \qquad (6.2.33) \\ L^{\mu\nu\rho\sigma}_{\alpha\beta\gamma\delta} &= T_{\alpha\mu}\delta_{\beta\nu}\delta_{\gamma\rho}\delta_{\delta\sigma} - \delta_{\alpha\mu}T_{\beta\nu}\delta_{\gamma\rho}\delta_{\delta\sigma} \\ &\quad +\delta_{\alpha\mu}\delta_{\beta\nu}T_{\gamma\rho}\delta_{\delta\sigma} - \delta_{\alpha\mu}\delta_{\beta\nu}\delta_{\gamma\rho}T_{\delta\sigma}, \qquad (6.2.34) \end{aligned}$$

$$N_{\alpha\beta\gamma\delta}(x) = \int dc\, \chi_\alpha\chi^*_\beta\chi_\gamma\chi^*_\delta N(x,c), \qquad (6.2.35)$$

$$J_{\alpha\beta\gamma\delta}(x) = \int dc\, \chi_\alpha\chi^*_\beta\chi_\gamma\chi^*_\delta J(x,c). \qquad (6.2.36)$$

The boundary conditions on the functions $N_{\alpha\beta\gamma\delta}$ and $J_{\alpha\beta\gamma\delta}$ are

$$N_{\alpha\beta\gamma\delta}(x=0) + \frac{\pi}{4}J_{\alpha\beta\gamma\delta}(x=0) = \delta_{\alpha1}\delta_{\beta1}\delta_{\gamma1}\delta_{\delta1}, \qquad (6.2.37)$$

$$N_{\alpha\beta\gamma\delta}(x=L) - \frac{\pi}{4}J_{\alpha\beta\gamma\delta}(x=L) = 0. \qquad (6.2.38)$$

The second moment $\overline{p^2}$ is determined by

$$\overline{p^2} = \left(\frac{\pi}{2} + \frac{L}{\ell}\right) [J_{1111}(x = L) - J_{1122}(x = L) - J_{2211}(x = L) + J_{2222}(x = L)] . \tag{6.2.39}$$

The numerical solution is plotted also in Fig. 6-2, together with the asymptotic expression

$$\operatorname{Var} p = \frac{1}{3} + \frac{2k\sqrt{3}}{3\sinh(k\sqrt{3})} - \frac{k^2}{\sinh^2 k}. \tag{6.2.40}$$

It is evident from Eqs. (6.2.30) and (6.2.40), and from Fig. 6-2, that the regime with $\overline{p} = 1$, $\operatorname{Var} p = 0$ is entered for $\omega_B\tau \gtrsim f$ [for $\sin\eta = \mathcal{O}(1)$], in agreement with Stern's criterion (6.1.1) for adiabaticity. For smaller $\omega_B\tau$ adiabaticity is lost. There is a transient regime $\omega_B\tau \ll (f\ell/L)^2$, in which the precession frequency is so low that the spin remains in the same state during the entire diffusion process. For $(f\ell/L)^2 \ll \omega_B\tau \ll f$ the average polarization reaches a plateau value close to zero with a finite variance. For a sufficiently non-uniform field, $f\sin\eta \gg 1$, we find in this regime $\overline{p} = 0$ and $\operatorname{Var} p = 1/3$, which means that the spin state is completely randomized. The transient regime, the randomized regime, and the adiabatic regime are indicated in Fig. 6-2 by the letters A, B, and C.

6.2.3 Comparison with Monte Carlo simulations

In order to check the diffusion approximation we solved the full Boltzmann equation by means of a Monte Carlo simulation. A particle is moved from $x = 0$ over a distance ℓ_1 in the direction ϕ_1, then over a distance ℓ_2 in the direction ϕ_2, and so on, until it is reflected back to $x = 0$ or transmitted to $x = L$. The step lengths ℓ_i are chosen randomly from a Poisson distribution with mean ℓ. The directions ϕ_i are chosen uniformly from $[0, 2\pi]$, except for the initial direction ϕ_1, which is distributed $\propto \cos\phi_1$. The spin components are given by

$$\begin{pmatrix} \chi_1 \\ \chi_2 \end{pmatrix} = \prod_i \mathrm{e}^{(S + T\cos\phi_i)\ell_i/\ell} \begin{pmatrix} 1 \\ 0 \end{pmatrix}. \tag{6.2.41}$$

To find $\overline{p^n}$, one has to average $(|\chi_1|^2 - |\chi_2|^2)^n$ over the transmitted particles. The results for $L/\ell = 25$ are shown in Fig. 6-2 (data points). They agree very well with the results of the previous subsection, thus confirming the validity of the diffusion approximation for $L/\ell \gg 1$.

6.3 Weak localization

6.3.1 Formulation of the problem

We turn to the effect of the non-uniform magnetic field on the weak-localization correction of a multiply-connected system. We consider the same geometry as in Fig. 6-1, but now with periodic boundary conditions — to model a ring of circumference L. Only the effects of the magnetic field on the spin are included, to isolate the Berry phase from the conventional Aharonov-Bohm phase. As in the previous subsection, we assume that the orbital motion is independent of the spin dynamics. We follow LSG in applying the semiclassical theory of Chakravarty and Schmidt [8] to the problem, however, we start at the level of the Boltzmann equation — rather than at the level of the diffusion equation — and make the diffusion approximation at a later stage of the calculation.

The weak-localization correction ΔG to the conductance is given by

$$\Delta G = -\frac{e^2 D}{\pi \hbar L} \int_0^\infty dt \, \mathrm{e}^{-t/\tau_\varphi} C(t), \tag{6.3.1}$$

where τ_φ is the phase coherence time and the diffusion coefficient $D = vl/d$ in d dimensions. (In our geometry $d = 2$.) The "return quasi-probability" $C(t)$ is expressed as a sum over "Boltzmannian walks" $\mathbf{R}(t)$ with $\mathbf{R}(0) = \mathbf{R}(t)$,

$$C(t) = \sum_{\{\mathbf{R}(t)\}} W \, \mathrm{Tr}\,(U^+ U^-). \tag{6.3.2}$$

Here $W[\mathbf{R}(t)]$ is the weight of the Boltzmannian walk for a spinless particle. The 2×2 matrices $U^\pm[\mathbf{R}(t)]$ are defined by

$$U^\pm = \mathcal{T} \exp\left\{ \pm \frac{ig\mu_\mathrm{B}}{2\hbar} \int_0^t dt' \, \mathbf{B}(\mathbf{R}(t')) \cdot \boldsymbol{\sigma} \right\}, \tag{6.3.3}$$

where $\mathcal{T}$ denotes a time ordering. The factor $\mathrm{Tr}\,(U^+ U^-)$ in Eq. (6.3.2) accounts for the phase difference of time-reversed paths.

The Cooperon can be written in terms of a propagator χ,

$$C(t) = \frac{1}{2\pi} \int_0^{2\pi} d\phi \int_0^{2\pi} d\phi_\mathrm{i} \sum_{\alpha,\beta} \chi_{\alpha\beta\beta\alpha}(x_\mathrm{i}, x_\mathrm{i}; \phi, \phi_\mathrm{i}; t), \tag{6.3.4}$$

that satisfies the kinetic equation

$$\begin{aligned} &\left(\frac{\partial}{\partial t} + \mathcal{B} \right) \chi_{\alpha\beta\gamma\delta}(x, x_\mathrm{i}; \phi, \phi_\mathrm{i}; t) \\ &- \frac{ig\mu_\mathrm{B}}{2\hbar} \sum_{\alpha',\gamma'} \left[(\mathbf{B}(x) \cdot \boldsymbol{\sigma})_{\alpha\alpha'} \delta_{\gamma\gamma'} - \delta_{\alpha\alpha'} (\mathbf{B}(x) \cdot \boldsymbol{\sigma})_{\gamma\gamma'} \right] \chi_{\alpha'\beta\gamma'\delta} \\ &= \delta(t) \delta(x - x_\mathrm{i}) \delta(\phi - \phi_\mathrm{i}) \delta_{\alpha\beta} \delta_{\gamma\delta}. \end{aligned} \tag{6.3.5}$$

The Boltzmann operator $\mathcal{B}$ is given by

$$\mathcal{B} = v \cos\phi \frac{\partial}{\partial x} + \frac{1}{\tau} - \frac{1}{\tau} \int_0^{2\pi} \frac{d\phi}{2\pi}. \tag{6.3.6}$$

The propagator χ is a moment of the probability distribution $P(x,\phi,U^+,U^-,t)$,

$$\chi_{\alpha\beta\gamma\delta} = \int dU^+ \int dU^-\, U^+_{\alpha\beta}U^-_{\gamma\delta}P, \tag{6.3.7}$$

that satisfies the Boltzmann equation

$$\left[\frac{\partial}{\partial t} + \mathcal{B} + \frac{\partial}{\partial U^+}\left(\frac{dU^+}{dt}\right) + \frac{\partial}{\partial U^-}\left(\frac{dU^-}{dt}\right)\right] P(x,\phi,U^+,U^-,t) = 0, \tag{6.3.8}$$

with initial condition

$$P(x,\phi,U^+,U^-,0) = \delta(x-x_{\rm i})\delta(\phi-\phi_{\rm i})\delta(U^+-\mathbb{1})\delta(U^--\mathbb{1}). \tag{6.3.9}$$

The notation dU^+ or dU^- indicates the differential of the real and imaginary parts of the elements of the 2 × 2 matrix U^+ or U^-. We will write this in a more explicit way in the next subsection.

The Boltzmann equation (6.3.8) has the same form as that which we studied in Sec. 6.2. The difference is that we have four times as many internal degrees of freedom. Instead of a single spinor ξ we now have two spinor matrices U^+ and U^-. A first doubling of the number of degrees of freedom occurs because we have to follow the evolution of both spin up and spin down. A second doubling occurs because we have to follow both the normal and the time-reversed evolution.

6.3.2 Diffusion approximation

We make the diffusion approximation to the Boltzmann equation (6.3.8), by following the steps outlined in Sec. 6.2. The 4×2 matrix $u^\pm$ containing the real and imaginary parts of $U^\pm$,

$$u^\pm = \begin{pmatrix} \operatorname{Re}U^\pm_{11} & \operatorname{Re}U^\pm_{12} \\ \operatorname{Im}U^\pm_{11} & \operatorname{Im}U^\pm_{12} \\ \operatorname{Re}U^\pm_{21} & \operatorname{Re}U^\pm_{22} \\ \operatorname{Im}U^\pm_{21} & \operatorname{Im}U^\pm_{22} \end{pmatrix}, \tag{6.3.10}$$

has a time evolution governed by

$$\tau\frac{du^\pm}{dt} = \pm Z(x)u^\pm, \tag{6.3.11}$$

$$\frac{Z(x)}{\omega_{\rm B}\tau} = \begin{pmatrix} 0 & -\cos\eta & \sin\eta\sin\psi & -\sin\eta\cos\psi \\ \cos\eta & 0 & \sin\eta\cos\psi & \sin\eta\sin\psi \\ -\sin\eta\sin\psi & -\sin\eta\cos\psi & 0 & \cos\eta \\ \sin\eta\cos\psi & -\sin\eta\sin\psi & -\cos\eta & 0 \end{pmatrix}, \tag{6.3.12}$$

$$\psi = 2\pi f x/L. \tag{6.3.13}$$

The Boltzmann equation (6.3.8) becomes, in a more explicit notation,

$$\begin{aligned}\tau\frac{\partial}{\partial t}P(x,\phi,u^+,u^-,t) &= -\ell\cos\phi\frac{\partial P}{\partial x}\\ &\quad -\sum_{i,j,k}\frac{\partial}{\partial u^+_{ij}}Z_{ik}(x)u^+_{kj}P+\sum_{i,j,k}\frac{\partial}{\partial u^-_{ij}}Z_{ik}(x)u^-_{kj}P\\ &\quad -P+\int_0^{2\pi}\frac{d\phi'}{2\pi}P(x,\phi',u^+,u^-,t). \qquad (6.3.14)\end{aligned}$$

We now make the diffusion ansatz in the form

$$\int_0^\infty dt\,\mathrm{e}^{-t/\tau_\varphi}\int_0^{2\pi}d\phi_\mathrm{i}\,P=N+J\cos\phi. \qquad (6.3.15)$$

By integrating the Boltzmann equation over ϕ, once with weight 1 and once with weight $\cos\phi$, we obtain two coupled equations for the functions $N(x,u^+,u^-)$ and $J(x,u^+,u^-)$. Next we multiply both equations with $U^+_{\alpha\beta}U^-_{\gamma\delta}$ and integrate over the real and imaginary parts of the matrix elements. The moments $N_{\alpha\beta\gamma\delta}$ and $J_{\alpha\beta\gamma\delta}$ defined by

$$\begin{aligned}N_{\alpha\beta\gamma\delta}(x) &= \int dU^+\int dU^-\,U^+_{\alpha\beta}U^-_{\gamma\delta}N, \qquad (6.3.16)\\ J_{\alpha\beta\gamma\delta}(x) &= \int dU^+\int dU^-\,U^+_{\alpha\beta}U^-_{\gamma\delta}J, \qquad (6.3.17)\end{aligned}$$

are found to obey the ordinary differential equations

$$\begin{aligned}\ell\frac{dN_{\alpha\beta\gamma\delta}}{dx} &= \frac{ig\mu_\mathrm{B}\tau}{2\hbar}\sum_{\alpha',\gamma'}\Big[(\mathbf{B}(x)\cdot\boldsymbol{\sigma})_{\alpha\alpha'}\delta_{\gamma\gamma'}-\delta_{\alpha\alpha'}(\mathbf{B}(x)\cdot\boldsymbol{\sigma})_{\gamma\gamma'}\Big]J_{\alpha'\beta\gamma'\delta}\\ &\quad -(1+\tau/\tau_\varphi)\,J_{\alpha\beta\gamma\delta}, \qquad (6.3.18)\\ \ell\frac{dJ_{\alpha\beta\gamma\delta}}{dx} &= \frac{ig\mu_\mathrm{B}\tau}{\hbar}\sum_{\alpha',\gamma'}\Big[(\mathbf{B}(x)\cdot\boldsymbol{\sigma})_{\alpha\alpha'}\delta_{\gamma\gamma'}-\delta_{\alpha\alpha'}(\mathbf{B}(x)\cdot\boldsymbol{\sigma})_{\gamma\gamma'}\Big]N_{\alpha'\beta\gamma'\delta}\\ &\quad -(2\tau/\tau_\varphi)N_{\alpha\beta\gamma\delta}+2\tau\delta_{\alpha\beta}\delta_{\gamma\delta}\delta(x-x_\mathrm{i}). \qquad (6.3.19)\end{aligned}$$

The periodic boundary conditions are

$$N_{\alpha\beta\gamma\delta}(0)=N_{\alpha\beta\gamma\delta}(L),\quad J_{\alpha\beta\gamma\delta}(0)=J_{\alpha\beta\gamma\delta}(L). \qquad (6.3.20)$$

The Cooperon C and the propagator χ of Eqs. (6.3.4) and (6.3.7) are related to the density N by

$$N_{\alpha\beta\gamma\delta}(x)=\int_0^\infty dt\,\mathrm{e}^{-t/\tau_\varphi}\frac{1}{2\pi}\int_0^{2\pi}d\phi\int_0^{2\pi}d\phi_\mathrm{i}\,\chi_{\alpha\beta\gamma\delta}(x,x_\mathrm{i};\phi,\phi_\mathrm{i};t), \qquad (6.3.21)$$

$$\sum_{\alpha,\beta}N_{\alpha\beta\beta\alpha}(x_\mathrm{i})=\int_0^\infty dt\,\mathrm{e}^{-t/\tau_\varphi}C(t). \qquad (6.3.22)$$

Hence the weak-localization correction (6.3.1) is obtained from N by

$$\Delta G = -\frac{e^2 D}{\pi\hbar L}\sum_{\alpha,\beta} N_{\alpha\beta\beta\alpha}(x_{\rm i}). \tag{6.3.23}$$

The transformation to the local basis of spin states (6.2.3) takes the form of a unitary transformation of the moments N and J,

$$\begin{aligned}
\tilde{N}_{\alpha\beta\gamma\delta} &= \sum_{\alpha',\beta',\gamma',\delta'} Q_{\alpha\alpha'}Q_{\gamma\gamma'}N_{\alpha'\beta'\gamma'\delta'}Q^{\dagger}_{\beta'\beta}Q^{\dagger}_{\delta'\delta}, && (6.3.24)\\
\tilde{J}_{\alpha\beta\gamma\delta} &= \sum_{\alpha',\beta',\gamma',\delta'} Q_{\alpha\alpha'}Q_{\gamma\gamma'}J_{\alpha'\beta'\gamma'\delta'}Q^{\dagger}_{\beta'\beta}Q^{\dagger}_{\delta'\delta}, && (6.3.25)\\
Q(x) &= \begin{pmatrix} {\rm e}^{i\pi f x/L}\cos\frac{\eta}{2} & {\rm e}^{-i\pi f x/L}\sin\frac{\eta}{2} \\ -{\rm e}^{i\pi f x/L}\sin\frac{\eta}{2} & {\rm e}^{-i\pi f x/L}\cos\frac{\eta}{2} \end{pmatrix}. && (6.3.26)
\end{aligned}$$

The transformed moments obey

$$\begin{aligned}
\ell\frac{d\tilde{N}_{\alpha\beta\gamma\delta}}{dx} &= \sum_{\alpha',\gamma'}\left(T_{\alpha\alpha'}\delta_{\gamma\gamma'} + \delta_{\alpha\alpha'}T_{\gamma\gamma'}\right)\tilde{N}_{\alpha'\beta\gamma'\delta} \\
&\quad + \sum_{\alpha',\gamma'}\left(S_{\alpha\alpha'}\delta_{\gamma\gamma'} - \delta_{\alpha\alpha'}S_{\gamma\gamma'}\right)\tilde{J}_{\alpha'\beta\gamma'\delta} \\
&\quad - (1+\tau/\tau_{\varphi})\,\tilde{J}_{\alpha\beta\gamma\delta}, && (6.3.27)\\
\ell\frac{d\tilde{J}_{\alpha\beta\gamma\delta}}{dx} &= 2\sum_{\alpha',\gamma'}\left(S_{\alpha\alpha'}\delta_{\gamma\gamma'} - \delta_{\alpha\alpha'}S_{\gamma\gamma'}\right)\tilde{N}_{\alpha'\beta\gamma'\delta} \\
&\quad + \sum_{\alpha',\gamma'}\left(T_{\alpha\alpha'}\delta_{\gamma\gamma'} + \delta_{\alpha\alpha'}T_{\gamma\gamma'}\right)\tilde{J}_{\alpha'\beta\gamma'\delta} \\
&\quad -(2\tau/\tau_{\varphi})\tilde{N}_{\alpha\beta\gamma\delta} + 2\tau\delta_{\alpha\beta}\delta_{\gamma\delta}\delta(x-x_{\rm i}), && (6.3.28)
\end{aligned}$$

with the same 2×2 matrices S and T as in Sec. 6.2. Because the transformation from N to $\tilde{N}$ is unitary, the weak-localization correction is still given by $\Delta G = -(e^2D/\pi\hbar L)\sum_{\alpha,\beta}\tilde{N}_{\alpha\beta\beta\alpha}(x_{\rm i})$, as in Eq. (6.3.23).

We have solved Eq. (6.3.27-6.3.28) with periodic boundary conditions by numerically computing the eigenvalues and (right) eigenvectors of the 8×8 matrix of coefficients. The resulting ΔG is plotted in Figs. 6-3,6-4 as a function of the tilt angle η. In the adiabatic regime $\omega_{\rm B}\tau \gg f$ we find the conductance oscillations due to the Berry phase. These are given by [5]

$$\Delta G = -\frac{e^2}{\pi\hbar}\frac{L_{\varphi}}{L}\frac{\sinh(L/L_{\varphi})}{\cosh(L/L_{\varphi}) - \cos\left(2\pi f\cos\eta\right)} \tag{6.3.29}$$

analogously to the Aharonov-Bohm oscillations [3]. (The length $L_{\varphi} = \sqrt{D\tau_{\varphi}}$ is the phase-coherence length.) In the randomized regime $(f\ell/L)^2 \ll \omega_{\rm B}\tau \ll f$

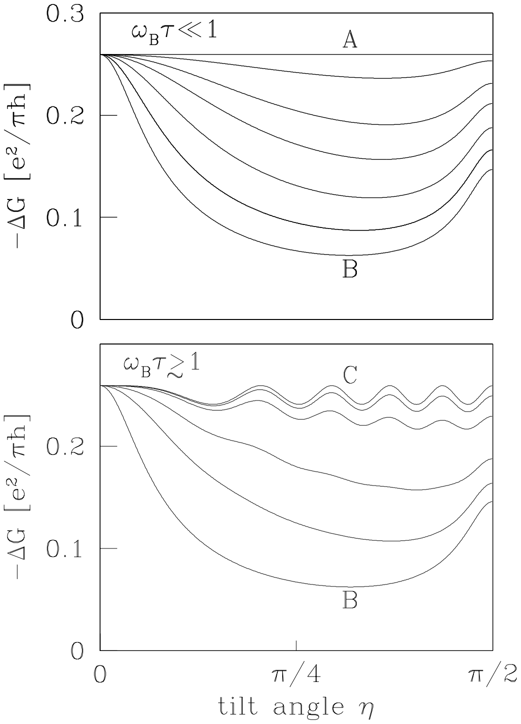

Figure 6-3. Weak-localization correction ΔG of a ring in a spatially rotating magnetic field, as a function of the tilt angle η. Plotted is the result of Eq. (6.3.27-6.3.28) for $f = 5$, $L = 500\,\ell$, and $L_\varphi = 125\,\ell$. The upper panel is for $\omega_B\tau \ll 1$. From top to bottom: $\omega_B\tau = 10^{-5}$, 10^{-4}, $2\cdot10^{-4}$, $3\cdot10^{-4}$, $5\cdot10^{-4}$, 10^{-3}, 10^{-2}. At $\omega_B\tau \simeq (f\ell/L)^2$, the weak-localization correction crosses over from the transient regime A of Eq. (6.3.30) to the randomized regime B of Eq. (6.3.39-6.3.41). The lower panel is for $\omega_B\tau \gtrsim 1$. From bottom to top: $\omega_B\tau = 0.1$, 1, 2, 5, 10, 100. Here the weak-localization correction reaches the adiabatic regime C of Eq. (6.3.29).

there are no conductance oscillations. Instead we find a reduction of the weak-localization correction, due to dephasing by spin scattering. In the transient regime $\omega_B\tau \ll (f\ell/L)^2$ the effect of the field on the spin can be ignored [9], and the weak-localization correction remains at its zero-field value

$$\Delta G = -\frac{e^2}{\pi\hbar}\frac{L_\varphi}{L}\operatorname{cotanh}\left(\frac{L}{2L_\varphi}\right). \qquad (6.3.30)$$

6.3.3 Comparison with Loss, Schoeller, and Goldbart

If we replace the Boltzmann operator $\mathcal{B}$ in Eq. (6.3.5) by the diffusion operator $-D\partial^2/\partial x^2$ and integrate over ϕ and ϕ_i, we end up with the diffusion equation

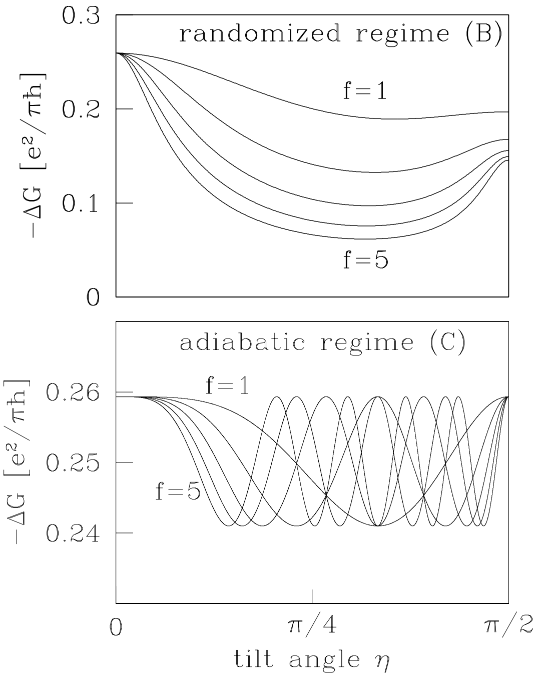

Figure 6-4. Same as Fig. 6-3, but now for $f = 1, 2, \ldots, 5$ with a fixed field strength in the randomized regime (upper panel) respectively adiabatic regime (lower panel).

studied by LSG,

$$\left(\frac{\partial}{\partial t} - \mathcal{H}\right) \chi_{\alpha\beta\gamma\delta}(x, x_{\rm i}; t) = \delta(t)\delta(x - x_{\rm i})\delta_{\alpha\beta}\delta_{\gamma\delta}, \tag{6.3.31}$$

$$\mathcal{H} = D\frac{\partial^2}{\partial x^2} + \frac{ig\mu_{\rm B}}{2\hbar}\left[\mathbf{B}(x) \cdot \boldsymbol{\sigma}_1 - \mathbf{B}(x) \cdot \boldsymbol{\sigma}_2\right], \tag{6.3.32}$$

$$\chi_{\alpha\beta\gamma\delta}(x, x_{\rm i}; t) = \frac{1}{2\pi}\int_0^{2\pi} d\phi \int_0^{2\pi} d\phi_{\rm i}\, \chi_{\alpha\beta\gamma\delta}(x, x_{\rm i}; \phi, \phi_{\rm i}; t). \tag{6.3.33}$$

Here $\boldsymbol{\sigma}_1$ and $\boldsymbol{\sigma}_2$ act, respectively, on the first and third indices of $\chi_{\alpha\beta\gamma\delta}$.

The difference between the diffusion equation (6.3.31) and the diffusion equation (6.3.18-6.3.19) is that the former holds only if $\omega_{\rm B}\tau \ll 1$, while the latter holds for any value of $\omega_{\rm B}\tau$. LSG used Eq. (6.3.31) to argue that there exists an adiabatic region within the regime $\omega_{\rm B}\tau \ll 1$. In contrast, our analysis of Eq. (6.3.18-6.3.19) shows that adiabaticity is not possible if $\omega_{\rm B}\tau \ll 1$. The argument of LSG is based on a mapping of the diffusion equation (6.3.31) onto the Schrödinger equation studied in Ref. [10]. However, the mapping is not carried out explicitly. In this subsection we will solve Eq. (6.3.31) exactly using this mapping, to demonstrate that the adiabatic regime of LSG is in fact the randomized regime B. This mis-identification perhaps occurred because both regimes are stationary with respect to the magnetic field strength (cf. Fig. 6-2). However, Berry-phase oscillations of the conductance are only supported in the adiabatic regime C, not in the randomized regime B (cf. Figs. 6-3,6-4).

We solve Eq. (6.3.31) for the weak-localization correction

$$\Delta G = -\frac{e^2 D}{\pi\hbar L}\sum_{\alpha,\beta}\left\langle x,\alpha,\beta\,\middle|\left(\tau_\varphi^{-1}-\mathcal{H}\right)^{-1}\middle|\,x,\beta,\alpha\right\rangle, \tag{6.3.34}$$

where we introduced the basis of eigenstates $|x,\alpha,\beta\rangle$ (with $\alpha,\beta=\pm 1$) of the position operator x and the spin operators σ_{1z} and σ_{2z}. The operator $\mathcal{H}$ commutes with

$$J = \frac{L}{2\pi i}\frac{\partial}{\partial x} + \tfrac{1}{2}f\,(\sigma_{1z}+\sigma_{2z}). \tag{6.3.35}$$

It is therefore convenient to use as a basis, instead of the eigenstates $|x,\alpha,\beta\rangle$, the eigenstates $|j,\alpha,\beta\rangle$ of J, σ_{1z}, and σ_{2z}. The eigenvalue j of J is an integer because of the periodic boundary conditions. The eigenfunctions are given by

$$\langle x,\alpha',\beta'|j,\alpha,\beta\rangle = \frac{1}{\sqrt{L}}\delta_{\alpha'\alpha}\delta_{\beta'\beta}\exp\left[\tfrac{2\pi i x}{L}(j-\tfrac{1}{2}f\alpha-\tfrac{1}{2}f\beta)\right]. \tag{6.3.36}$$

In the basis $\{|j,1,1\rangle,|j,1,-1\rangle,|j,-1,1\rangle,|j,-1,-1\rangle\}$ the operator $\mathcal{H}$ has matrix elements

$$\begin{aligned}\langle j',\alpha',\beta'|\mathcal{H}|j,\alpha,\beta\rangle = {}& -D\left(\frac{2\pi}{L}\right)^2\delta_{j'j}\begin{pmatrix}(j-f)^2 & 0 & 0 & 0\\ 0 & j^2 & 0 & 0\\ 0 & 0 & j^2 & 0\\ 0 & 0 & 0 & (j+f)^2\end{pmatrix}\\ & -i\omega_{\mathrm{B}}\delta_{j'j}\begin{pmatrix}0 & \sin\eta & -\sin\eta & 0\\ \sin\eta & -2\cos\eta & 0 & -\sin\eta\\ -\sin\eta & 0 & 2\cos\eta & \sin\eta\\ 0 & -\sin\eta & \sin\eta & 0\end{pmatrix}.\end{aligned} \tag{6.3.37}$$

Substitution into Eq. (6.3.34) yields

$$\begin{aligned}\Delta G = {}& -\frac{e^2 D}{\pi\hbar}\frac{1}{L^2}\sum_{\alpha,\beta}\sum_{j=-\infty}^{\infty}\left\langle j,\alpha,\beta\,\middle|\left(\tau_\varphi^{-1}-\mathcal{H}\right)^{-1}\middle|\,j,\beta,\alpha\right\rangle\\ = {}& -\frac{e^2}{2\pi^3\hbar}\sum_{j=-\infty}^{\infty}\left[(\gamma+j^2)^2(f^2+\gamma+j^2)+\kappa^2(3f^2+4\gamma+4j^2+f^2\cos 2\eta)\right]\\ & \times\Big[(\gamma+j^2)^2(f^4+2f^2\gamma+\gamma^2-2f^2j^2+2\gamma j^2+j^4)+2\kappa^2\big(f^4+3f^2\gamma\\ & +2\gamma^2-f^2j^2+4\gamma j^2+2j^4+f^2(f^2+\gamma-3j^2)\cos 2\eta\big)\Big]^{-1}.\end{aligned} \tag{6.3.38}$$

We abbreviated $\kappa = 2\omega_B\tau(L/2\pi\ell)^2$ and $\gamma = (L/2\pi L_\varphi)^2$. The sum over j can be done analytically for $\kappa \gg 1$, with the result

$$\begin{aligned} \Delta G &= -\frac{e^2}{\pi\hbar}\frac{1}{4\pi Q}\left[\frac{4a_- + 4\gamma + (3+\cos 2\eta)f^2}{\sqrt{a_-}\tan\pi\sqrt{a_-}}\right. \\ &\qquad\qquad \left. -\frac{4a_+ + 4\gamma + (3+\cos 2\eta)f^2}{\sqrt{a_+}\tan\pi\sqrt{a_+}}\right], \qquad (6.3.39) \\ Q &= \left[f^4(9\cos^2 2\eta - 2\cos 2\eta - 7) - 32\gamma f^2(1+\cos 2\eta)\right]^{1/2}, \qquad (6.3.40) \\ a_\pm &= -\gamma + \tfrac{1}{4}(1+3\cos 2\eta)f^2 \pm \tfrac{1}{4}Q. \qquad (6.3.41) \end{aligned}$$

We have checked that our solution (6.3.38) of Eq. (6.3.31) coincides with the solution of Eq. (6.3.18-6.3.19) in the regime $\omega_B\tau \ll 1$. (The two sets of curves are indistinguishable on the scale of the figures.) In particular, Eq. (6.3.39-6.3.41) coincides with the curves labeled B in Figs. 6-3 and 6-4, demonstrating that it represents the randomized regime — without Berry phase-oscillations.

6.4 Conclusions

In conclusion, we have computed the effect of a non-uniform magnetic field on the spin polarization (Sec. 6.2) and weak-localization correction (Sec. 6.3) in a disordered conductor. We have identified three regimes of magnetic field strength: the transient regime given by $\omega_B\tau \ll (f\ell/L)^2$, the randomized regime $(f\ell/L)^2 \ll \omega_B\tau \ll f$, and the adiabatic regime $\omega_B\tau \gg f$. In the transient regime (labeled A in Figs. 6-2 and 6-3), the effect of the magnetic field can be neglected. In the randomized regime (labeled B), the depolarization and the suppression of the weak-localization correction are maximal. In the adiabatic regime (labeled C), the polarization is restored and the weak-localization correction exhibits oscillations due to the Berry phase.

The criterion for adiabaticity is $\omega_B t_c \gg 1$, with ω_B the spin-precession frequency and t_c a characteristic timescale of the orbital motion. We find $t_c = \tau$, in agreement with Stern [2], but in contradiction with the result $t_c = \tau(L/\ell)^2$ of Loss, Schoeller, and Goldbart [5]. By solving exactly the diffusion equation for the Cooperon derived in Ref. [5], we have demonstrated unambiguously that the regime which in that paper was identified as the adiabatic regime, is in fact the randomized regime B — without Berry-phase oscillations.

We have focused on transport properties, such as conductance and spin-resolved transmission. Thermodynamic properties, such as the persistent current, in a non-uniform magnetic field have been studied by Loss, Goldbart, and Balatsky [10, 11] in connection with Berry-phase oscillations. These papers assumed ballistic systems. We believe that the adiabaticity criterion $\omega_B\tau \gg 1$ for disordered systems should apply to thermodynamic properties as well as transport properties. This strong-field criterion presents a pessimistic outlook for the prospect of experiments on the Berry phase in disordered systems.

In a recent preprint (cond-mat/9805128), Loss, Schoeller and Goldbart have reconsidered the condition for adiabaticity. We agree on the equations (our exact solution (3.2a) is their starting point), but differ in the interpretations. They interpret our randomized regime B as being the adiabatic regime and explain the absence of Berry-phase oscillations as being due to the effects of field-induced dephasing. We reserve the name “adiabatic” for regime C, because if the spin would follow the magnetic field adiabatically in regime B, it should not suffer dephasing.

References

[1] M. V. Berry, Proc. R. Soc. Lond. A **392**, 45 (1984).

[2] A. Stern, Phys. Rev. Lett. **68**, 1022 (1992); in *Quantum Coherence and Reality*, eds. J. S. Anandan and J. L. Safko (World Scientific, Singapore, 1992).

[3] B. L. Altshuler, A. G. Aronov, and B. Z. Spivak, Pis'ma Zh. Eksp. Teor. Fiz. **33**, 101 (1981) [JETP Lett. **33**, 94 (1981)]; D. Yu. Sharvin and Yu. V. Sharvin, Pis'ma Zh. Eksp. Teor. Fiz. **34**, 285 (1981) [JETP Lett. **34**, 272 (1981)]; A. G. Aronov and Yu. V. Sharvin, Rev. Mod. Phys. **59**, 755 (1987).

[4] A. Stern, in *Mesoscopic Electron Transport*, eds. L. P. Kouwenhoven, G. Schön, and L. L. Sohn (Kluwer, Dordrecht, 1997).

[5] D. Loss, H. Schoeller, and P. M. Goldbart, Phys. Rev. B **48**, 15218 (1993).

[6] L. P. Kouwenhoven (private communication). Experiments in a ballistic system were reported by A. F. Morpurgo, J. P. Heida, T. M. Klapwijk, B. J. van Wees, and G. Borghs, Phys. Rev. Lett. **80**, 1050 (1998).

[7] Yu. Lyanda-Geller, I. L. Aleiner, and P. M. Goldbart, preprint (cond-mat/9801113).

[8] S. Chakravarty and A. Schmid, Phys. Rep. **140**, 193 (1986).

[9] Because we include only the effect of the magnetic field on the spin, we do not find the suppression of weak-localization due to time-reversal-symmetry breaking of the orbital motion, nor do we find the Aharonov-Bohm oscillations due to the coupling of the magnetic field to the charge.

[10] D. Loss and P. M. Goldbart, Phys. Rev. B **45**, 13544 (1992).

[11] D. Loss, P. Goldbart, and A. V. Balatsky, Phys. Rev. Lett. **65**, 1655 (1990).

Samenvatting

Thermische en elektrische verschijnselen in chaotische geleiders

Dit proefschrift gaat over de chaotische beweging van elektronen. In wanordelijke metalen botsen de elektronen op onzuiverheden en maken daardoor een chaotische “dronkemanswandeling” door het metaal. Er zijn ook systemen zonder onzuiverheden waarin de elektronen toch een chaotische beweging uitvoeren door botsingen met de wanden. Een voorbeeld van zo’n chaotisch systeem is een “elektronenbiljart” in de vorm van een stadion (twee halve cirkels verbonden door lijnstukken). De beweging in zo’n stadion is chaotisch in tegenstelling tot de beweging in een rechthoekig of rond biljart. We onderzoeken de invloed van de chaotische beweging op de warmtegeleiding en de elektrische geleiding.

In hoofdstuk 1 wordt een algemene inleiding gegeven en worden de gebruikte technieken nader toegelicht. Uitgangspunt is de relatie tussen transportgrootheden bij lage temperaturen en quantummechanische verstrooiingsparameters. Het elektrische geleidingsvermogen, bijvoorbeeld, is evenredig met de transmissiekans door het metaal. Alle informatie over hoe een object invallende golven doorlaat of terugkaatst, is bevat in de verstrooiingsmatrix. De verstrooiingsmatrix van één enkel chaotisch systeem valt niet te voorspellen, zonder een ingewikkelde berekening te doen. Maar de statistische eigenschappen van een ensemble van chaotische systemen zijn wel eenvoudig te voorspellen. Voor een chaotisch biljart bijvoorbeeld is de verstrooiingsmatrix een willekeurig gekozen unitaire matrix. Deze aanpak heet de *toevalsmatrixtheorie*.

De theorie ontwikkeld voor de chaotische beweging van elektronen is ook van toepassing op de chaotische verstrooiing van licht. In hoofdstuk 2 van dit proefschrift onderzoeken we de statistiek van optische spikkelpatronen. Een spikkelpatroon is een schakering van lichte en donkere vlekjes op een scherm dat ontstaat na verstrooiing van laserlicht aan een ruw object. Wij bestuderen de transmissie van licht door een buis gevuld met verstrooiers. Voor korte buizen is de gemiddelde intensiteit van de spikkels omgekeerd evenredig met de buislengte. Dit is het optische equivalent van de wet van Ohm en beschrijft “diffuus licht”. Voor langere buizen neemt de gemiddelde intensiteit van de spikkels exponentieel af met de lengte. Dit heet “lokalisatie” van licht. Door destructieve interferentie van veelvoudig verstrooide lichtstralen raakt het licht “verstrikt” in de wanorde. Wij berekenen de kansverdeling van de intensiteit van de spikkels, als functie van de lengte van de buis. Het resultaat beschrijft de volledige overgang van diffuus licht naar gelokaliseerd licht. Recentelijk is deze overgang waargenomen door een groep uit New York.

In hoofdstuk 3 bestuderen we een elektronisch spikkelpatroon in een chaotisch biljart. De statistiek van de intensiteit hangt ervan af of tijdsomkeersymmetrie al dan niet aanwezig is. Tijdsomkeersymmetrie wordt gebroken door een magnetisch veld. Dit is een geleidelijk proces. We onderzoeken de invloed van het magnetisch veld op de ruimtelijke correlaties van de intensiteit. Is het veld afwezig of juist heel groot, dan zijn de intensiteiten op verschillende plaatsen ongecorreleerd. Voor een niet al te groot magnetisch veld zijn er opmerkelijk genoeg *wel* ruimtelijke correlaties, van lange dracht. Deze werden recentelijk ontdekt met behulp van een microscopische theorie. In dit hoofdstuk laten wij zien dat de correlaties ook volgen uit de toevalsmatrixtheorie. We tonen tevens het verband aan van deze ruimtelijke correlaties met een ander verschijnsel, namelijk de niet-Gaussische kansverdeling van de snelheid waarmee een energieniveau reageert op een verstoring van het systeem.

In de volgende twee hoofstukken beschouwen we twee andere transportverschijnselen, hagelruis en thermokracht.

De elektrische stroom door een geleider fluctueert in de tijd, zelfs bij zeer lage temperaturen en een constante aangelegde spanning. Deze tijdsafhankelijkheid is het gevolg van de discreetheid van elektrische lading en staat bekend als hagelruis. (De naam verwijst naar het geluid veroorzaakt door hagel op het dak.) Bij een geleider met meer dan twee stroomcontacten zijn om dezelfde reden de stromen door verschillende contacten gecorreleerd. Recentelijk zijn deze correlaties in Stanford gemeten, voor een tunnelbarrière met twee ingaande en twee uitgaande stroomcontacten — het elektrische analogon van een optische bundelsplitser. Terwijl optische correlaties vergroot worden door het bosonische karakter van de fotonen, veroorzaakt het uitsluitingsprincipe van Pauli een onderdrukking van de elektrische correlaties. In hoofdstuk 4 berekenen wij de correlaties en fluctuaties van stromen door een chaotische geleider met vier contacten. De mate van onderdrukking ten gevolge van het principe van Pauli hangt onder andere af van de kwaliteit van de contacten.

Als twee uiteinden van een geleider op verschillende temperaturen worden gebracht, zal er een elektrische stroom gaan lopen van het warme naar het koude gedeelte. Deze stroom kan worden gecompenseerd door een spanning aan te leggen die een even grote stroom opwekt in de tegenovergestelde richting. De verhouding van temperatuurverschil en spanningverschil heet thermokracht. Deze grootheid hangt af van de energie-gevoeligheid van de verstrooiingsprocessen die de elektrische geleiding beperken. In hoofstuk 5 berekenen wij de verdeling van de thermokracht voor een één-dimensionale wanordelijke draad en voor een chaotisch biljart. In het eerste geval vertoont de transmissie scherpe en ongecorreleerde pieken als functie van de energie; in het tweede geval zijn de transmissiepieken gecorreleerd doordat ze elkaar overlappen. De respectievelijke kansverdelingen van de thermokracht zijn dan ook verschillend en in beide gevallen niet-Gaussisch. Voor het chaotische biljart is deze verdeling recentelijk gemeten door een groep uit Aken.

Het laatste hoofdstuk behandelt een actuele controverse uit de literatuur: hoe sterk moet een magneetveld zijn om de fase van Berry waar te nemen in een wanordelijk metaal? De fase van Berry is een gevolg van de adiabatische rotatie van de elektronspin in een ruimtelijk roterend magneetveld. In de literatuur staan twee sterk uiteenlopende schattingen voor de minimaal vereiste veldsterkte. Als de hoogste schatting correct is, is een experiment praktisch onmogelijk; de lagere schatting daarentegen geeft een veel optimistischer perspektief. Onze berekening bevestigt de eerstgenoemde schatting. Door een exacte oplossing te geven van de kinetische vergelijking hopen we de controverse uit de wereld geholpen te hebben.

List of publications

- *Nonperturbative calculation of the probability distribution of plane-wave transmission through a disordered waveguide*, S. A. van Langen, P. W. Brouwer, and C. W. J. Beenakker, Physical Review E **53**, R1344–1347 (1996) [Chapter 2].

- *Fluctuating phase rigidity for a quantum chaotic system with partially broken time-reversal symmetry*, S. A. van Langen, P. W. Brouwer, and C. W. J. Beenakker, Physical Review E **55**, R1–4 (1997) [Chapter 3].

- *Quantum-statistical current correlations in multilead chaotic cavities*, S. A. van Langen and M. Büttiker, Physical Review B **56**, R1680–1683 (1997) [Chapter 4].

- *Thermopower of single-channel disordered and chaotic conductors*, S. A. van Langen, P. G. Silvestrov, and C. W. J. Beenakker, Superlattices and Microstructures **23**, 691–698 (1998) [Chapter 5].

- *Berry phase and adiabaticity of a spin diffusing in a non-uniform magnetic field*, S. A. van Langen, H. P. A. Knops, J. C. J. Paasschens, and C. W. J. Beenakker, submitted to Physical Review B [Chapter 6].

- *Distribution of parametric conductance derivatives of a quantum dot*, P. W. Brouwer, S. A. van Langen, K. M. Frahm, M. Büttiker, and C. W. J. Beenakker, Physical Review Letters **79**, 913–916 (1997).

- *Charge fluctuations in quantum point contacts and chaotic cavities in the presence of transport*, M. H. Pedersen, S. A. van Langen, and M. Büttiker, Physical Review B **57**, 1838–1846 (1998).

- *Exchange effects in shot noise in multi-terminal devices*, Ya. M. Blanter, S. A. van Langen, and M. Büttiker, Uspekhi Fizicheskikh Nauk **168**, 159–162 (1998) [Physics-Uspekhi **41**, 149–152 (1998)].

Curriculum Vitae

Ik ben geboren op 31 augustus 1971 te Nijmegen. Vanaf 1983 bezocht ik in deze stad het RK Dominicus College tot ik in 1989 het diploma Atheneum B behaalde.

Datzelfde jaar ging ik natuurkunde studeren aan de Katholieke Universiteit Nijmegen, waar ik in 1990 cum laude slaagde voor het propaedeutisch examen. Tijdens mijn studie heb ik een negental studentassistentschappen vervuld bij diverse natuur- en wiskundevakken. Bij de studievereniging Marie Curie was ik actief met onder andere het organiseren van twee buitenlandse studiereizen. Mijn afstudeerwerk in de groep van prof. dr. T. W. J. M. Janssen betrof de theorie van structurele defecten in aperiodieke kristallen. Een deel van dit werk heb ik verricht gedurende een verblijf van zes maanden aan de Université de Paris VI in de groep van dr. M. Kléman. In februari 1995 studeerde ik cum laude af.

Vanaf maart 1995 was ik als onderzoeker in opleiding in dienst van de Stichting voor Fundamenteel Onderzoek der Materie (FOM). Ik werkte op het Instituut-Lorentz van de Rijksuniversiteit Leiden onder begeleiding van prof. dr. C. W. J. Beenakker aan het onderzoek beschreven in dit proefschrift. Een deel van het onderzoek is uitgevoerd in samenwerking met prof. dr. M. Büttiker van de Université de Genève. Met steun van de Europese Unie verbleef ik twee maal enkele maanden in Genève. Mijn onderwijstaak in Leiden bestond uit het verzorgen van de werkcolleges bij het vak Statistische Fysica I. De resultaten van mijn promotie-onderzoek heb ik onder andere gepresenteerd op zomerscholen in Bad Lauterberg en Trieste en op conferenties in Miraflores, Mauterndorf en Ioannina.

Vanaf augustus 1998 ben ik werkzaam als onderzoeker op het Philips Natuurkundig Laboratorium te Eindhoven.

STELLINGEN

1. De adiabatische evolutie van een elektronspin in een niet-uniform magneetveld is onverenigbaar met verstrooiing door wanorde.

2. Indien H een hermitische matrix is en H' een matrix verkregen uit H door weglating van de j-de rij en kolom, dan bevindt zich tussen elke twee eigenwaarden van H een eigenwaarde van H'.

3. De verdeling van het warmte-vermogen S van een chaotisch biljart met enkel-kanaals stroomcontacten, gemiddelde toestandsdichtheid ρ en inelastische verstrooiingstijd $\tau_\phi \ll \hbar\rho$ is bij gebroken tijdsomkeersymmetrie gegeven door

$$P(\sigma) = \frac{1}{96}\left(|\sigma|^3 + 6\sigma^2 + 15|\sigma| + 15\right) \mathrm{e}^{-|\sigma|}, \quad \sigma \equiv \frac{3e\rho}{\pi k_\mathrm{B}^2 T}\left(\frac{\hbar}{\tau_\phi}\right)^2 S.$$

4. De lading gepompt door een chaotisch biljart tijdens een adiabatische cyclische verandering van parameters is alleen statistisch onafhankelijk van het geleidingsvermogen in de afwezigheid van tijdsomkeersymmetrie.

5. De DMPK-vergelijking was reeds bekend in 1972.

   R. Burridge and G. Papanicolaou,
   Comm. Pure Appl. Math. **25**, 715 (1972).

6. De zogenaamd universele onderdrukking van de hagelruis met een factor 1/3 in een *niet-ontaard* wanordelijk elektronengas is in werkelijkheid modelafhankelijk.

   T. González, C. González, J. Mateos, D. Pardo, L. Reggiani,
   O. M. Bulashenko, and J. M. Rubí, Phys. Rev. Lett. **80**, 2901 (1998).

7. De intensiteit van thermische straling uitgezonden door een niet-ideaal zwart lichaam is gecorreleerd over afstanden langer dan de transversale optische coherentielengte.

8. Reproduceerbare fluctuaties in de coda van een aardbeving zijn het seismische analogon van universele geleidingsfluctuaties.

9. Een houten klarinet klinkt niet beter dan een van kunststof.

Stijn van Langen
Leiden, 3 september 1998